CR-134647
LYC 73-48

NASA

(NASA-CR-134647) DEVELOPMENT OF HELICOPTER ENGINE SEALS (Avco Lycoming Div.) 108 p HC $6.50 CSCL 21A
N74-28229
Unclas
G3/28 42472

DEVELOPMENT OF HELICOPTER ENGINE SEALS

by

Peter Lynwander

AVCO LYCOMING DIVISION
550 South Main Street
Stratford, Connecticut 06497

prepared for

NATIONAL AERONAUTICS AND SPACE ADMINISTRATION

CONTRACT NAS 3-16720

NASA Lewis Research Center
Cleveland, Ohio

1. Report No. NASA CR-134647	2. Government Accession No.	3. Recipient's Catalog No.
4. Title and Subtitle Development of Helicopter Engine Seals		5. Report Date November 1973
		6. Performing Organization Code
7. Author(s) P. Lynwander		8. Performing Organization Report No. LYC 73-48
		10. Work Unit No.
9. Performing Organization Name and Address Avco Lycoming Division, 550 South Main Street, Stratford, Connecticut 06497		11. Contract or Grant No. NAS 3-16720
		13. Type of Report and Period Covered Contractor Report
12. Sponsoring Agency Name and Address U. S. Army Air Mobility Research and Development Laboratory, Moffett Field, California and National Aeronautics and Space Administration, Washington, D.C. 20546		14. Sponsoring Agency Code

15. Supplementary Notes

Project Manager, Lawrence P. Ludwig, Fluid Systems Components Division
NASA Lewis Research Center, Cleveland, Ohio

16. Abstract

An experimental evaluation of main shaft seals for helicopter gas turbine engines was conducted with shaft speeds to 213 m/s (700 ft/sec), air pressures to 148 N/cm^2 (215 psia), and air temperatures to 645 K (675°F).

Three conventional carbon seal designs were evaluated; these were the face, the circumferential segmented, and the rotating ring types. In addition, two advanced carbon seal configurations, the face and circumferential incorporating self-acting geometry for lift augmentation, were evaluated.

Gas leakage test results indicate that conventional seals will not be satisfactory for high-pressure sealing because of excessive leakage. The self-acting face seal, however, had significantly lower leakage and operated with insignificant wear during a 150-hour endurance test at sliding speeds to 145 m/s (475 ft/sec), air pressures to 124 N/cm^2 (180 psia), and air temperatures to 408 K (275°F). Wear measurements indicate that noncontact operation was achieved at shaft speeds of 43,000 rpm.

Evaluation of the self-acting circumferential seal was inconclusive because of seal dimensional variations.

17. Key Words (Suggested by Author(s)) shaft seals, gas seals, rotating seals, main shaft seals	18. Distribution Statement Unclassified - Unlimited

19. Security Classif. (of this report) Unclassified	20. Security Classif. (of this page) Unclassified	21. No. of Pages 106	22. Price*

* For sale by the National Technical Information Service, Springfield, Virginia 22151

FOREWORD

This program was funded by the U. S. Army Air Mobility Research and Development Laboratory. Program management was by the Lewis Research Center of the National Aeronautics and Space Administration under Contract NAS 3-16720. The period of performance was May 1972 to December 1973.

Technical direction was provided by the NASA project manager, Mr. Lawrence P. Ludwig of the Fluid Systems Components Division. Mr. Leonard W. Schopen, NASA Lewis Research Center, was the Contracting Officer.

The Avco Lycoming test program was carried out by Mr. Harry Thornton. Acknowledgement is also made to the engineering staff of Stein Seal Company for their assistance in this program.

TABLE OF CONTENTS

LIST OF ILLUSTRATIONS

LIST OF ILLUSTRATIONS (Cont)

LIST OF ILLUSTRATIONS (Cont)

LIST OF TABLES

SUMMARY

An experimental evaluation was conducted on main shaft seals for helicopter gas turbine engines. Seals were operated at conditions more stringent than those of existing engines.

Three conventional carbon seal designs were tested: face, circumferential segmented, and rotating ring.

In addition, two advanced carbon seal configurations incorporating self-acting geometry for lift augmentation were evaluated. One was a face seal and the other a circumferential (shaft-riding) seal.

Evaluation tests were conducted on all seal configurations at ambient temperature over a range of sliding speeds and sealed pressures. The maximum sliding speed was 213 m/s (700 ft/sec) and maximum air pressure was 148 N/cm^2 (215 psia). Basic design data such as air leakage and seal temperature were developed. Results indicated that conventional seals have high leakage rates. The conventional circumferential segmented seal and the self-acting circumferential seal had high wear rates, but results on the self-acting circumferential were inconclusive because of dimensional variations.

The self-acting face seal limited airflow effectively, and has the potential to operate successfully in high-pressure applications. A series of evaluation tests over a temperature range(maximum temperature, 645 K (675°F)) was conducted on the self-acting face seal. During this temperature evaluation testing of the self-acting face seal, several random failures occurred during which the carbon primary ring contacted the rotating seat and created excessive heat and wear. These failures were attributed to a combination of dynamic effects and thermal distortion of the seal seat.

High rotating speed (43, 000 rpm) capability of the self-acting face seal was demonstrated in a 150-hour endurance test that was successfully completed. Test conditions were sliding speed to 145 m/s (475 ft/sec), air pressure to 124 N/cm^2 (180 psia), and air temperature to 408 K (275°F). Wear was insignificant.

INTRODUCTION

Main shaft seals are becoming increasingly critical in advanced gas turbine engines for helicopters. As shaft speeds, air temperatures, and air pressures increase, engine size decreases, leaving less envelope to accomplish the sealing function.

The purpose of this program was to evaluate the performance of conventional seals and self-acting seals at operating conditions more severe than those experienced in current engines and to develop seals capable of operating in these environments.

Advanced Avco Lycoming engines in the 1.36 to 4.54 kg/s (3 to 10 lb/sec) class incorporate main shaft seals that operate with surface speeds to 137 m/s (450 ft/sec), air pressures to 72 N/cm^2 (104 psia), and air temperatures to 810 K (1000°F). Positive-contact carbon seals are used. In future high-performance engines, seal operating conditions will be more severe and existing positive-contact seal configurations may not be adequate. At high speeds and pressures, positive-contact carbon seals have a tendency to wear, generate heat, and coke up.

An alternative to positive-contact seals are labyrinth seals. Because of their noncontacting feature, labyrinth seals offer infinite life; however, at high air pressures and temperatures, simple labyrinths will not suffice, and complicated multistage labyrinths must be used. These latter seals incorporate venting and pressurization passages that are costly to produce and difficult to accommodate in small, high-performance engines. Compared with positive-contact seals, labyrinths also permit higher leakage airflows, (which must be absorbed by the lubrication system) that cause a loss in engine performance.

The self-acting seal concept incorporates the best features of positive-contact seals (low leakage) and labyrinth seals (noncontacting). During operation, self-acting seals are noncontacting, the sealing surfaces being separated by a thin gas film (sealing gap) which limits gas leakage. At shutdown the seal is positively contacting. Self-acting seal designs incorporate Rayleigh step lift pads on the primary (carbon) sealing faces. These lift pads provide hydrodynamic force to separate the sealing surfaces, and the gas film is sufficiently stiff so that the primary (carbon) ring tracks the runout motions of the seat without rubbing contact.

Analysis of the self-acting seal concept and experimental feasibility studies for large gas turbine engines have been detailed in many NASA-sponsored programs (References 1 through 10). However, as engine size decreases, the seal size decreases and it becomes increasingly more difficult to design in adequate lift pad geometry. Further, engine speeds increase as engine size decreases, and seal inertia forces (which increase as the square of the shaft speed) start to become a significant force to cause rubbing contact. Therefore the subject program was designed to investigate the operating conditions and problems peculiar to small, high-performance helicopter gas turbine engines.

The experimental evaluation was carried out in a test rig that simulates engine conditions in an advanced gas producer turbine bearing location. All seal and bearing package hardware was lightweight and typical of Avco Lycoming engine design practice.

Three conventional seal configurations used in Avco Lycoming engines were tested: face, shaft riding, and rotating ring.

In addition, two self-acting seal configurations were evaluated. One configuration had an internally pressurized, shaft-riding, circumferential seal design, and the other had a positive-contact face seal design. The basic seal designs were defined by NASA.

Test data pertaining to airflow, cavity pressure and seal temperature for all seals were developed for a range of speeds and pressures at ambient temperatures. These data provided design criteria and a basis for comparison of the seal configurations. A labyrinth configuration was analytically evaluated as part of the seal performance comparison.

The self-acting face seal configuration (which showed the best potential for successful operation at advanced engine conditions) was endurance tested and evaluated at elevated temperatures.

During the course of the program, 282 hours of rig evaluation was conducted.

TEST VEHICLE

The test rig bearing compartment (Figure 1) is typical of advanced, high-speed gas turbine packages. Sealing positions are located forward and aft of the bearing, which enabled two seal samples to be tested simultaneously.

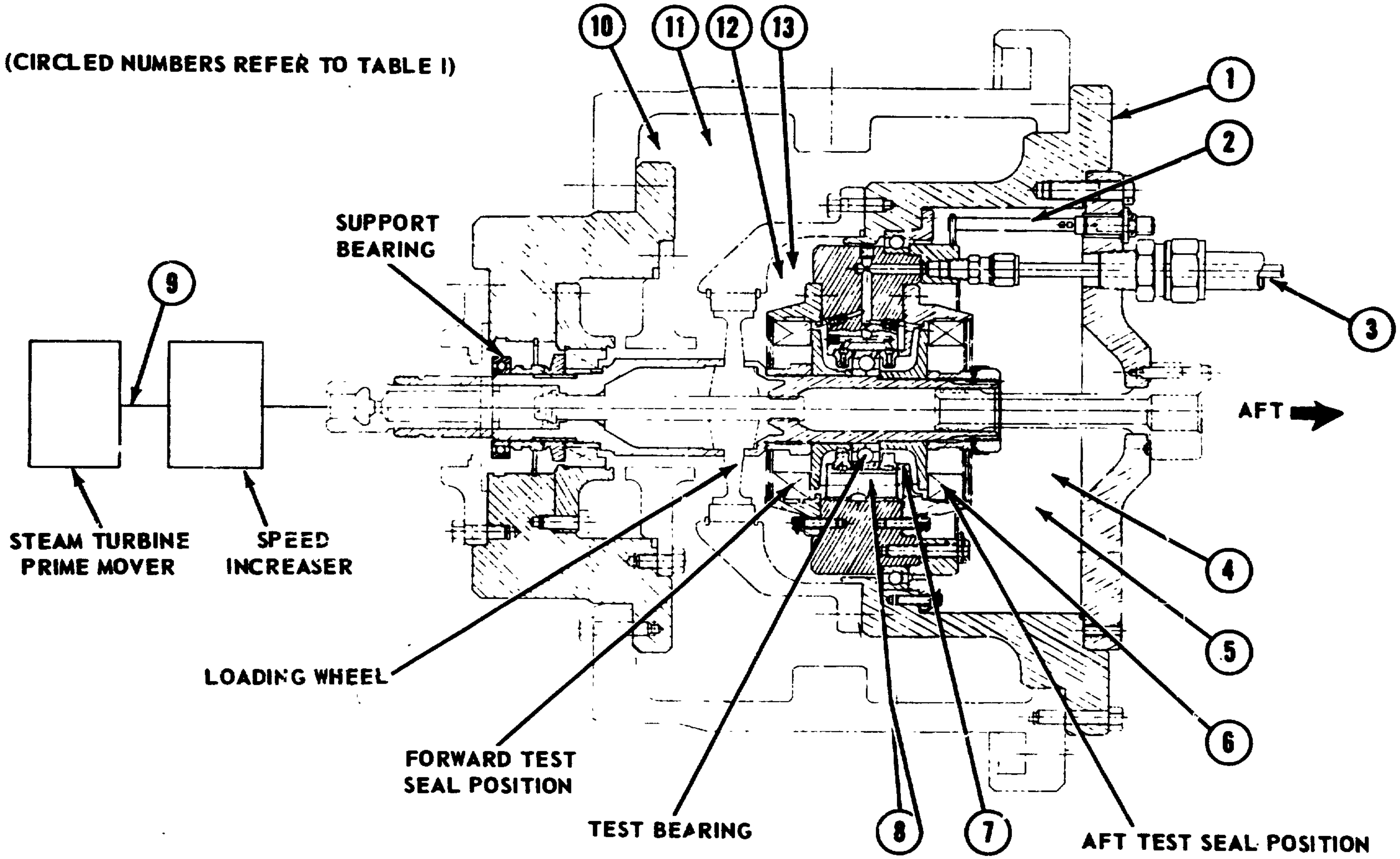

Figure 1. Test Vehicle and Instrumentation Plan.

The rig prime mover is a 100-horsepower, 20,000-rpm steam turbine. Connecting the steam turbine to the rig is a 3:1 ratio speed increaser. The test installation is shown in Figure 2.

The shaft is supported by a 35-mm, split-inner-race ball bearing in the test position, and by a 25-mm, split-inner-race bearing in the support position. Both bearings are hydraulically mounted, and thrust loading is supplied by coil springs acting on the outer race of the support bearing and by pressure differentials across the loading wheel.

A single batch of MIL-L-23699 oil at 367 ± 5 K (200 ± 10°F) was used throughout the test program.

The bearing compartment drains by gravity into a static air-oil separator. The minimum scavenge area is 93 mm^2 (0.144 in^2). Desired air pressure is introduced into the cavities adjacent to the test seals, and the air that leaks past the test seals in conveyed through a flowmeter from the air-oil separator to obtain a measure of seal performance.

Instrumentation incorporated in the test rig is listed in Table I. The location of the pertinent instrumentation is shown in Figure 1. All measurements were made with instruments using English units. These were then converted to SI units for reporting purposes.

An attempt was made to measure seal operating torque by recording the housing reaction torque, but this was discontinued because the seal and bearing torque was so small it was being absorbed in the lines going to and from the housing and in friction in the large support bearing.

Much of the test data are reported as a function of seal sliding speed; the corresponding shaft RPM for the self-acting face seal is as follows:

Sliding Speed		Shaft Speed
m/s	ft/sec	rpm
61	200	18,200
91	300	27,300
122	400	36,400
152	500	45,500
183	600	54,600
213	700	63,700

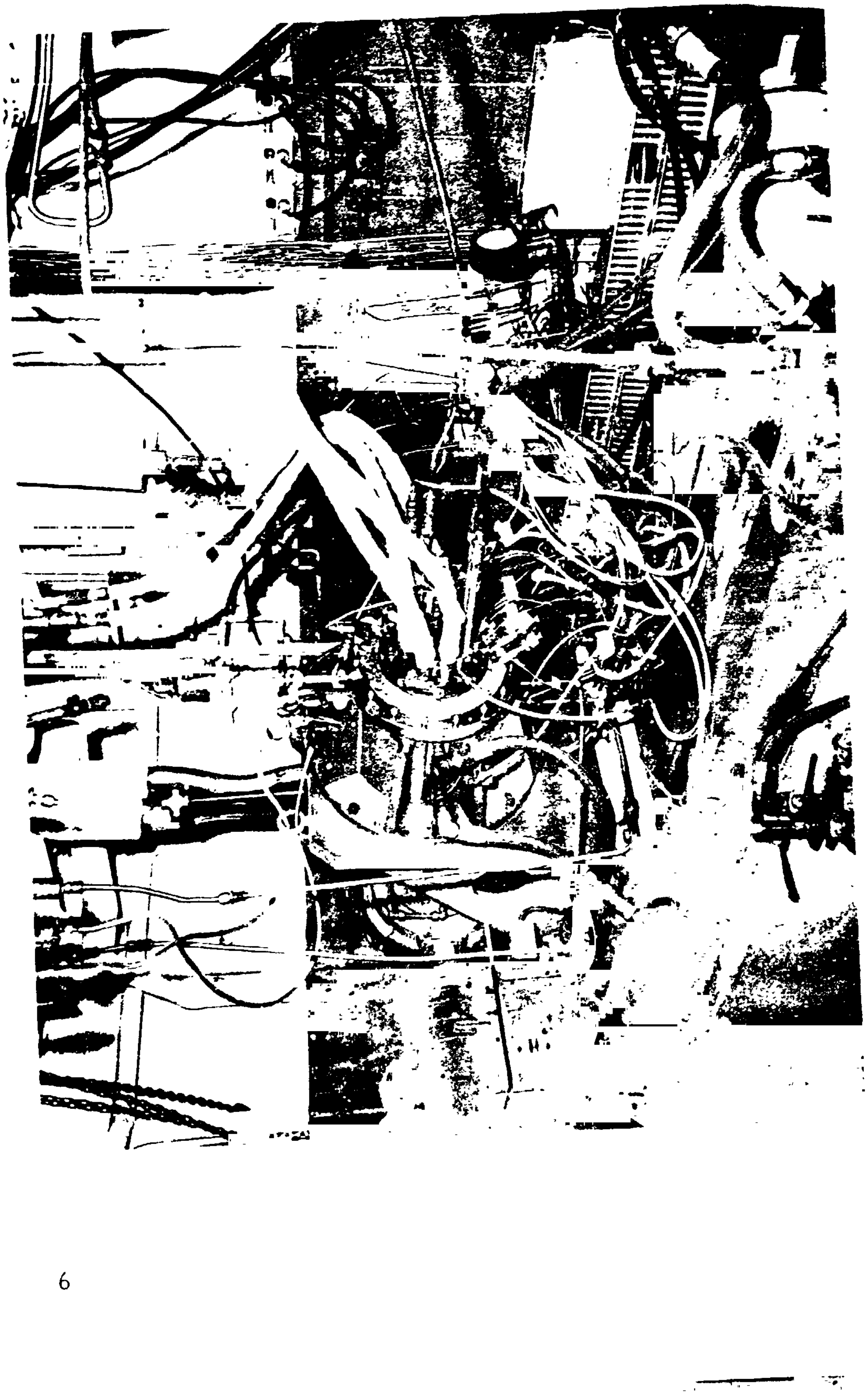

Figure 2. Test Rig Installation.

TABLE I. INSTRUMENTATION PLAN

Parameter To Be Measured	Sensing Device	Location	Corresponding Number in Figure 1
Shaft Speed	Magnetic pickup	Steam turbine shaft	9
Air Pressure	Gage	Fwd wheel cavity	10
	Gage	Fwd seal cavity	13
	Gage	Aft seal cavity	4
Air Temperature	Thermocouple	Fwd wheel cavity	11
	Thermocouple	Fwd seal cavity	12
	Thermocouple	Aft seal cavity	5
Seal Air Leakage	Glass tube rotameter	Scavenge air-oil mixture is passed through a static separator and the dry airflow is passed through the flowmeter	8
Oil Temperature	Thermocouple	Oil feed line	3
	Thermocouple	Scavenge line	8
Oil Flow	Glass tube rotameter	Oil feed line	3
Oil Pressure	Gage	Oil feed line	3
Bearing Cavity Pressure	Gage	Within bearing cavity	7
Scavenge Pressure	Gage	Scavenge line	8
Shaft Torque (reaction torque measured)	Strain gage	Beam assembly	2
Seal Temperature	Thermocouple	Seal case or carbon	6
Vibration	Velocity pickup		1
Chips	Chip detector	Scavenge line	8

EVALUATION OF CONVENTIONAL AND ADVANCED SEALS

Conventional Rotating Ring Seal

Design

The rotating ring seal (Figure 3) is essentially a close clearance labyrinth that is free to rotate in the seal case. The rotating ring sealing element is composed of a carbon ring shrunk into a steel retaining band. The retaining band is used to control the expansion rate of the composite ring and to reinforce it against rotational stress.

The carbon-steel composite ring is designed to have a coefficient of thermal expansion similar to that of the seal runner. The purpose of matching thermal expansion characteristics is to hold a temperature-constant clearance between the runner outside diameter and the carbon inside diameter.

The carbon-steel composite ring is shaft driven (by friction) and is designed to rotate at a speed less than shaft speed. The expansion of the composite ring with speed is utilized to provide a minimum air leakage gap at all operating conditions. If the gap tends to increase, the driving torque decreases and the ring speed decreases. The opposite occurs if the gap decreases: the driving torque increases, the ring speed increases. The seal, therefore, is designed to be self-regulating.

The rotating ring configuration used in the test program is shown in Figure 3. Seal materials and critical dimensions are listed. Seal components are shown in Figure 4.

For the test program, the forward seal position was built with a static diametral gap of 0.0610 mm (0.0024 in.) and the aft seal with a static diametral gap of 0.1346 mm (0.0053 in.).

Test Results

Five tests were conducted, each test covering a range of speeds and air pressures at ambient temperature. Test data are shown in Table II, which lists test conditions and resulting airflows, bearing cavity pressures, and seal temperatures. Seal temperature was measured at the location shown in Figure 3. Only the aft seal was temperature instrumented.

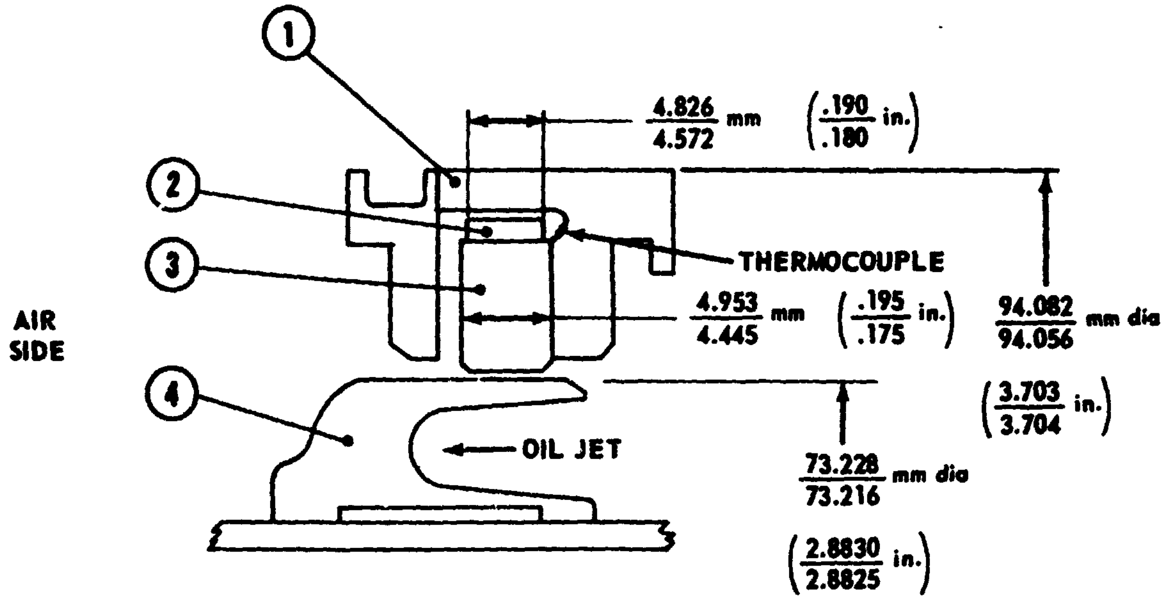

1. SEAL CASE	AMS 5610
2. RETAINING BAND	431 SST
3. CARBON RING	HIGH-TEMPERATURE CARBON
4. RUNNER	AMS 6382 CHROME PLATE PER AMS 2406

INTERFERENCE FIT BETWEEN RETAINING BAND AND CARBON RING $\frac{.356}{.305}$ mm $\left(\frac{.014}{.012}\text{ in.}\right)$

Figure 3. Rotating Ring Seal.

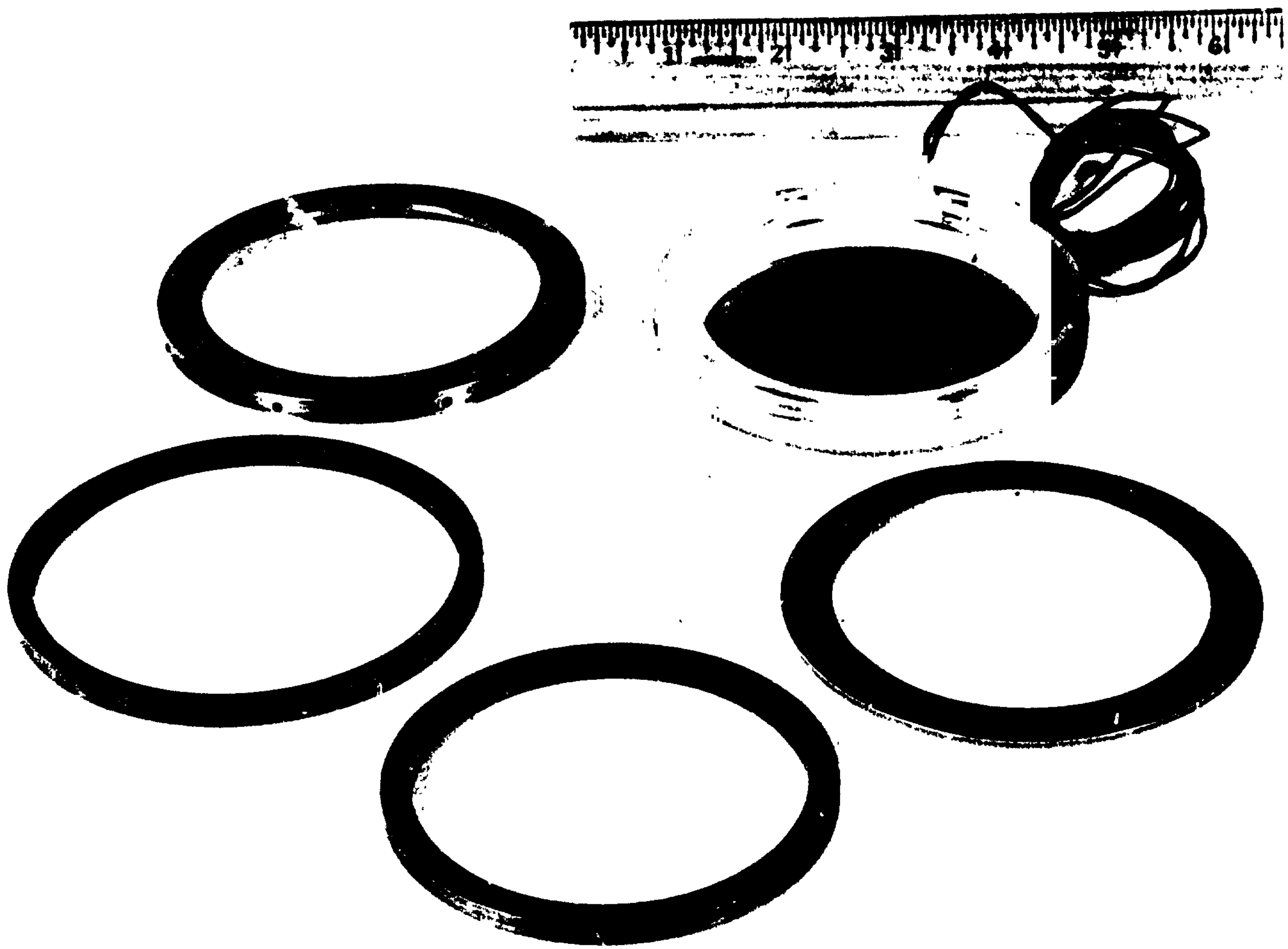

Figure 4. Rotating Ring Components.

TABLE II . ROTATING RING SEAL TEST DATA

Test	Run	Speed (m/s)	Speed (ft/sec)	Air Pressure (N/cm²)	Air Pressure (psia)	Cavity Pressure (N/cm²)	Cavity Pressure (psia)	Airflow (Two Seals) (kg/s)	Airflow (Two Seals) (scfm)	Airflow (Two Seals) (lb/sec)	Seal Temperature (K)	Seal Temperature (°F)
I	1	61	200	30.8	44.7	20.4	29.7	.011	18.5	.024	-	-
	2	91	300	30.8	44.7	19.8	28.7	.010	16.5	.021	352	175
	3	61	200	46	66.7	26.7	38.7	-	-	-	363	195
	4	91	300	46.7	67.7	26.0	37.7	-	-	-	367	203
	5	61	200	79.1	114.7	36.4	52.7	.028	48	.061	377	220
	6	91	300	79.1	114.7	35.6	51.7	.025	43.5	.055	386	235
II	7	61	200	34.3	49.7	26.7	38.7	.014	25	.032	322	120
	8	91	300	34.3	49.7	26	37.7	.013	23	.029	337	145
	9	122	400	34.3	49.7	24.6	35.7	.012	20	.025	363	195
	10	61	200	55	79.7	37.8	54.7	.027	47.5	.061	339	150
	11	91	300	55	79.7	36.4	52.7	.025	43	.055	361	190
	12	122	400	55	79.7	34.3	49.7	.021	37	.047	368	205
	13	61	200	73.6	106.7	48.1	69.7	.038	65	.083	361	190
	14	91	300	73.6	106.7	46.7	67.7	.036	60.5	.077	363	195
	15	122	400	77.7	112.7	45.3	65.7	.032	56	.071	371	210
III	16	61	200	34.3	49.7	24.6	32.7	.014	23.5	.030	300	80
	17	91	300	34.3	49.7	22.6	32.7	.011	18.5	.024	337	145
	18	122	400	34.3	49.7	20.5	29.7	.009	15	.019	350	170
	19	152	500	34.3	49.7	18.4	26.7	.006	11	.014	366	200
	20	61	200	55	79.7	30.8	44.7	.023	40	.051	333	140
	21	91	300	55	79.7	29.5	42.7	.019	33.5	.043	344	160
	22	122	400	55	79.7	27.4	39.7	.016	28	.036	361	190
	23	152	500	55	79.7	23.2	33.7	.011	19.5	.025	375	215
	24	61	200	78.4	113.7	39.2	56.7	-	-	-	361	190
	25	91	300	79.1	114.7	39.2	56.7	-	-	-	363	195
	26	122	400	79.1	114.7	36.4	52.7	-	-	-	366	200
	27	152	500	79.1	114.7	30.8	44.7	-	-	-	378	220
IV	28	122	400	34.3	49.7	19.8	28.7	.010	16.5	.021	339	150
	29	152	500	34.3	49.7	18.4	26.7	.006	11	.014	361	190
	30	183	600	34.3	49.7	15.[illegible]	22.7	.003	5.5	.007	388	240
	31	122	400	55	79.7	25.[illegible]	36.7	.016	27	.034	339	150
	32	152	500	55.7	80.7	22.[illegible]	32.7	.012	20	.025	361	190
	33	183	600	55	79.7	19.1	27.7	.007	12	.015	392	245
	34	122	400	77.7	112.7	34.3	49.7	.024	42	.054	366	200
	35	152	500	79.1	114.7	30.8	44.7	.016	28	.036	375	215
	36	183	600	79.1	114.7	23.9	34.7	.011	19	.024	399	260
	37	122	400	103.2	149.7	42.6	61.7	.034	59.5	.076	366	200
	38	152	500	103.2	149.7	37.8	54.7	.025	43	.055	388	240
	39	183	600	103.2	149.7	30.8	44.7	.013	23	.029	399	260
V	40	61	200	34.3	49.7	21.9	31.7	.013	23	.029	344	160
	41	91	300	34.3	49.7	20.6	29.7	.011	18.5	.024	358	185
	42	122	400	34.3	49.7	19.8	28.7	.009	15	.019	368	205
	43	152	500	34.3	49.7	18.4	26.7	.007	12	.015	385	235
	44	183	600	35	50.7	15.7	22.7	.003	6	.008	399	260
	45	213	700	35	50.7	14.3	20.7	.001	2.5	.003	428	315
	46	61	200	55	79.7	32.2	46.7	.023	40	.051	338	145
	47	91	300	55	79.7	30.8	44.7	.020	34	.043	341	155
	48	122	400	55	79.7	28	40.7	.016	28	.036	358	185
	49	152	500	55	79.7	24.6	35.7	.011	19.5	.025	388	240
	50	183	600	55	79.7	20.6	29.7	.006	11	.014	410	280
	51	213	700	55	79.7	16.4	23.7	.002	4	.005	435	330
	52	91	300	77.7	112.7	39.2	56.7	.029	50	.064	361	190
	53	122	400	78.4	113.7	36.7	52.7	.025	44	.056	366	200
	54	152	500	79.1	114.7	30.8	44.7	.019	33.5	.043	375	215
	55	183	600	79.1	114.7	25.3	36.7	.011	19	.024	394	250
	56	213	700	79.1	114.7	21.9	31.7	.008	13.5	.017	420	300
	57	122	400	103.2	149.7	50.9	73.7	-	-	-	358	185
	58	152	500	103.2	149.7	43.3	62.7	.029	50	.064	388	240
	59	183	600	103.2	149.7	35.7	51.7	.020	35	.045	405	270
	60	213	700	103.2	149.7	28.8	41.7	.013	23	.029	405	270
	61	183	600	123.9	179.7	41.9	60.7	-	-	-	382	230
	62	213	700	123.9	179.7	34.3	49.7	.019	33	.042	394	250
	63	183	600	148.2	214.7	47.4	68.7	.035	60	.076	382	230
	64	213	700	146.8	212.7	51.6	74.7	-	-	-	399	260

Carbon-runner static diametral gaps showing the carbon wear experienced after each test are listed in Table III.

It can be seen that the forward seal gap increased to 0.1245 mm (0.0049 in.) after test I. The aft seal did not change from the original gap of 0.1346 mm (0.0053 in.). These gaps did not change again until test V, where further wear occurred.

Test II values of airflow are high compared with those of the other test runs. This disparity was attributed to a distorted aft seal housing that was first used in this test. The distortion was due to a hole drilled in the housing to lead out the thermocouple wires, which raised a 0.0127 mm (0.0005 in.) bump on the axial face that contacts the carbon ring. The housing was lapped flat for subsequent operation.

Data for tests III through V are presented in Figure 5. As a design guide, airflow versus pressure differential is plotted for various operating gaps. The operating gaps were calculated at various speeds under the following assumptions:

1. Static gaps of 0.132 mm (0.0052 in.) were assumed for both seals.

2. The runner is treated as an unsupported thin ring.

3. The growth of the runner and the carbon-metal composite due to temperature are equal.

4. The composite ring does not rotate.

Runner growth due to speed and the resulting operational gap at each speed point are listed in Table IV.

During test V, substantial carbon wear occurred (Table III). This is why some points for the 0.005 mm (0.0002 in.) and 0.03 mm (0.0012 in.) gaps trail off from the straight lines shown in Figure 5. Wear was to be expected at the 213 m/s (700 ft/sec) point, since the calculated diametral operating gap closes to 0.005 mm (0.0002 in.).

The following traces were taken after each test:

1. Carbon axial flatness and roughness

2. Casing axial flatness and roughness

TABLE III. ROTATING RING SEAL TEST RESULTS--COMPARISON

	New	I	II	III	IV	V
Fwd Carbon ID (mm)	73.29170	73.35520	73.35520	73.35774	73.35774	73.43394
Fwd Runner OD (mm)	73.23074	73.23074	73.22820	73.23074	73.23074	73.21804
Diametral Gap (mm)	.06096	.12446	.12700	.12700	.12700	.21590
Fwd Carbon ID (in.)	2.8855	2.8880	2.8880	2.8881	2.8881	2.8911
Fwd Runner OD (in.)	2.8831	2.8831	2.8830	2.8831	2.8831	2.8826
Diametral Gap (in.)	.0024	.0049	.0050	.0050	.0050	.0085
Aft Carbon ID (mm)	73.36028	73.36028	73.36028	73.36028	73.37044	73.39076
Aft Runner OD (mm)	73.22566	73.22566	73.22312	73.22566	73.22566	73.22566
Diametral Gap (mm)	.13462	.13462	.13716	.13462	.14478	.16510
Aft Carbon ID (in.)	2.8882	2.8882	2.8882	2.8882	2.8886	2.8894
Aft Runner OD (in.)	2.8829	2.8829	2.8828	2.8829	2.8829	2.8829
Diametral Gap (in.)	.0053	.0053	.0054	.0053	.0057	.0065

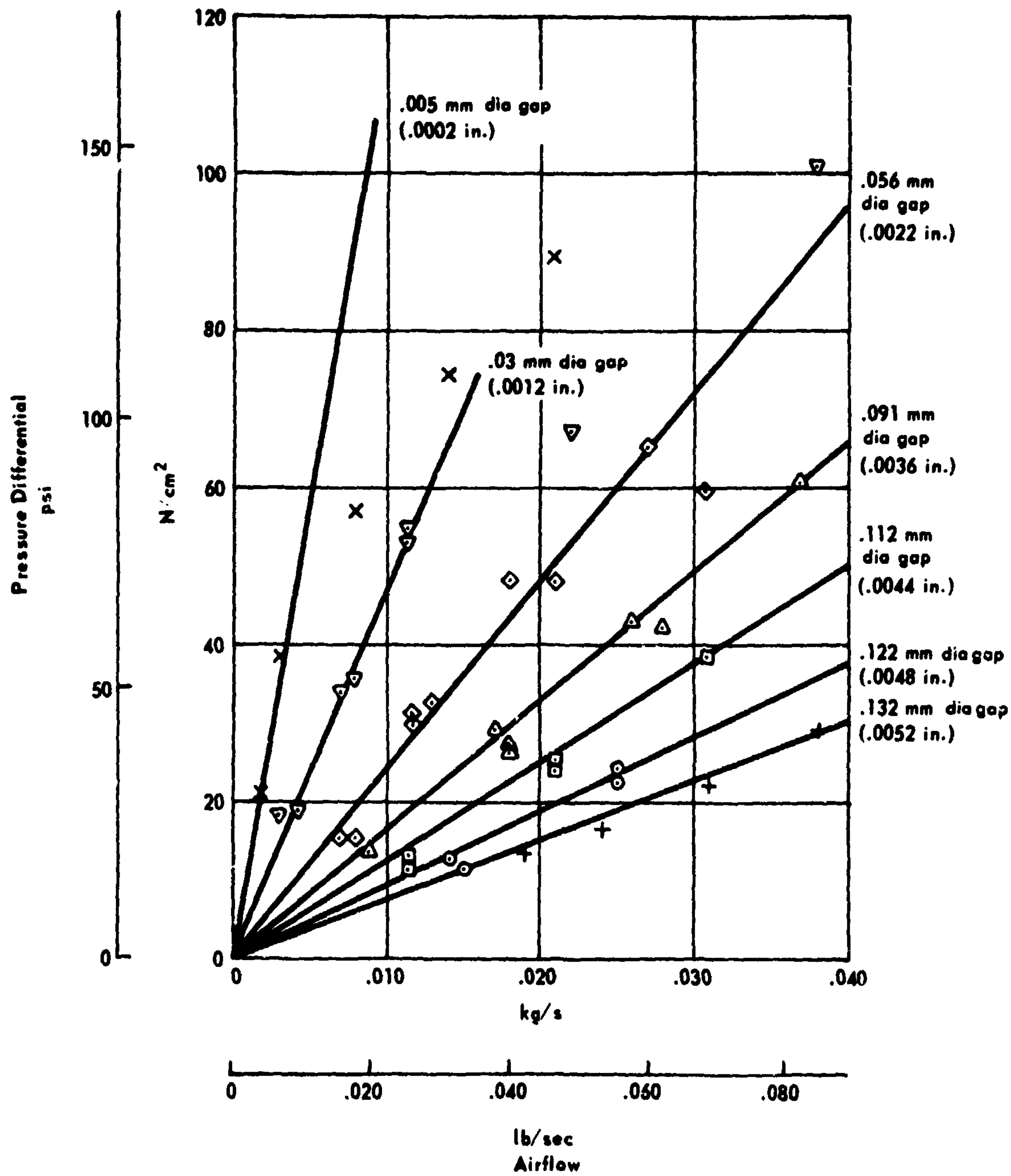

Figure 5. Airflow Through Two Rotating Ring Seals Versus Pressure Differential Between Air Side and Oil Side, Tests III Through V.

TABLE IV. OPERATING GAP AT SPEED					
Speed		Diametral Increase of Runner OD		Resulting Operating Gap	
(m/s)	(ft/sec)	(mm)	(in.)	(mm)	(in.)
0	0	0	0	.132	.0052
61	200	.01016	.0004	.122	.0048
91	300	.02032	.0008	.112	.0044
122	400	.04064	.0016	.091	.0036
152	500	.06604	.0026	.056	.0022
183	600	.09144	.0036	.030	.0012
213	700	.12700	.0050	.005	.0002

3. Runner roughness, waviness, and roundness

Inspection results of carbon flatness and roughness and runner roughness, waviness, and roundness are listed in Table V. Casing flatness, roughness and waviness did not change significantly during the test program. Typical values were:

Casing flatness	7.62 μm (0.0003 in.)
Casing roughness	0.127 μm (5 μin. AA)
Casing waviness	1.27 μm (0.00005 in.)

The carbon rings did not wear axially throughout the test program.

Charts showing the aft carbon axial sealing face condition following test V are shown in Figures 6 and 7. Forward runner condition after test V is shown in Figures 8 and 9. Both the forward and aft runners after testing are shown in Figure 10. Carbon deposits can be seen on the runners. Inspection revealed 0.038 mm (0.0005 in.) wear on the forward carbon.

Total oil flow to the bearing compartment was varied with speed as follows:

Shaft Speed		Oil Flow	
m/s	ft/sec	kg/hr	lb/hr
61	200	48	106
91	300	75	166
122	400	95	210
152	500	115	254
183	600	142	314
213	700	170	374

The bearing was fed by four 0.81 mm (0.032 in.) jets and each seal runner was cooled by one 0.81 mm (0.032 in.) jet. Oil-in temperature was 366 K (200°F). MIL-L-23699 oil was used.

Runs 1 - 15 were of 30-minute duration each. All succeeding runs were of 15-minute duration.

TABLE V. ROTATING RING SEAL INSPECTION DATA

	Test				
	I	II	III	IV	V
Fwd Carbon					
Flatness (μm)	6.35	5.84	4.32	5.84	3.05
(in.)	.00025	.00023	.00017	.00023	.00012
Roughness (μm)	.13	.18-.20	.20-.23	.15	.18-.20
(μ in. AA)	5	7-8	8-9	6	7-8
Aft Carbon					
Flatness (μm)	2.54	9.39	2.54	3.05	22.35
(in.)	.00010	.00037	.00010	.00012	.00088
Roughness (μm)		.15-.18	.18	.13	.53
(μ in. AA)		6-7	7	5	21
Fwd Runner					
Roundness (μm)		1.27	3.05	2.54	13.96
(in.)		.00005	.00012	.00010	.00055
Roughness (μm)	.25-.28	.30-.33	.25-.28	.25	.25-.28
(μ in. AA)	10-11	12-13	10-11	10	10-11
Waviness (μm)		1.14	1.52	1.01	1.19
(in.)		.000045	.000060	.000040	.00047
Aft Runner					
Roundness (μm)		5.58	8.88	5.08	2.54
(in.)		.00022	.00035	.00020	.00010
Roughness (μm)	.25-.28	.28-.30	.25-.28	.28-.30	.30
(μ in. AA)	10-11	11-12	10-11	11-12	12
Waviness (μm)		2.04	1.78	2.04	3.04
(in.)		.000080	.000070	.000080	.00011

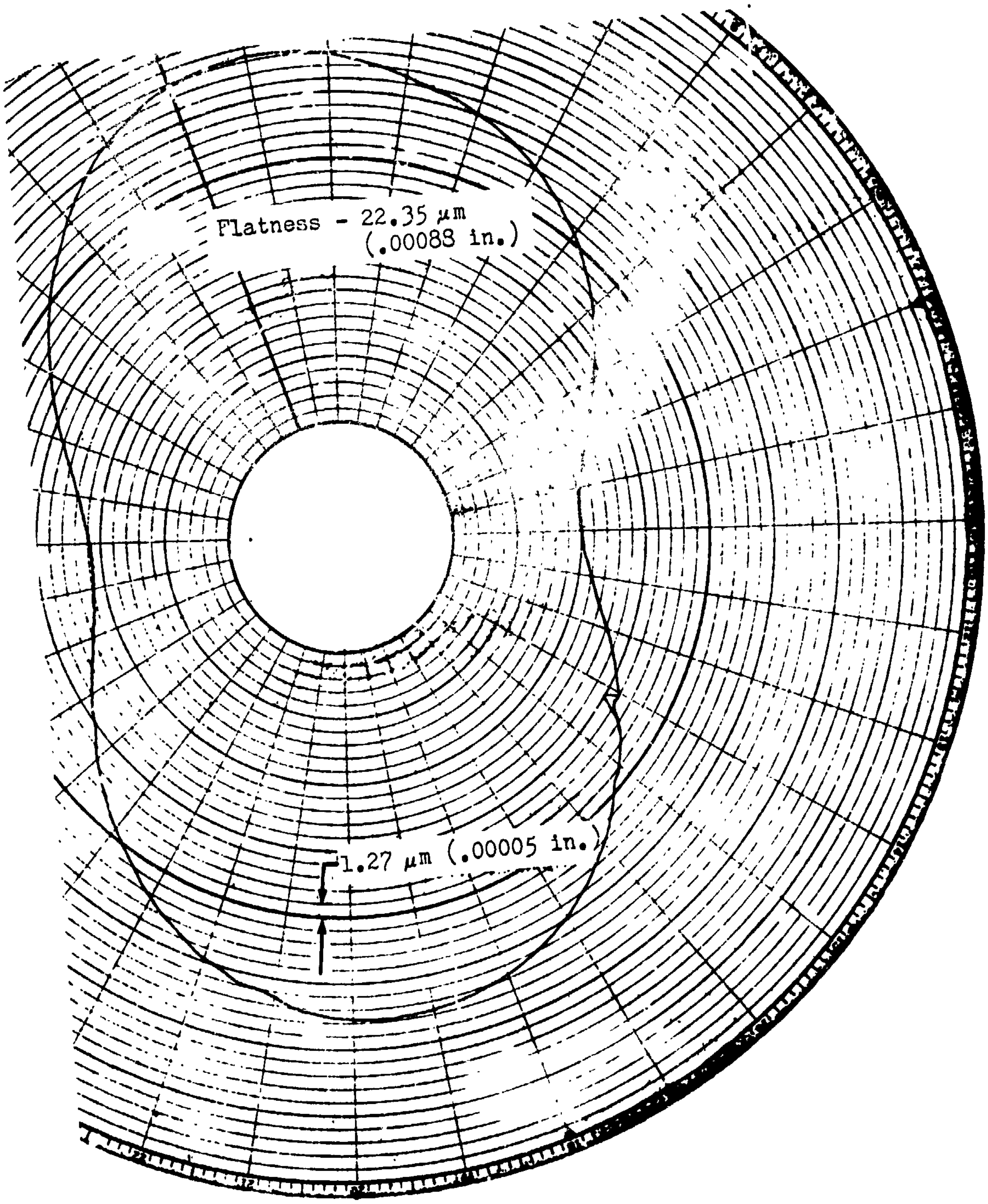

Figure 6. Aft Rotating Ring Seal--Flatness Trace of Axial Seal Face of Carbon Ring After Test V.

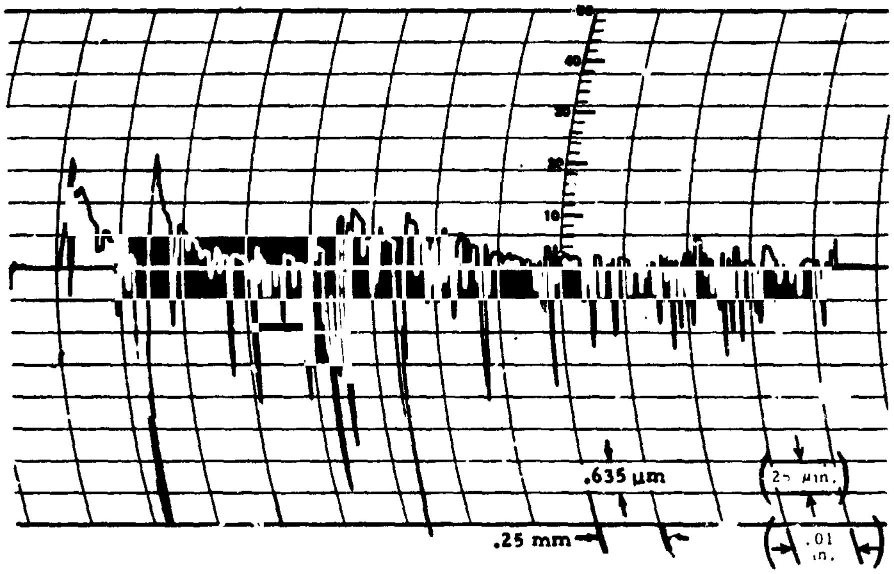

Figure 7. Aft Rotating Ring Seal--Roughness Trace of Axial Sealing Face of Carbon Ring After Test V.

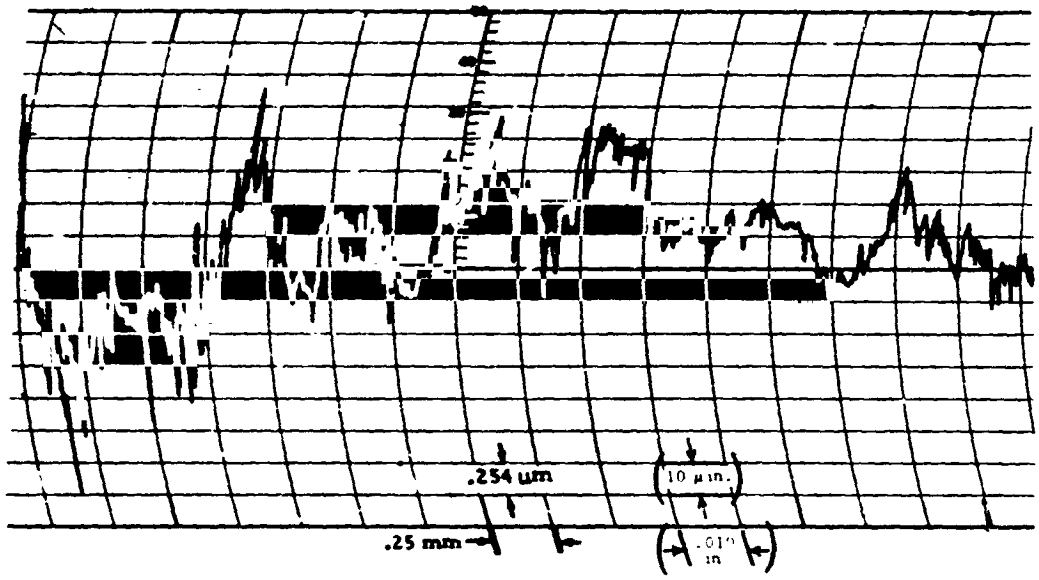

Figure 8   Forward Rotating Ring Seal--Trace of Runner Contact Area After Test V.

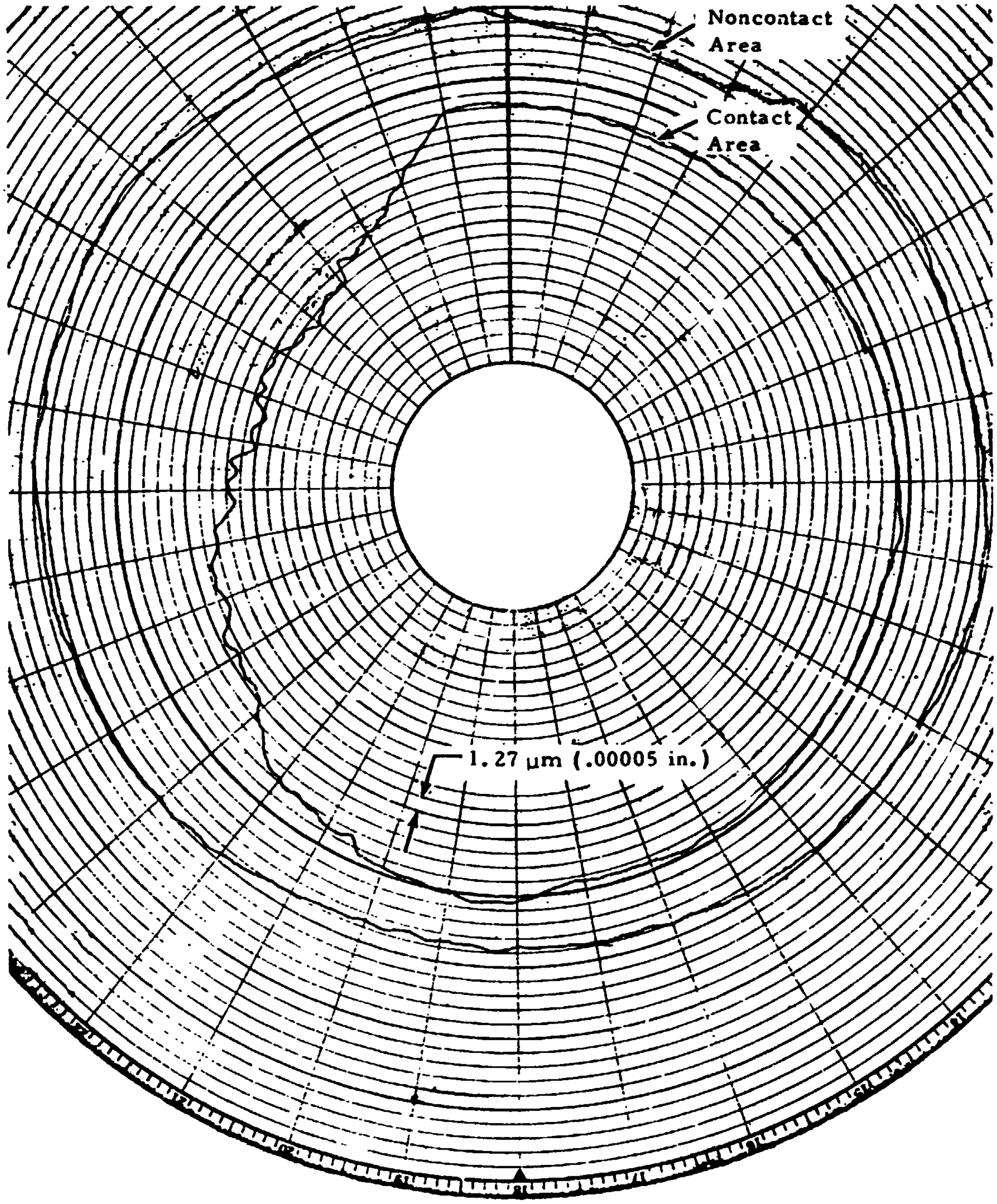

Figure 9 . Forward Rotating Ring Seal--Trace of Runner Roundness After Test V.

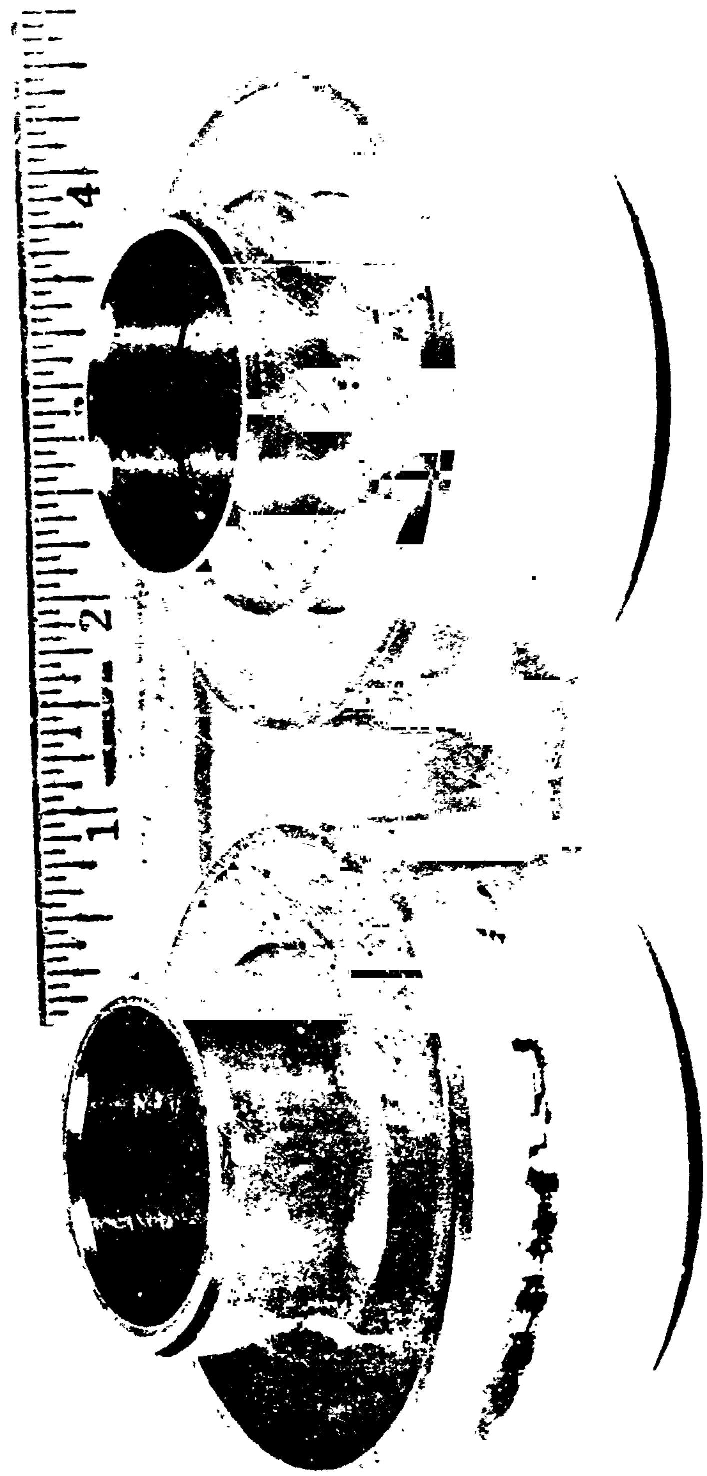

Figure 10. Rotating Ring Seal Runners After Test.

Circumferential Segmented Seal

Design

The circumferential segmented seal (Figure 11) is a carbon ring consisting of three 120-degree segments held together by a garter soring on the outside diameter. When the ring is installed on the runner, clearance between the adjacent ends of the segments allows a limited airflow into the bearing cavity. Design clearance, at each gap, is 0.229/0.305 mm (0.009/0.012 in.). During operation, if the carbon wears from shaft contact, the garter spring forces the segments radially inward. When the clearance between the adjacent carbon segment ends is zero, the ends butt up and the carbon inside diameter no longer contacts the runner. Approximately 0.127 mm (0.005 in.) of radial carbon wear will cause this condition. The seal then operates as a close clearance labyrinth. The minimum gap is formed at the maximum speed, pressure, and temperature conditions, where the runner is at its largest diameter.

The circumferential segmented seal configuration used in the test program is shown in Figure 11. Seal materials and critical dimensions are listed. Seal components are shown in Figure 12, and the seal assembly is shown in Figure 13.

Test Results

Five tests were conducted, each test covering a range of speeds and air pressures at ambient temperatures. Table VI lists test conditions and resulting airflows, bearing cavity pressures, and seal temperatures. Seal temperature was measured at the location shown in Figure 11. Only the aft seal was temperature instrumented.

Test I. - Disassembly of the seal following test I revealed that one forward seal carbon segment was cracked in two places. It was determined that the damage had occurred at assembly prior to testing when the forward seal was slipped over the runner. A larger lead-in chamfer on the forward runner was incorporated to correct the problem. The airflows in test I are high as a result of the cracked carbon element. Average radial wear on the carbon elements following test I was 0.0178 mm (0.0007 in.) on the forward seal and 0.0102 mm (0.0004 in.) on the aft seal. The cracked forward seal was replaced.

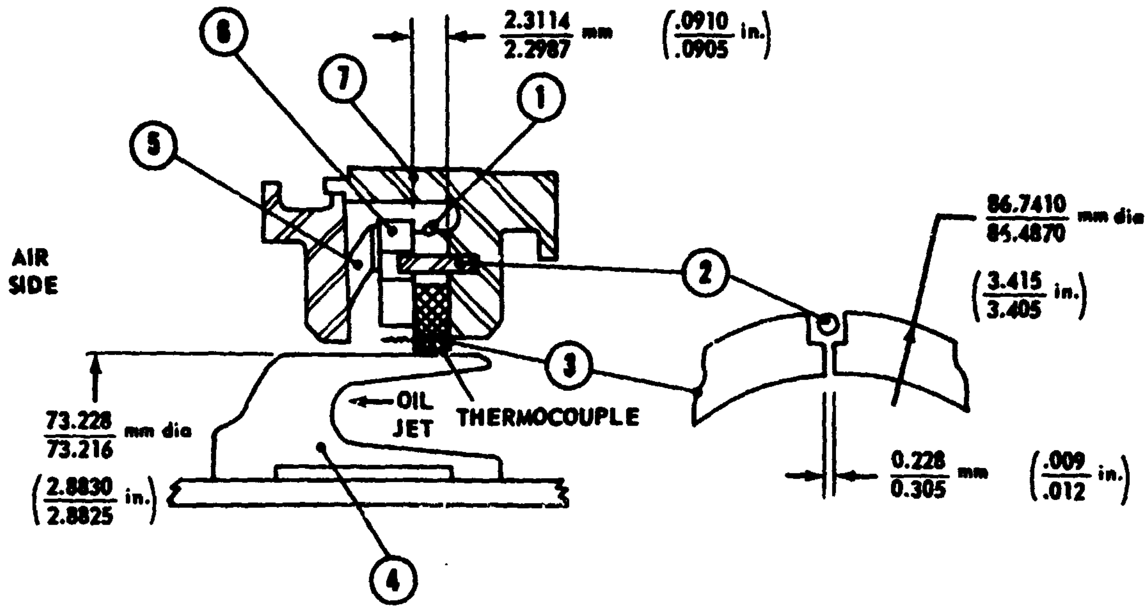

1. GARTER SPRING	AMS 5698 3.1 N LOAD (0.7 lb)
2. ANTIROTATION PIN	AMS 5610
3. CARBON SEGMENT	HIGH-TEMPERATURE CARBON
4. RUNNER	AMS 6382 FLAME SPRAYED WITH LCIC CHROME CARBIDE
5. WAVE SPRING	AMS 5542 16.9 N LOAD (3.8 lb)
6. SPACER	AMS 5610
7. SEAL CASE	AMS 5610

Figure 11. Circumferential Segmented Seal.

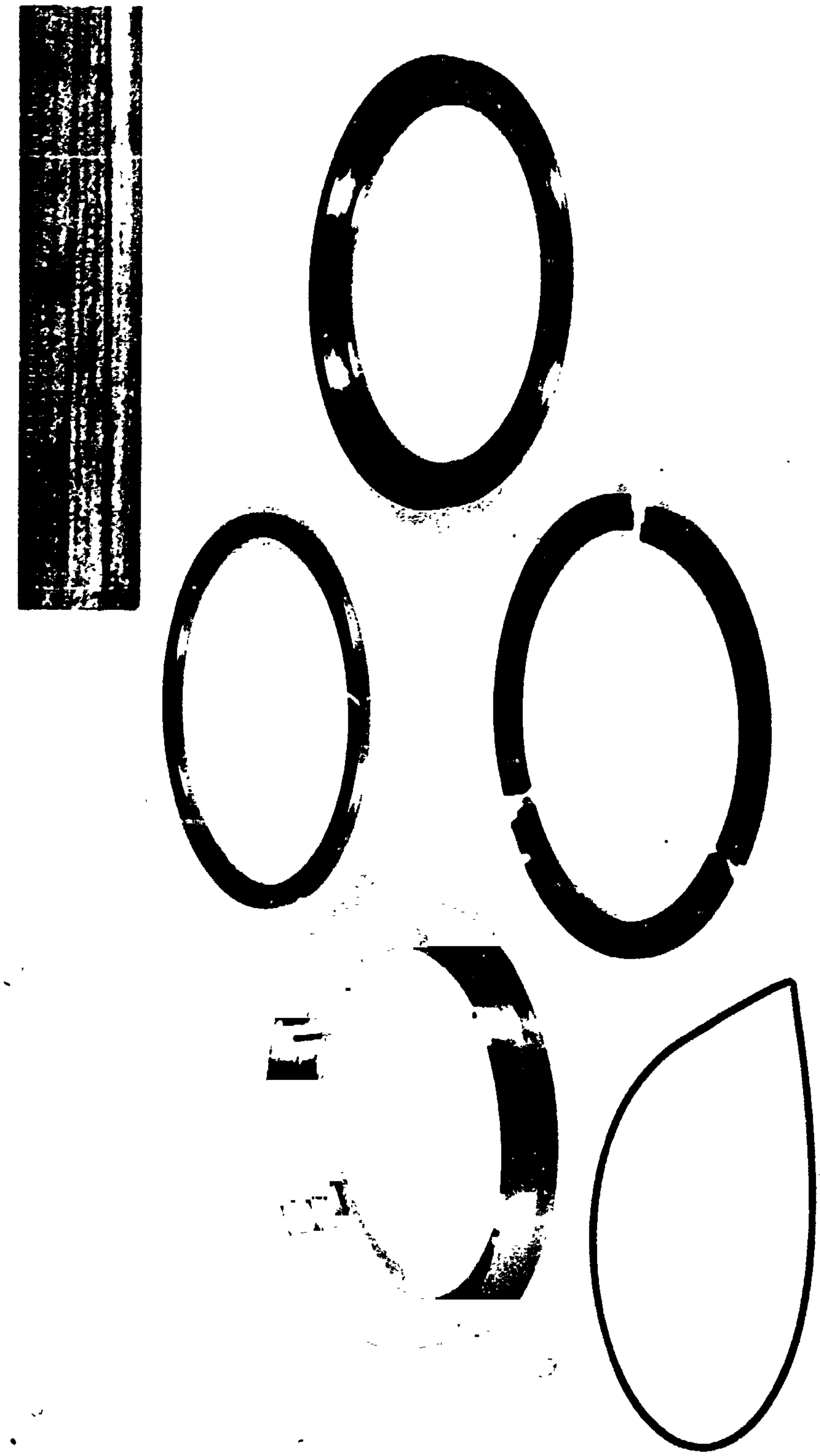

Figure 12. Circumferential Segmented Seal Components.

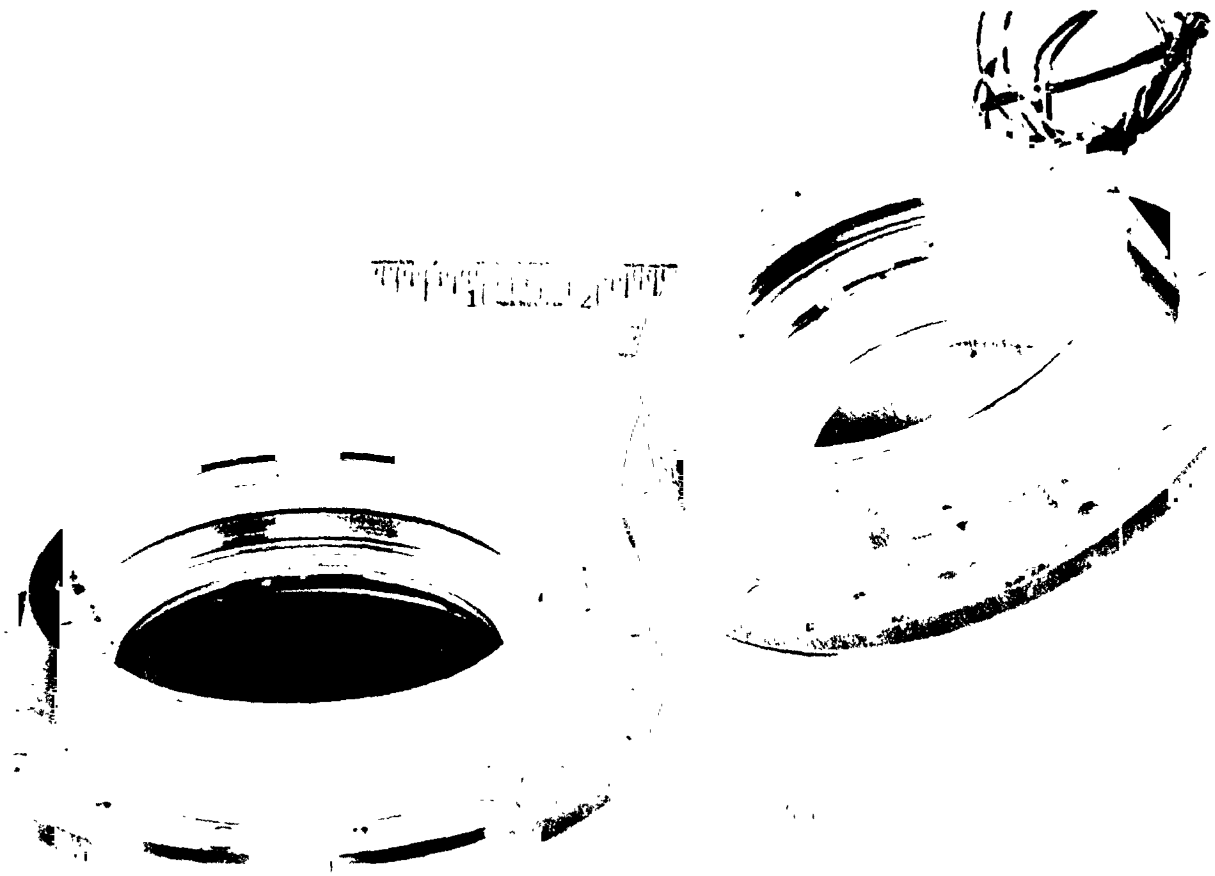

Figure 13. Circumferential Segmented Seal Assembly and Instrumentation.

TABLE VI. CIRCUMFERENTIAL SEGMENTED SEAL TEST DATA												
Test	Run	Speed (m/s)	Speed (ft/sec)	Air Pressure (N/cm²)	Air Pressure (psia)	Cavity Pressure (N/cm²)	Cavity Pressure (psia)	Airflow (Two Seals) (kg/s)	Airflow (Two Seals) (scfm)	Airflow (Two Seals) (lb/sec)	Seal Temperature (K)	Seal Temperature (°F)
I	1	61	200	34.3	49.7	17.0	24.7	.006	10	.013	378	220
	2	91	300	34.3	49.7	17.0	24.7	.006	11	.014	405	270
	3	61	200	55	79.7	19.8	28.7	.009	16	.020	399	260
	4	91	300	55	79.7	19.8	28.7	.009	15	.019	407	275
	5	61	200	79.1	114.7	22.6	32.7	.013	22.5	.029	433	320
	6	91	300	79.1	114.7	24.6	35.7	.013	22	.028	455	360
II	7	61	200	34.3	49.7	12.5	18.2	.002	3.4	.004	352	175
	8	91	300	34.3	49.7	12.5	18.2	.002	3.3	.004	389	240
	9	122	400	34.3	49.7	12.9	18.7	.002	3.2	.004	407	275
	10	61	200	55	79.7	12.9	18.7	.003	5.9	.008	383	230
	11	91	300	55	79.7	12.9	18.7	.003	5.9	.008	408	285
	12	122	400	55	79.7	13.6	19.7	.003	5.6	.007	425	305
	13	61	200	79.1	114.7	28.8	41.7	.035	60	.076	405	270
	14	91	300	79.1	114.7	34.3	49.7	.034	58	.074	410	280
	15	122	400	79.1	114.7	34.3	49.7	.033	57	.073	425	305
III	16	61	200	34.3	49.7	11.9	17.2	.003	4.8	.006	378	220
	17	91	300	34.3	49.7	12.2	17.7	.003	4.4	.006	383	230
	18	122	400	34.3	49.7	12.5	18.2	.003	4.5	.006	410	280
	19	61	200	55	79.7	13.2	19.2	.004	7.5	.010	383	230
	20	91	300	55	79.7	13.6	19.7	.004	7.3	.009	415	285
	21	122	400	55	79.7	14.3	20.7	.004	7.5	.010	433	320
	22	61	200	79.1	114.7	13.9	20.2	.006	10.2	.013	422	300
	23	91	300	79.1	114.7	15.0	21.7	.006	10.5	.013	472	390
	24	122	400	79.1	114.7	15.6	22.7	.006	10.7	.014	483	410
	25	61	200	34.3	49.7	12.9	18.7	.003	5.0	.006	385	230
	26	91	300	34.3	49.7	13.2	19.2	.003	4.7	.006	399	260
	27	122	400	34.3	49.7	13.2	19.2	.003	5.0	.006	415	285
	28	152	500	34.3	49.7	13.6	19.7	.003	4.8	.006	433	320
	29	61	200	55	79.7	13.2	19.2	.004	7.5	.010	399	260
	30	91	300	55	79.7	13.6	19.7	.004	7.4	.009	416	290
	31	122	400	55	79.7	14.3	20.7	.004	7.3	.009	427	310
	32	152	500	55	79.7	14.6	21.2	.004	7.3	.009	444	340
	33	61	200	76.3	110.7	13.9	20.2	.005	8.3	.011	428	315
	34	91	300	76.3	110.7	14.6	21.2	.006	9.7	.012	433	320
	35	122	400	77.0	111.7	15.3	22.2	.006	9.8	.012	444	340
	36	152	500	77.7	112.7	16.0	23.2	.006	10.0	.013	480	405
IV	37	61	200	34.3	49.7	12.2	17.7	.002	3	.004	-	-
	38	122	400	34.3	49.7	12.9	18.7	.002	3.2	.004	-	-
	39	152	500	34.3	49.7	12.9	18.7	.002	3.1	.004	-	-
	40	183	600	34.3	49.7	13.6	19.7	.002	3.4	.004	-	-
	41	152	500	55	79.7	13.9	20.2	.003	5.4	.007	-	-
	42	183	600	55	79.7	14.3	20.7	.003	4.7	.006	-	-
	43	122	400	79.1	114.7	17.4	25.2	.008	14.5	.018	-	-
	44	152	500	79.1	114.7	19.8	28.7	.009	16.0	.020	-	-
	45	183	600	79.1	114.7	19.8	28.7	.008	14.0	.018	-	-
V	46	122	400	55	79.7	16.3	23.7	.005	8.4	.011	-	-
	47	152	500	55	79.7	17.0	24.7	.005	9	.011	-	-
	48	183	600	55	79.7	17.4	25.2	.005	8.4	.011	-	-
	49	213	700	55	79.7	18.4	26.7	.004	7.7	.010	-	-
	50	122	400	79.1	114.7	24.6	35.7	.012	21.5	.027	-	-
	51	152	500	79.1	114.7	22.6	32.7	.011	19	.024	-	-
	52	183	600	79.1	114.7	24.6	35.7	.012	20	.025	-	-
	53	213	700	79.1	114.7	25.3	36.7	.011	18.5	.024	-	-
	54	152	500	103	149.7	46	66.7	.030	52.5	.067	-	-
	55	183	600	103	149.7	36.3	52.7	.020	35	.045	-	-
	56	213	700	103	149.7	39.7	57.7	-	-	-	-	-
	57	183	600	55	79.7	32.2	46.7	.017	30	.038	-	-
	58	152	500	55	79.7	33.5	48.7	.020	35	.045	-	-
	59	122	400	55	79.7	35.6	51.7	.025	43	.055	-	-
	60	91	300	55	79.7	37	53.7	.028	48	.061	-	-
	61	61	200	55	79.7	37.7	54.7	.029	50.5	.066	-	-
	62	61	200	34.3	49.7	27.4	39.7	.019	32.5	.041	-	-
	63	91	300	34.3	49.7	27.4	39.7	.016	28.5	.036	-	-
	64	122	400	34.3	49.7	26.7	38.7	.014	24	.031	-	-
	65	152	500	34.3	49.7	25.3	36.7	.012	21	.027	-	-
	66	183	600	34.3	49.7	24.6	35.7	.010	16.5	.021	-	-
	67	213	700	34.3	49.7	20.5	29.7	.006	10.2	.013	-	-

Test II. - During run 13 of test II (see Table VI), airflow was noted to increase drastically. The test was aborted, and disassembly revealed that an air leak had developed in the bearing package scavenge line. The leak was repaired, and a static check was made with dummy seals to ensure that no airflow entered the bearing cavity other than through the shaft seals.

Test III. - Test III data were consistent, and they were representative of circumferential segmented seals that are not worn out. Test III data for airflow through the seals versus the pressure differential between the air and oil sides for various speeds are shown in Figure 14. It can be seen that speed does not affect the amount of airflow. Carbon temperature versus pressure differential is shown in Figure 15.

Average radial carbon wear of 0.005 mm (0.0002 in.) on both the forward and aft seal was measured for test III.

Test IV. - Prior to test IV, the temperature instrumentation on the aft seal was damaged, and new instrumentation was installed. Static checks revealed that reinstrumentation caused the seal to hang up and allow large airflows, so the aft instrumented seal was replaced by a new seal that was not instrumented.

During run 43 of test IV, the airflow increased sharply. Upon disassembly, the new aft seal was found to have worn out to 0.17 mm (0.0067 in.) average radial wear, and it had worn a 0.025 mm (0.001 in.) groove in the runner. The forward seal average radial wear was 0.018 mm (0.0007 in.) in test IV. For further testing, the aft and forward seals were shimmed so as to run on an unworn portion of the runner.

Test V. - The objective of test V was to wear out the forward seal and obtain an airflow plot for both seals operating as labyrinths.

Measurements following test V revealed that the forward seal had worn 0.150 mm (0.0059 in.) during test V and had a total average radial wear of 0.170 mm (0.0069 in.). In test V the forward seal wore a 0.051 mm (0.002 in.) groove in the runner.

The aft seal wore an additional 0.06 mm (0.0023 in.) and again wore a 0.025 mm (0.001 in.) groove in the runner.

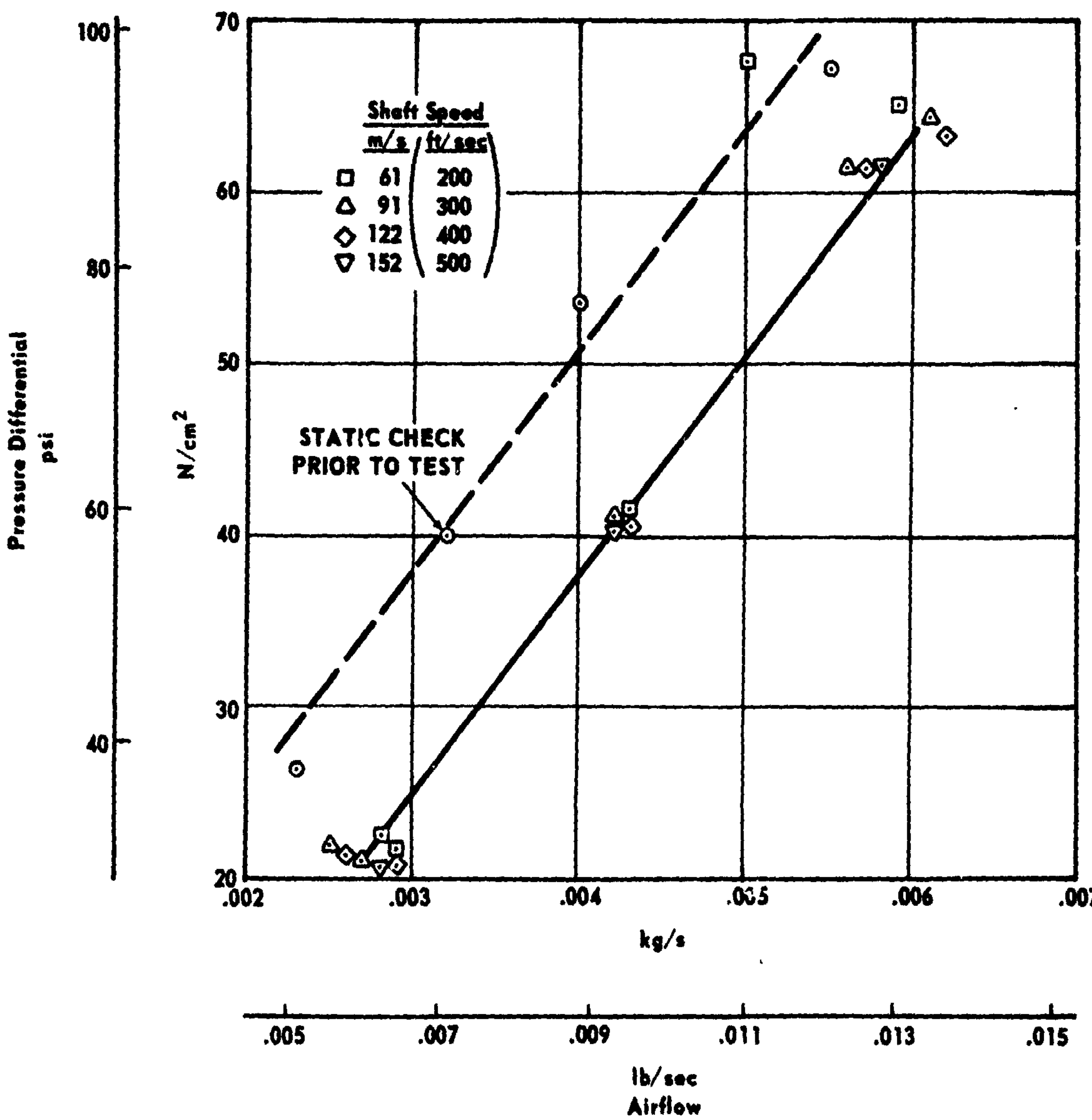

Figure 14. Airflow Through Two Circumferential Segmented Seals Versus Pressure Differential Between Air Side and Oil Side, Test III.

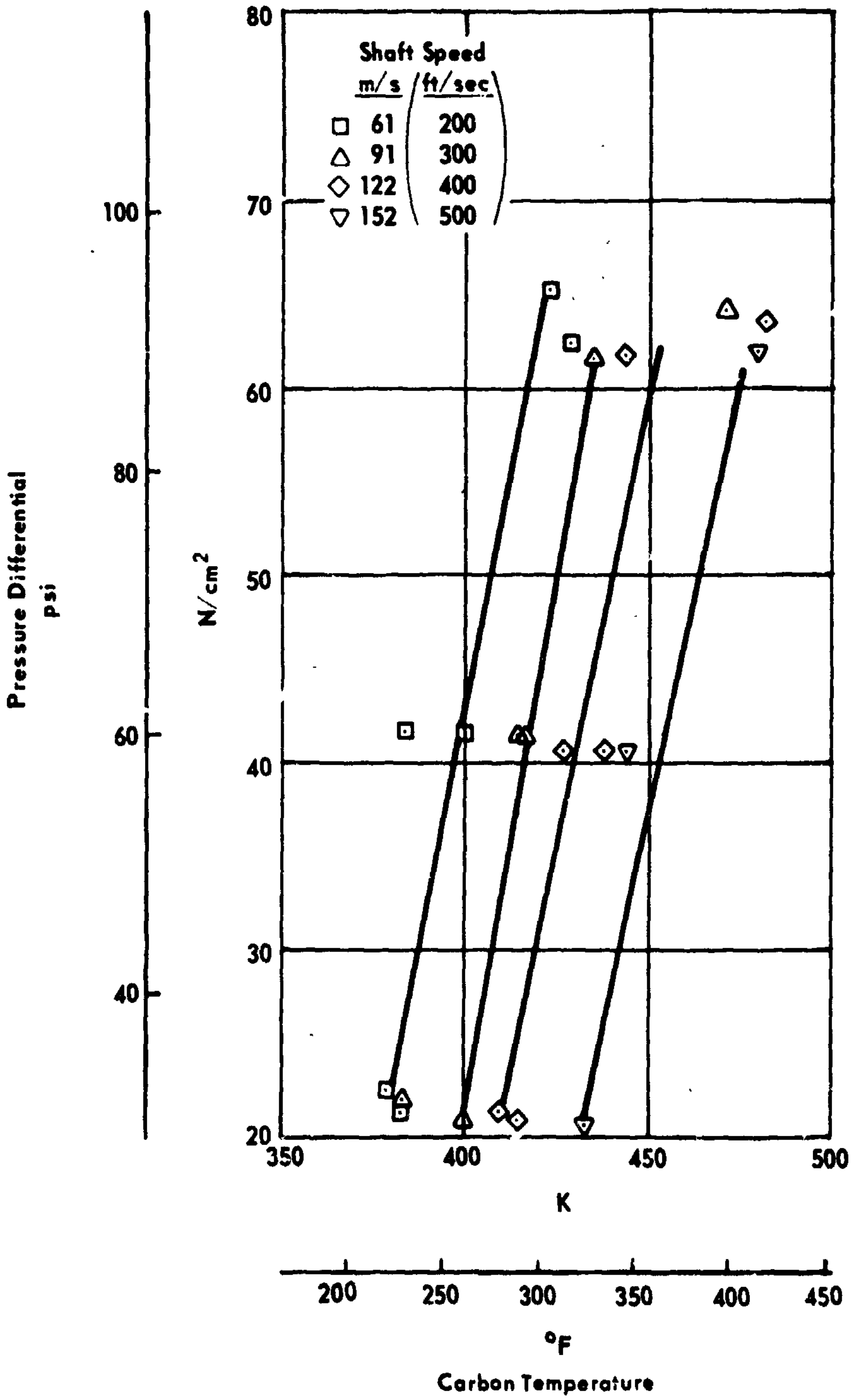

Figure 15. Circumferential Segmented Seal Temperature Versus Pressure Differential Between Air Side and Oil Side, Test III.

Airflow versus pressure differential for test V is shown in Figure 16. The curves showing the least pressure differential reflect the two worn out seals as the airflow was speed sensitive. As the runner grows with speed, the airflow decreases. The upper points reflect data taken early in the test before the forward seal wore out.

The following traces were taken after each test:

1. Casing axial flatness, roughness, and waviness

2. Runner roughness, waviness, and roundness

Inspection results of runner roundness, roughness, and waviness are listed in Table VII. Casing flatness, roughness, and waviness did not change significantly during the test program. Typical values were:

Casing flatness	50.8 μm	(0.002 in.)
Casing roughness	0.304 μm	(12 μin. AA)
Casing waviness	5.08 μm	(0.0002 in.)

A chart showing the condition of the forward runner after test V is presented in Figure 17. Runner runout was measured at assembly and was found to be 0.015 mm (0.0006 in.) on the forward runner and 0.038 mm (0.0015 in.) on the aft runner.

Total oil flow to the bearing compartment was varied with speed as follows:

Shaft Speed		Oil Flow	
m/s	ft/sec	kg/hr	lb/hr
61	200	48	106
91	300	75	166
122	400	95	210
152	500	115	254
183	600	142	314
213	700	170	374

The bearing was fed by four 0.81 mm (0.032 in.) jets and each seal runner was cooled by one 0.81 mm (0.032 in.) jet. Oil-in temperature was 366 K (200°F). MIL-L-23699 oil was used.

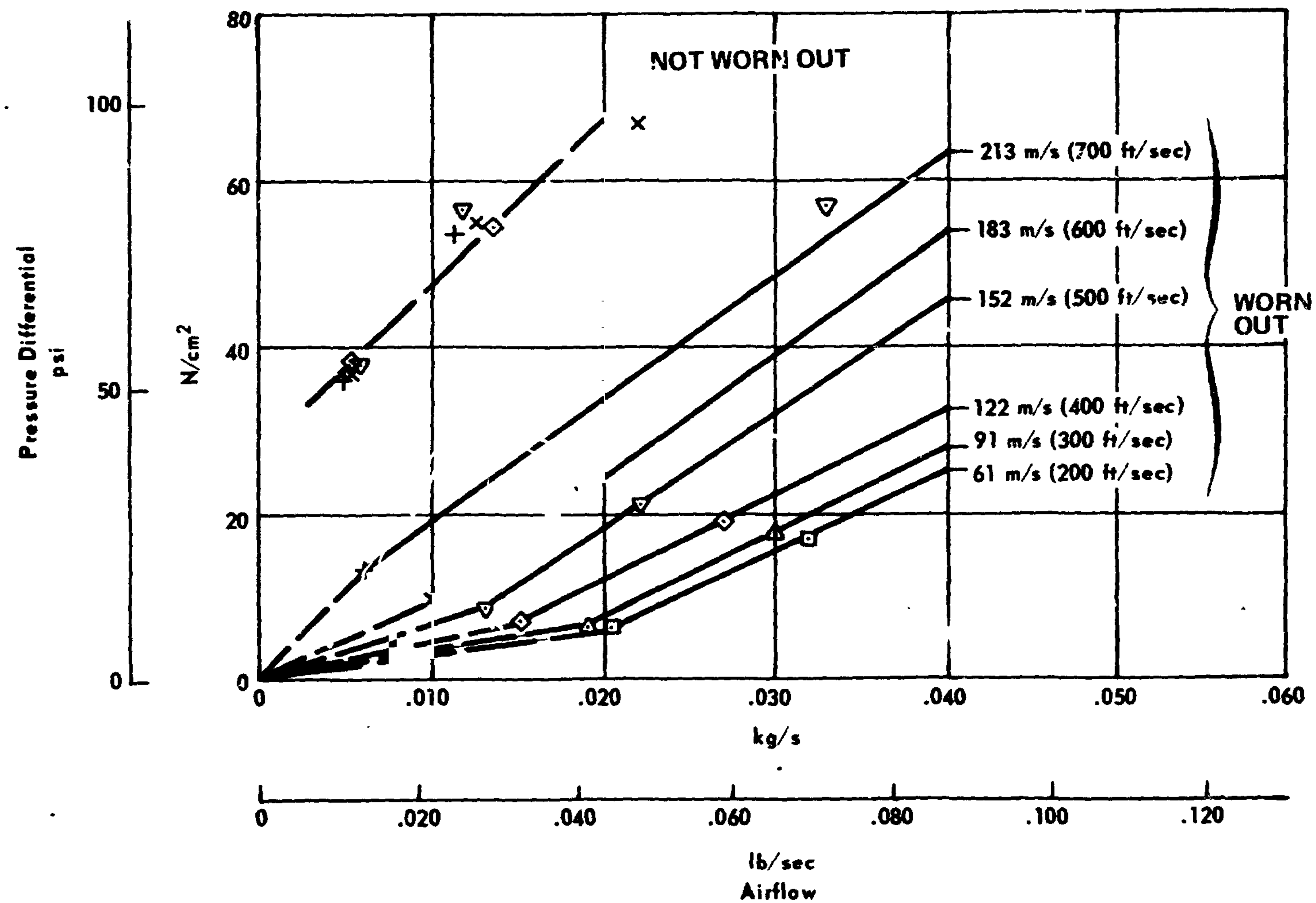

Figure 16. Airflow Through Two Circumferential Segmented Seals Versus Pressure Differential Between Air Side and Oil Side, Test V.

TABLE VII. CIRCUMFERENTIAL SEGMENTED SEAL INSPECTION DATA

	New	After Test I	II	III	IV	V
Fwd Runner						
Roundness (μm)	2.54	2.54	2.54	2.54	2.54	50.8
(in.)	.0001	.0001	.0001	.0001	.0001	.002
Roughness (μm)		.381	.15	.15	.18	.51
(μin. AA)	16	15	6	6	7	20
Waviness (μm)	2.54	2.54	2.54	.13	.18	50.8
(in.)	.0001	.0001	.0001	.00005	.00007	.002
Aft Runner						
Roundness (μm)	1.27	1.01	5.08	3.81	3.04	2.80
(in.)	.00005	.00004	.0002	.00015	.0012	.0011
Roughness (μm)	.36	.30	.15	.08	.41	.18
(μin. AA)	14	12	6	3	16	7
Waviness (μm)	2.54	2.54	.51	.15	24.2	25.4
(in.)	.0001	.0001	.00002	.00006	.00095	.001

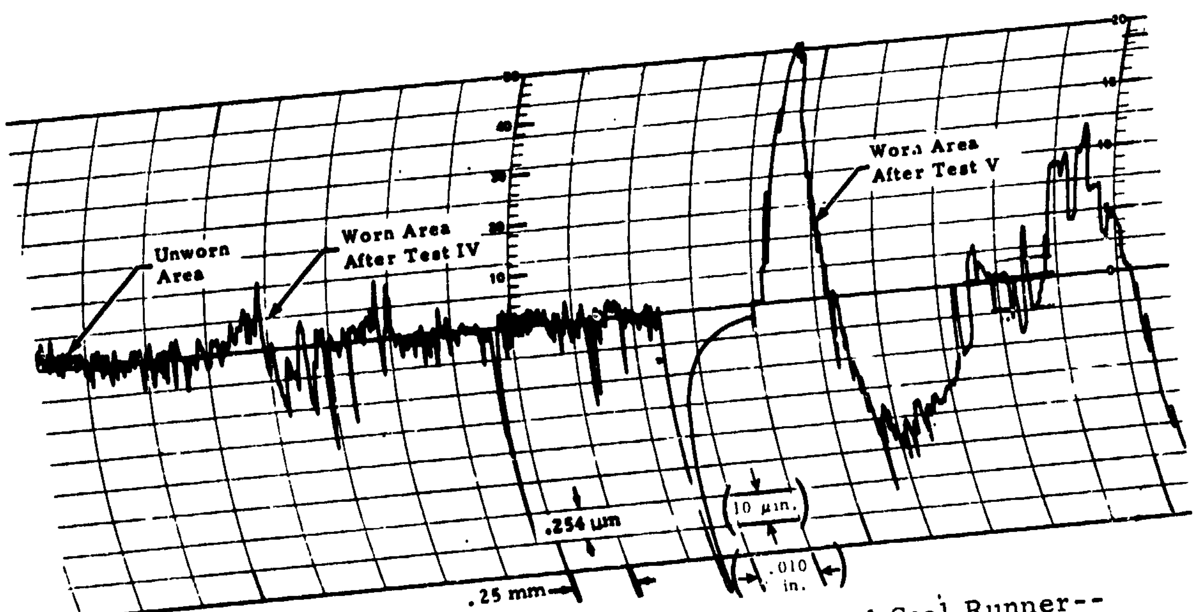

Figure 17. Forward Circumferential Segmented Seal Runner--
Trace of Contact Area After Test V.

Runs 1-15 were of 30 minutes duration each. All succeeding runs were of 15 minutes duration.

Conventional Face Seal

Design

The conventional face seal design is shown in Figure 18. Seal materials and critical dimensions are listed. The primary ring (carbon) is pressure balanced with an area ratio of 0.645. Pressure balancing is also applied to the secondary carbon piston ring seal both axially and radially. A chronium carbide flame spray is applied to the seal seat. The seal was assembled with a 3.02 N (6.8 lb) spring force, which results in an interface pressure of 67 N/cm^2 (9.7 psi).

Test Results

Five tests were conducted, each test covering a range of speeds and air pressures at ambient temperatures. Test conditions and resulting airflows, bearing cavity, pressures, and seal temperatures are listed in Table VIII. Each run was of 15 minutes duration. Seal temperature was measured at the location shown in Figure 18. Only the aft seal was temperature instrumented.

Airflow through two seals versus the pressure differential between the air side and oil side is shown in Figure 19. Airflow values varied from test to test, particularly at the higher pressures. Within each test, airflow decreased with increasing speed at any external air pressure setting.

Face seal carbon nose wear was minimal throughout the test program: 0.0051 mm (0.0002 in.) on the forward seal and 0.0102 mm (0.0004 in.) on the aft seal. This wear and the fact that the temperature did not exceed 372 K (210°F) indicate the seals were operating on an air film.

The following traces were taken after each test:

1. Primary ring (carbon) flatness, roughness, and waviness

2. Seat flatness, roughness, and waviness

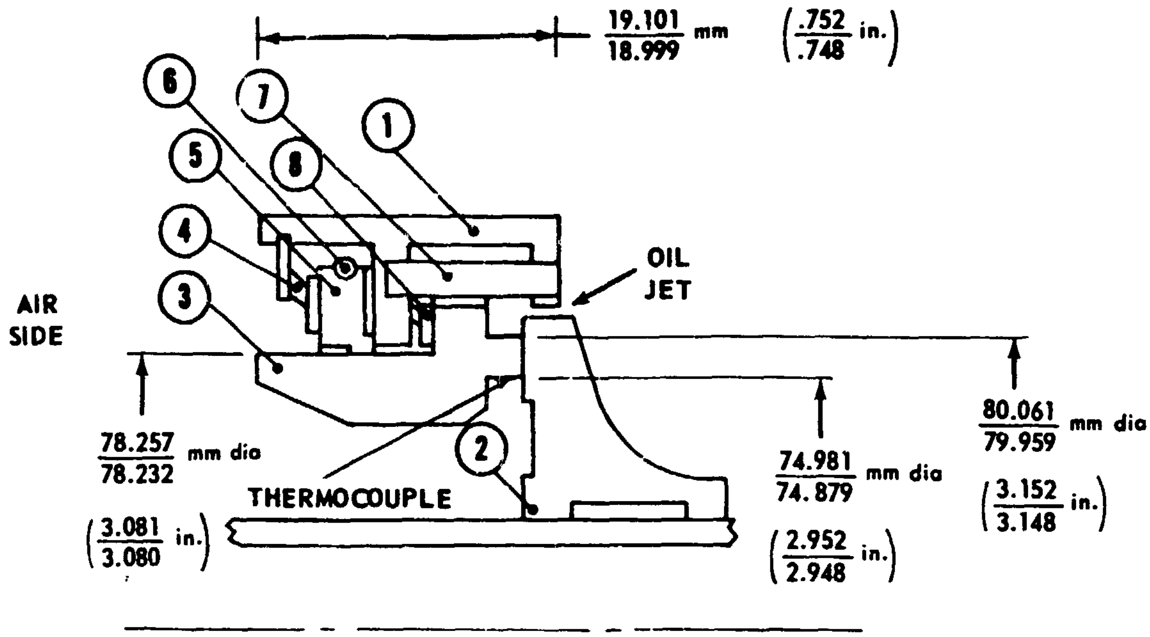

1. SEAL CASE	AMS 5610
2. SEAT	AMS 6382 FLAME SPRAYED WITH LCIC CHROME CARBIDE COATING
3. PRIMARY RING	HIGH-TEMPERATURE CARBON
4. WAVE SPRING	AMS 5542
5. SECONDARY SEAL	HIGH-TEMPERATURE CARBON
6. GARTER SPRING	AMS 5698 2.21 N LOAD (.5 lb)
7. ANTIROTATION PIN	AMS 5610
8. WAVE SPRING	AMS 5542 TOTAL WAVE SPRING LOAD 31.1 N (7 lb)

Figure 18. Conventional Face Seal

TABLE VIII. CONVENTIONAL FACE SEAL TEST DATA

Test	Run	Speed (m/s)	Speed (ft/sec)	Air Pressure (N/cm²)	Air Pressure (psia)	Cavity Pressure (N/cm²)	Cavity Pressure (psia)	Airflow (Two Seals) (kg/s)	Airflow (Two Seals) (scfm)	Airflow (Two Seals) (lb/sec)	Seal Temperature (K)	Seal Temperature (°F)
I	1	65	214	34.3	49.7	12.2	17.7	.001	2.3	.003	322	120
	2	126	414	35	50.7	12.5	18.2	.001	2.3	.003	358	185
	3	162	532	34.3	49.7	12.5	18.2	.001	2.3	.003	363	195
	4	65	214	55	79.7	15.7	22.7	.004	7	.009	330	135
	5	97	318	55	79.7	15	21.7	.004	6.6	.008	347	165
	6	65	214	77.7	112.7	18.8	27.2	.009	15.0	.014	350	170
	7	97	318	77	111.7	19.5	28.2	.008	13.0	.017	357	180
II	8	61	200	34.3	49.7	11.9	17.2	.001	1.7	.002	344	160
	9	91	300	34.3	49.7	11.9	17.2	.001	1.7	.002	357	180
	10	122	400	34.3	49.7	12.2	17.7	.001	1.7	.002	372	210
	11	152	500	34.3	49.7	12.2	17.7	-	-	-	366	200
	12	61	200	55	79.7	12.5	18.2	.002	4.3	.005	318	110
	13	91	300	55	79.7	12.5	18.2	.002	3.7	.005	339	150
	14	122	400	55	79.7	12.9	18.7	.002	3.5	.004	350	170
	15	152	500	55	79.7	12.9	18.7	.002	3.3	.004	361	190
	16	61	200	79.1	114.7	16.1	23.2	.006	11	.014	350	170
	17	91	300	79.1	114.7	16.3	23.7	.006	10	.013	350	170
	18	122	400	79.1	114.7	16.3	23.7	.005	9	.011	357	180
	19	152	500	79.1	114.7	16.1	23.2	.005	8	.010	363	195
	20	61	200	103	149.7	19.4	28.2	.010	18	.023	352	175
	21	91	300	103	149.7	19.8	28.7	.009	15	.019	358	185
	22	122	400	103	149.7	19.4	28.2	.008	14	.018	366	200
	23	152	500	103	149.7	18.8	27.2	.007	12.5	.016	372	210
III	24	91	300	79.1	114.7	17.7	25.7	.007	12.5	.016	350	170
	25	122	400	79.1	114.7	18.1	26.2	.007	12	.015	363	195
	26	152	500	79.1	114.7	17	24.7	.006	10	.013	394	250
	27	91	300	103	149.7	21.5	31.2	.011	19	.024	383	230
	28	122	400	103	149.7	21.8	31.7	.010	17.5	.022	350	170
	29	152	500	103	149.7	20.6	29.7	.008	14.5	.018	366	200
	30	91	300	123.9	179.7	23.9	34.7	.014	24	.031	352	175
	31	122	400	123.9	179.7	25.3	36.7	.013	23	.029	333	140
	32	152	500	123.9	179.7	23.9	34.7	.011	19	.024	344	160
	33	91	300	148.2	214.7	28.8	41.7	.017	30	.038	347	165
	34	122	400	148.2	214.7	27.4	39.7	.015	26	.033	330	135
	35	152	500	148.2	214.7	30.8	44.7	.017	29	.037	340	155
	36	122	400	148.2	214.7	31.6	45.7	.019	32.5	.041	333	140
	37	91	300	148.2	214.7	30.2	43.7	.018	31.5	.040	306	90
	38	61	200	148.2	214.7	30.2	43.7	.019	33.5	.043	303	85
	39	61	200	123.9	179.7	26.7	30.7	.016	27	.034	306	90
	40	91	300	123.9	179.7	27.4	39.7	.016	27.5	.035	312	100
	41	122	400	123.9	179.7	26.7	38.7	.014	24.5	.031	322	120
	42	152	500	123.9	179.7	27.4	37.7	.012	21.5	.027	333	140
IV	43	91	300	77.7	112.7	19.5	28.2	.008	14.5	.018	-	-
	44	122	400	79.1	114.7	19.8	28.7	.008	14	.018	-	-
	45	152	500	79.1	114.7	19.8	28.7	.008	13	.017	-	-
	46	183	600	79.1	114.7	19.8	28.7	.008	13	.017	-	-
	47	91	300	103	149.7	23.7	34.7	.013	23	.024	-	-
	48	122	400	103	149.7	23.7	34.7	.012	21	.027	-	-
	49	152	500	103	149.7	23.7	34.7	.011	19	.024	-	-
	50	183	600	103	149.7	23.7	34.7	.010	17	.022	-	-
	51	91	300	123.9	179.7	28.1	40.7	.018	30.5	.034	-	-
	52	122	400	123.9	179.7	28.1	40.7	.017	30	.038	-	-
	53	152	500	123.9	179.7	28.1	40.7	.015	26.5	.034	-	-
	54	183	600	123.9	179.7	28.1	40.7	.014	23.5	.030	-	-
	55	91	300	148.2	214.7	34.3	49.7	.023	39.	.050	-	-
	56	122	400	148.2	214.7	33.6	48.7	.021	35.5	.045	-	-
	57	152	500	148.2	214.7	32.9	47.7	.019	33	.042	-	-
	58	183	600	148.2	214.7	32.2	46.7	.017	29.5	.038	-	-
V	59	122	400	77	111.7	17.7	25.7	.007	12	.015	-	-
	60	152	500	79.1	114.7	18.4	26.7	.007	12	.015	-	-
	61	183	600	79.1	114.7	17.7	25.7	.005	9.5	.012	-	-
	62	213	700	79.1	114.7	19.8	28.7	.006	10.5	.013	-	-
	63	122	400	103	149.7	23.9	34.7	.012	21.5	.027	-	-
	64	152	500	103	149.7	23.2	33.7	.010	18	.023	-	-
	65	183	600	103	149.7	21.2	30.7	.008	14	.018		-
	66	213	700	103	149.7	23.9	34.7	.010	16.5	.021	-	-
	67	122	400	123.9	179.7	31.6	45.7	.020	34.5	.044	-	-
	68	152	500	123.9	179.7	31.6	45.7	.017	30	.038	-	-
	69	183	600	123.9	179.7	28.8	41.7	.015	26	.033	-	-
	70	213	700	123.9	179.7	29.5	42.7	.014	24	.031	-	-
	71	122	400	148.2	214.7	36.4	52.7	.025	43	.055	-	-
	72	152	500	148.2	214.7	35	50.7	.023	39	.050	-	-
	73	183	600	148.2	214.7	34.3	49.7	.021	35.5	.045	-	-
	74	213	700	148.2	214.7	30.8	44.7	.016	27.5	.035	-	-

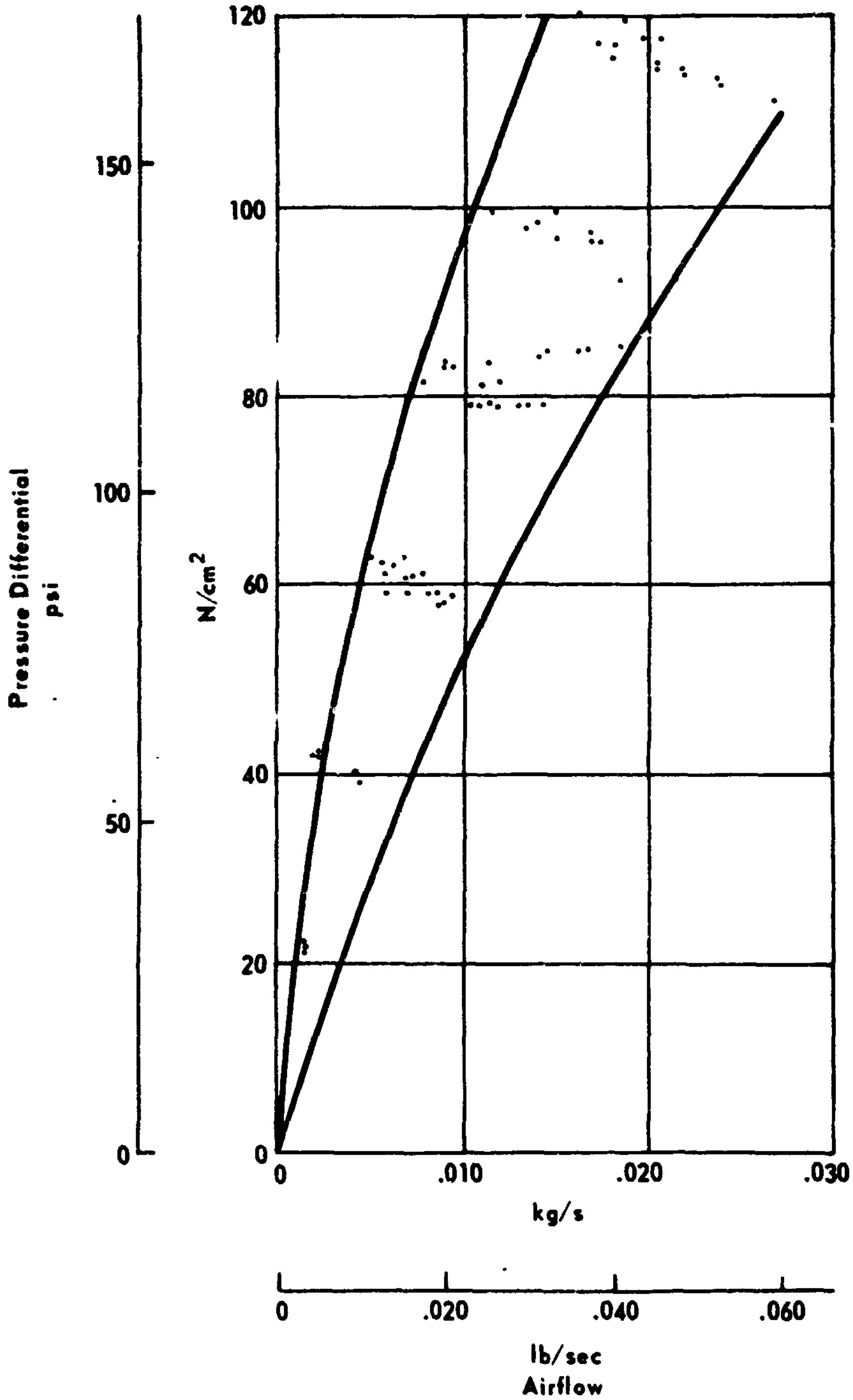

Figure 19. Airflow Through Two Conventional Face Seals Versus Pressure Differential Between Air Side and Oil Side.

Surface texture measurements before and after the test program are shown in Table IX.

Seal components after testing are shown in Figure 20. Total oil flow to the bearing compartment was varied with speed as follows:

Shaft Speed		Oil Flow	
m/s	ft/sec	kg/hr	lb/hr
61	200	45	100
91	300	68	150
122	400	89	195
152	500	114	250
183	600	136	300
213	700	161	355

The bearing was fed by four 0.81 mm (0.032 in.) jets, and each seal face plate was cooled by one 0.81 mm (0.032 in.) jet. Oil-in temperature was 366 K (200°F). MIL-L-23699 oil was used.

Traces of component surface texture following testing are shown in Figures 21 and 22.

Labyrinth Seal

An analytical evaluation was made of a labyrinth seal that could be compared with the experimental results of the conventional and self-acting seals. Labyrinth geometry was chosen that would fit into the envelope of the test seals. The labyrinth seal is shown in Figure 23.

The method used to calculate airflow is that of Reference 11. The bearing cavity pressure versus airflow relationship, which is known from the experimental program, is presented in Figure 24. This relationship is used in the leakage analysis. The airflow through two labyrinth seals versus pressure differential from the air side to the oil side is shown in Figure 25. Airflow through two seals is used for ease of comparison with airflow from the test rig programs, in which two seals were incorporated flanking the bearing cavity to simulate an engine installation. Airflow is calculated for several different diametral operating gaps at 294 K (70°F) air temperature.

TABLE IX. CONVENTIONAL FACE SEAL SURFACE TEXTURE MEASUREMENTS

	New	After Test
Fwd Carbon		
Flatness (μm)	.381	2.54
(in.)	.000015	.0001
Roughness (μm)	.381	.280
(μ in. AA)	15	11
Waviness (μm)	-	1.02
(in.)	-	.00004
Aft Carbon		
Flatness (μm)	2.54	7.62
(in.)	.0001	.0003
Roughness (μm)	.381	.127
(μ in. AA)	15	5
Waviness (μm)	2.28	.51
(in.)	.00009	.00002
Fwd Seat		
Flatness (μm)	.254	1.52
(in.)	.00001	.00006
Roughness (μm)	.051	.280
(μ in. AA)	2	11
Waviness (μm)	.254	1.78
(in.)	.00001	.00007
Aft Seat		
Flatness (μm)	1.78	1.27
(in.)	.00007	.00005
Roughness (μm)	.025	.203
(μ in. AA)	1	8
Waviness (μm)	.254	1.02
(in.)	.00001	.00004

Figure 20. Conventional Face Seal Components After Test.

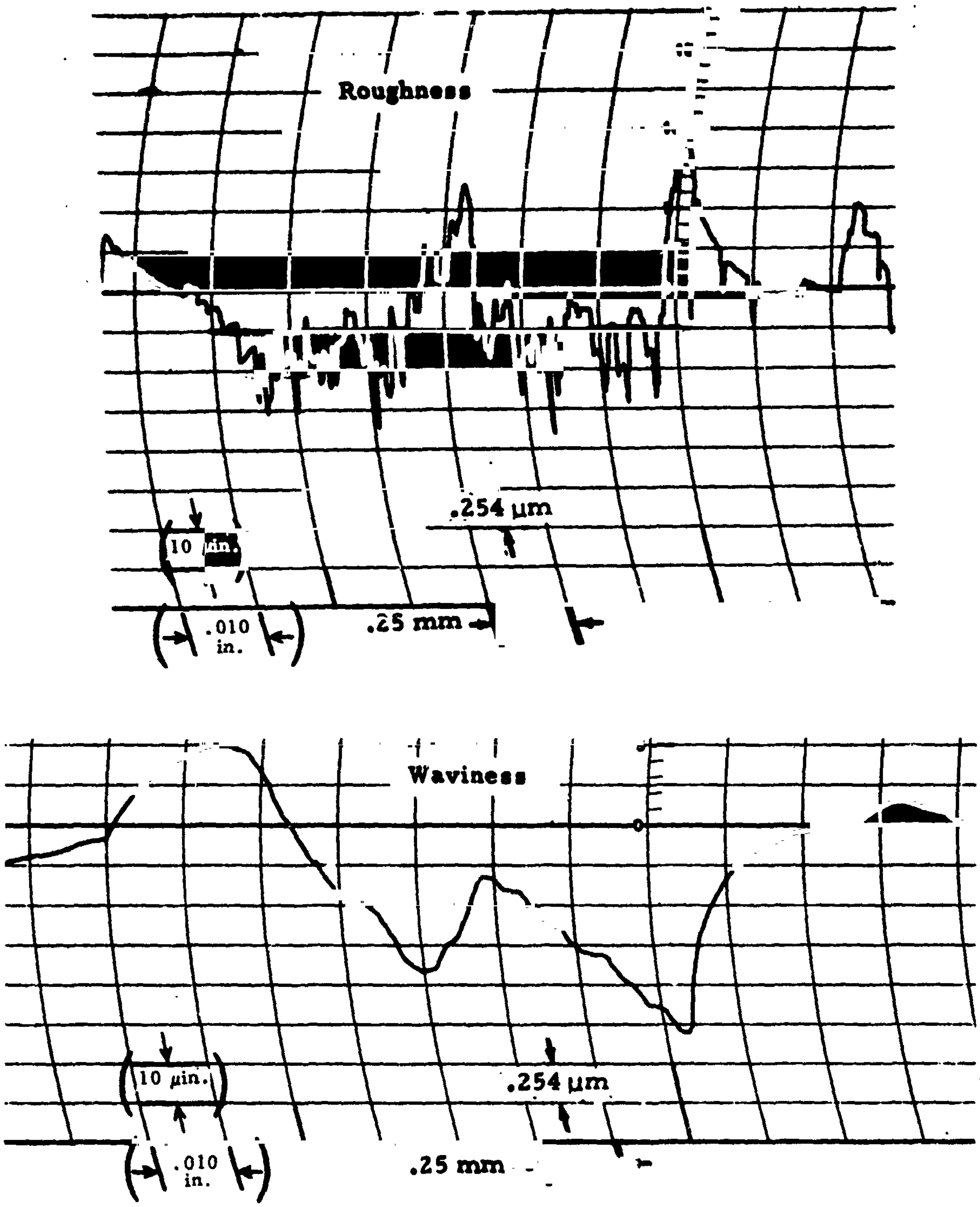

Figure 21. Conventional Face Seal Seat Trace of Roughness and Waviness After Test.

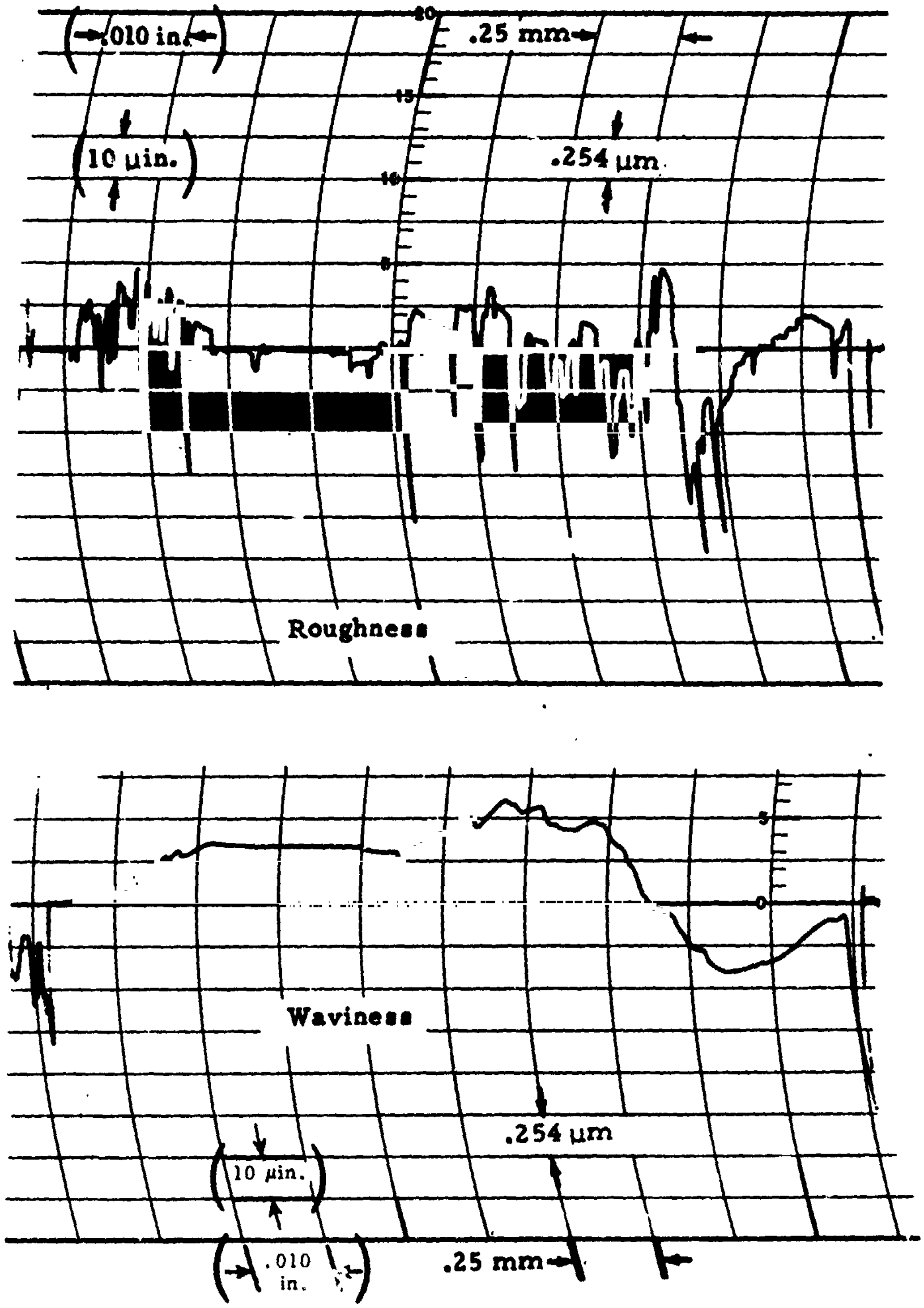

Figure 22. Conventional Face Forward Seal Carbon Ring, Trace of Roughness and Waviness After Test.

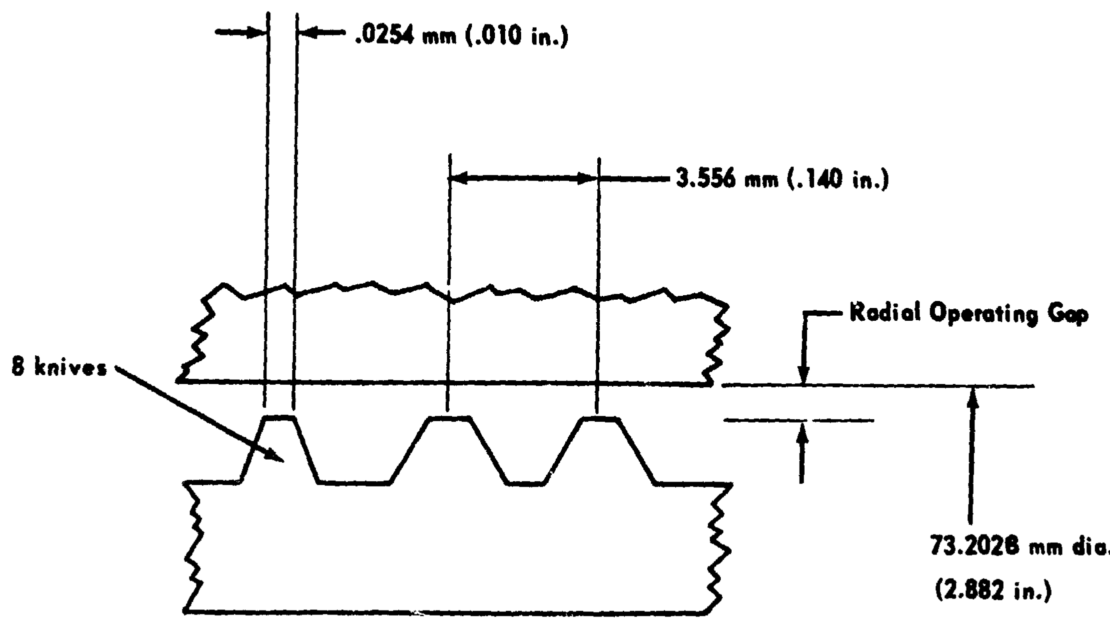

Figure 23. Labyrinth Geometry.

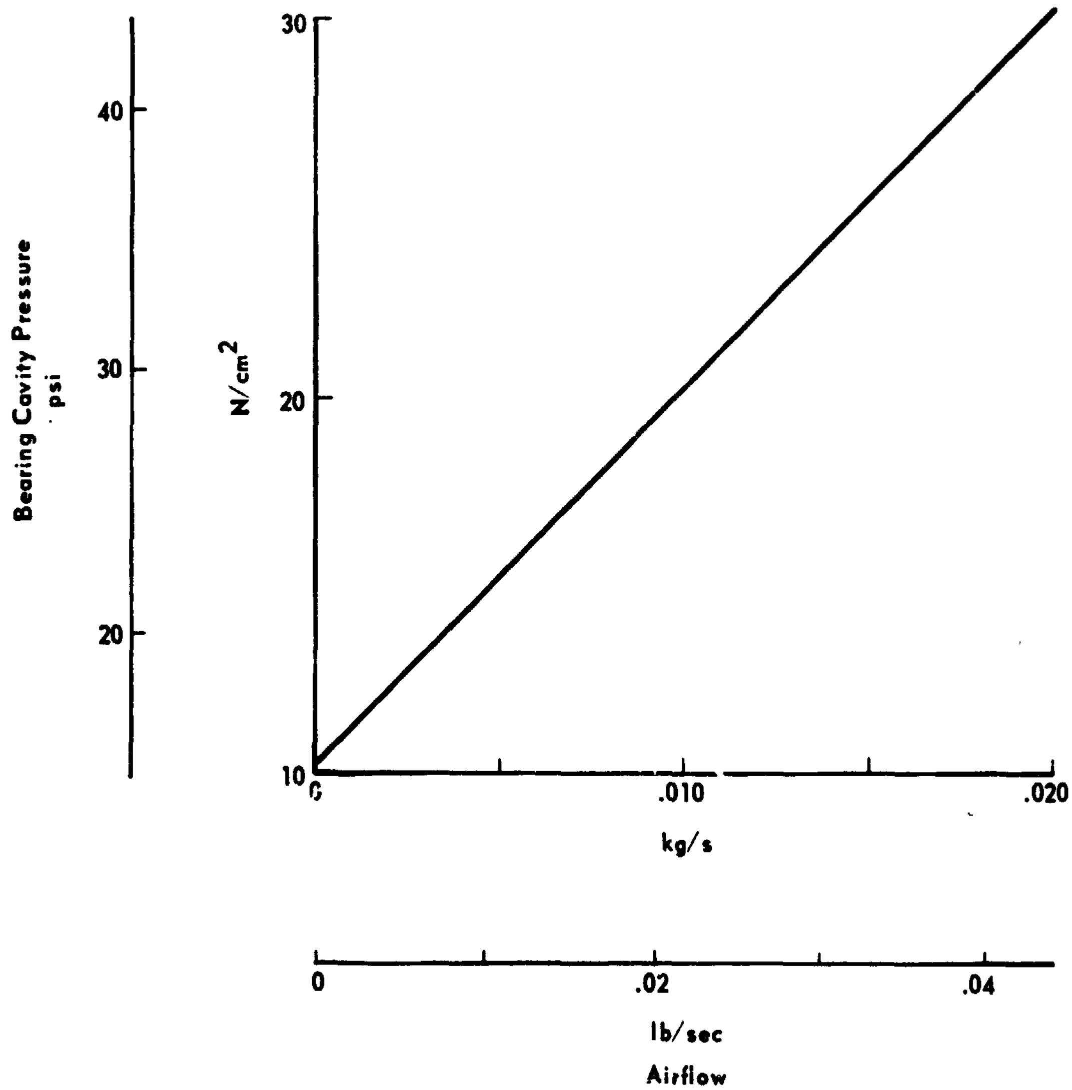

Figure 24. Bearing Cavity Pressure Versus Airflow.

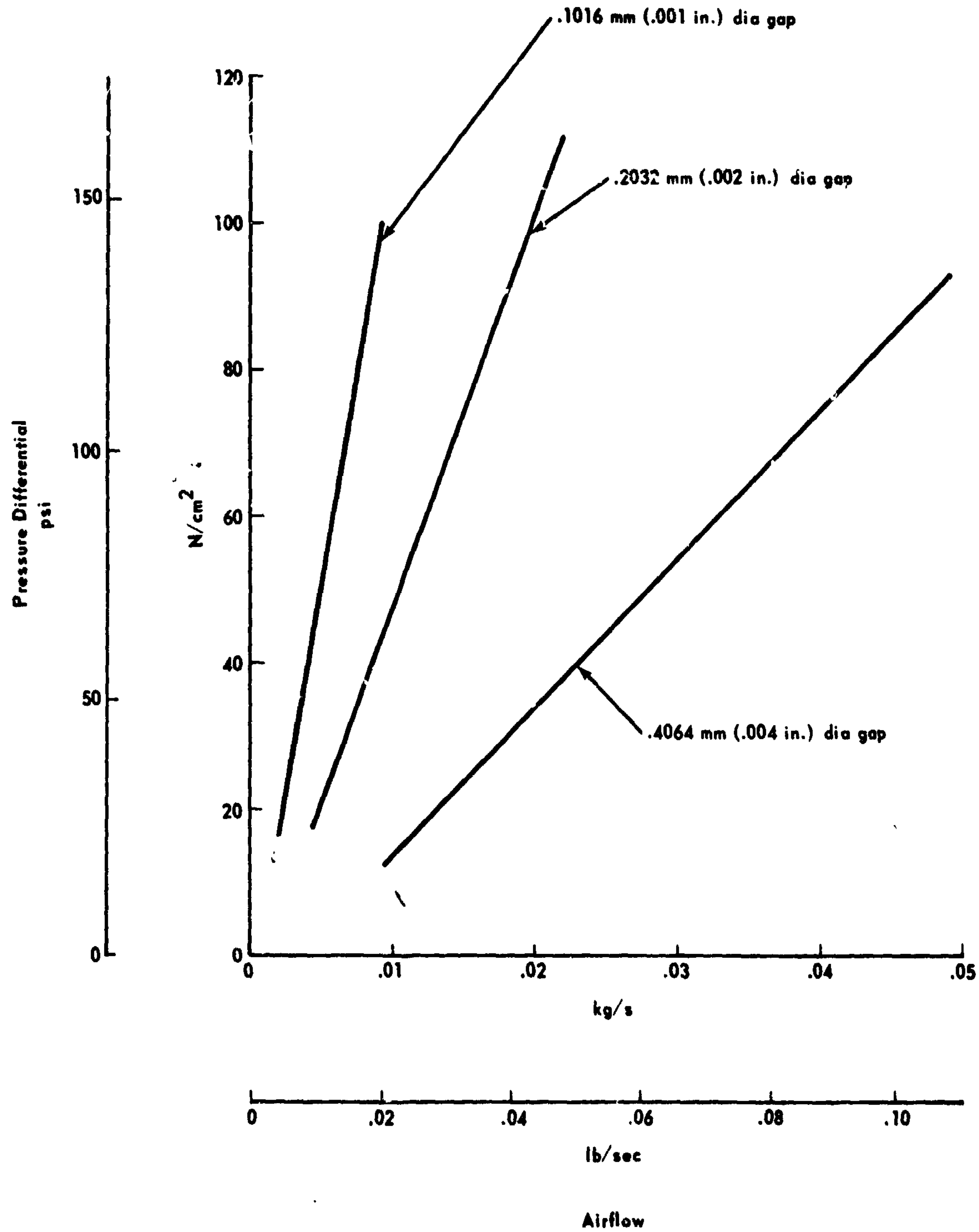

Figure 25. Airflow Through Two Labyrinth Seals Versus Pressure Differential.

Self-Acting Face Seal

Design

The self-acting face seal used in the test program is shown in Figure 26. It is similar to a conventional face seal with the addition of the self-acting geometry for lift augmentation.

The primary sealing interface consists of the rotating face plate, which is keyed to the shaft, and the nonrotating primary ring assembly, which is free to move in an axial direction, thus accommodating axial motions due to thermal expansion. Axial springs provide the mechanical force that maintains contact between the seat and primary ring at shutdown. Initially the seal incorporated 16 springs producing an axial load of 58 N (13 lb). The secondary seal is a carbon piston ring, which is subjected only to the axial motion of the carrier assembly.

Great care is taken to ensure flatness of the sealing surfaces. The seat is keyed to the shaft spacer and is axially clamped by a machined bellows which minimizes distortion of the seat since the major part of the clamping force goes through the shaft spacers. The bellows also acts as a static seal between the seat and the shaft spacer. Cooling oil is passed through the seat to reduce thermal gradients, and the oil dam disc also serves as a heat shield. Windbacks are used to prevent contaminants from approaching the sealing surfaces.

In operation, the sealing faces are separated slightly, in the order of 0.00508 mm (0.0002 in.), by action of the self-acting lift geometry. This positive separation results from the balance of seal forces and the gas film stiffness of the self-acting geometry. The primary ring carbon face with the lift pads is shown in Figure 27.

To determine film thickness and air leakage in a self-acting face seal, the axial forces acting on the primary ring assembly must be determined for each operating condition. These forces comprise the self-acting lift force, the spring force, and the pneumatic forces due to the sealed pressure. Essentially the analysis requires finding the film thickness for which the opening forces balance the closing forces. When this equilibrium film thickness is known, the leakage rate can be calculated. References 3 through 9 detail the design procedure.

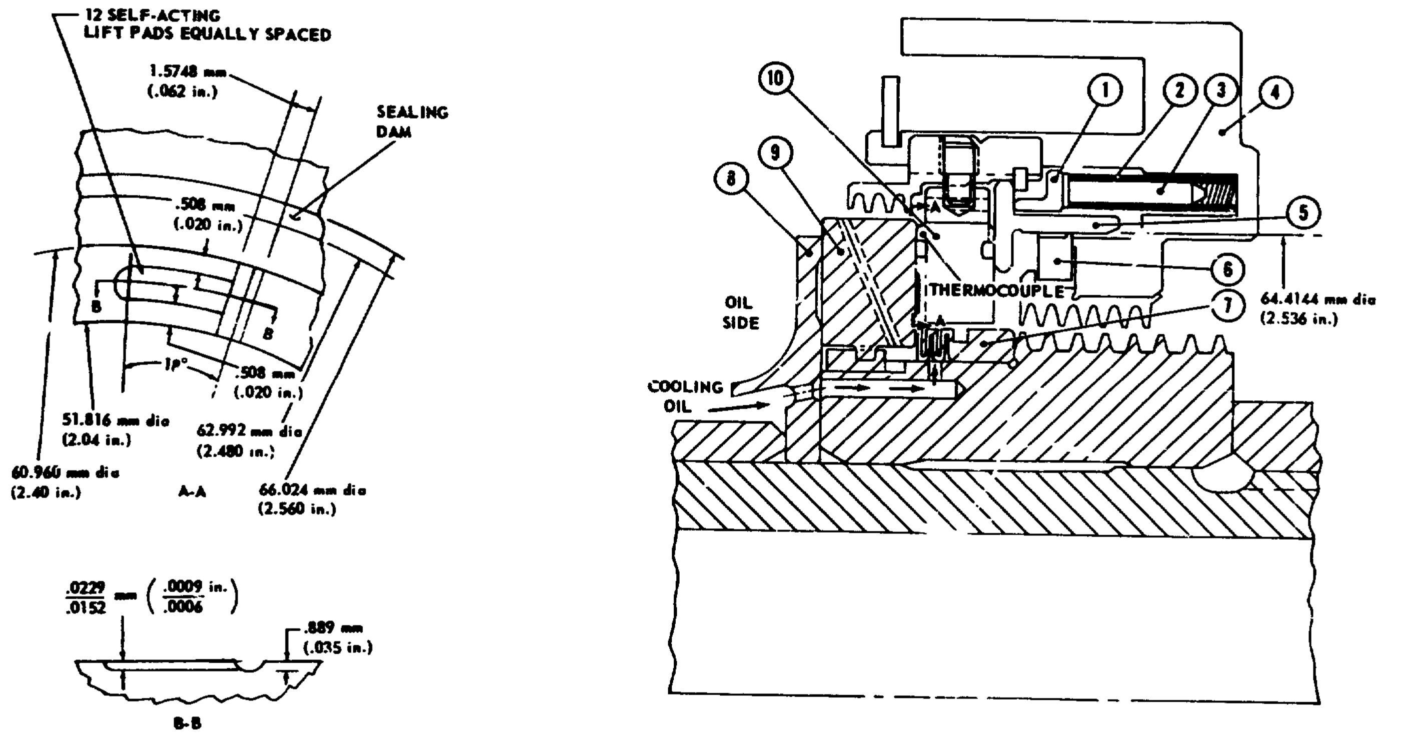

1. SPRING PLATE	INCONEL X750	6. PISTON RING	HIGH-TEMPERATURE CARBON
2. COMPRESSION SPRING	INCONEL X750	7. BELLOWS SPACER	INCONEL X750
3. SPRING PIN	18-8 SST	8. OIL DAM AND HEAT SHIELD	440 SST
4. HOUSING	INCONEL X750	9. SEAT	4340 FLAME SPRAYED WITH LINDE LCIC (CHROME CARBIDE)
5. CARRIER	INCONEL X750	10. PRIMARY RING	HIGH TEMPERATURE CARBON AND TZM

Figure 26. Self-Acting Face Seal Design.

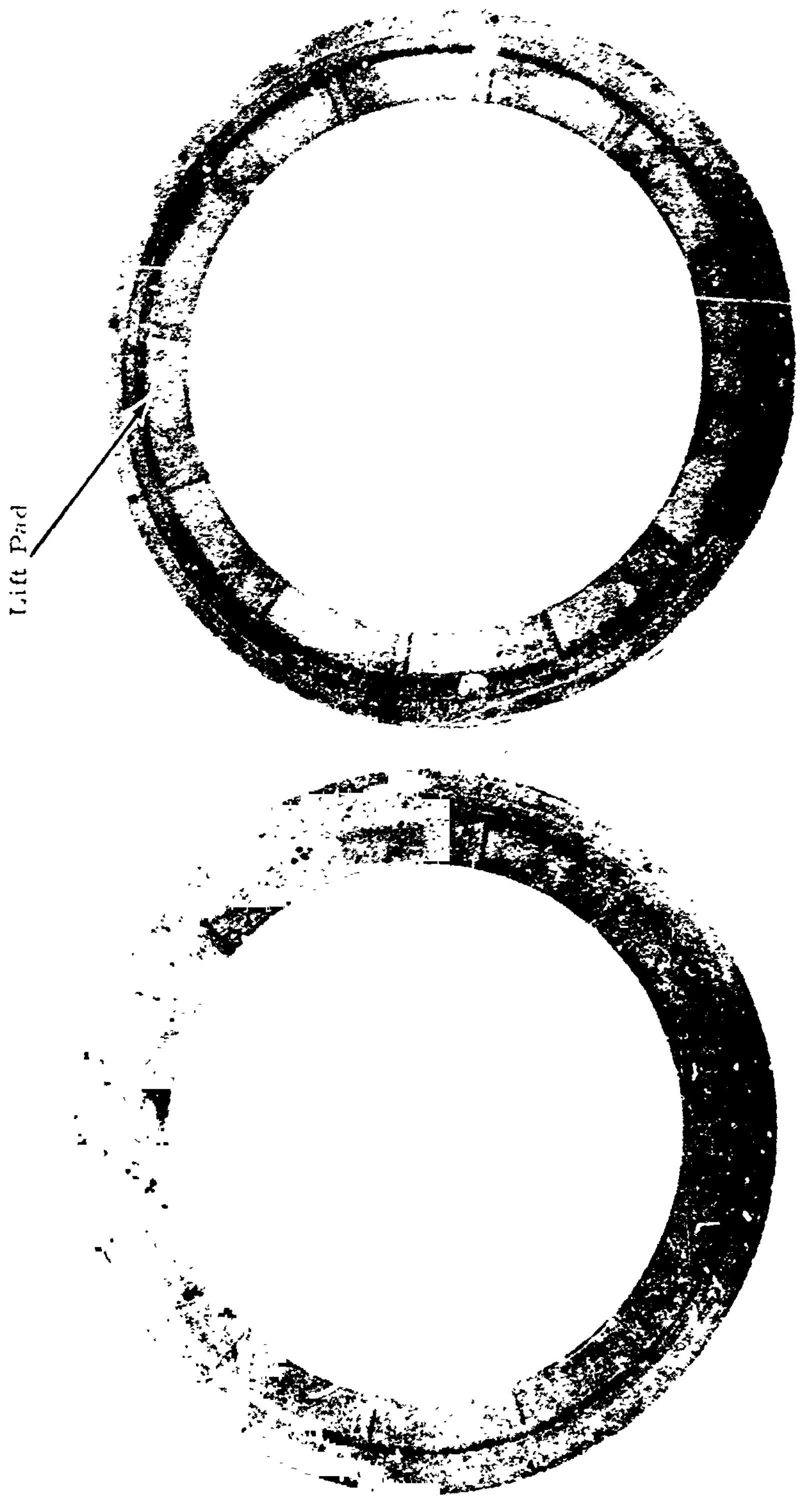

Figure 27. Detail of Lift Pads.

Test Results

Testing of the self-acting face seal was accomplished in three phases. First, evaluation tests were conducted at ambient temperature over a range of speeds and air pressures. During the evaluation testing and initial endurance testing, failure modes were uncovered. A second series of tests was conducted at elevated temperatures to investigate seal failures. Finally, 150 hours of endurance operation were accomplished.

Initially, seven evaluation tests were conducted, each test covering a range of speeds and air pressures. Operating conditions for the first three tests are documented in Table X. It was found that there were air leaks into the rig during the first three tests, and therefore the seal air leakages recorded were erroneous. Inspection following test I revealed no measurable wear of the carbon ring nor of the rotating seat. The carbon ring of both seals wore approximately 0.0025 mm (0.0001 in.) during test II. During test III, the aft seal wore an additional 0.0050 mm (0.0002 in.) while the forward carbon remained the same. The seal spring force had been set at 58 N (13 lb). In view of the wear that occurred, the spring force was reset at 42 N (9.5 lb) by reducing the number of coil springs.

Rig air leakage was corrected and four more tests were conducted. Test conditions and resulting airflows, bearing cavity pressures, and seal temperatures are listed in Table XI. Only the aft seal was temperature instrumented with a thermocouple implanted close to the sealing nose (Figure 26). Each run of tests I to VI was 15 minutes. Test VII points were held for 5 minutes.

Neither the forward nor the aft carbon ring or seat wore during tests IV and V. During test VI, at each pressure setting as the speed was increased above 203 m/s (660 ft/sec), it was noted that the aft seal temperature rose rapidly indicating that the carbon was contacting the runner. After the test it was found that the aft seal lift pads were almost worn out. The forward seal had not worn. The seal carbon rings and seats are shown in Figure 28.

A new aft seal was used for test VII.

Data taken during tests IV to VII were consistent for each test; however, there was some scatter from test to test. Airflow and seal temperature data for test V, which was typical, are shown in Figures 29 and 30.

TABLE X. SELF-ACTING FACE SEAL TEST DATA (TESTS I - III)

Test	Run	Speed (m/s)	Speed (ft/sec)	Air Pressure (N/cm^2)	Air Pressure (psia)	Time (min)
I	1	91	300	34.3	49.7	15
	2	122	400	34.3	49.7	15
	3	91	300	55.0	79.7	15
	4	122	400	55.0	79.7	15
	5	91	300	79.1	114.7	15
	6	122	400	79.1	114.7	15
	7	91	300	34.3	49.7	15
	8	122	400	34.3	49.7	15
	9	91	300	55.0	79.7	15
	10	122	400	55.0	79.7	15
	11	91	300	77.7	112.7	15
	12	122	400	73.5	106.7	15
II	13	91	300	34.3	49.7	15
	14	122	400	34.3	49.7	15
	15	152	500	34.3	49.7	15
	16	91	300	51.6	74.7	15
	17	122	400	54.2	78.7	15
	18	152	500	55.0	79.7	15
	19	91	300	78.3	113.7	15
	20	122	400	79.1	114.7	15
	21	152	500	79.1	114.7	15
	22	91	300	103.0	149.7	15
	23	122	400	103.0	149.7	15
	24	152	500	103.0	149.7	15
III	25	91	300	34.3	49.7	15
	26	122	400	34.3	49.7	15
	27	152	500	34.3	49.7	15
	28	91	300	55.0	79.7	15
	29	122	400	55.0	79.7	15
	30	152	500	55.0	79.7	15
	31	91	300	103.0	149.7	15
	32	122	400	103.0	149.7	15
	33	152	500	103.0	149.7	15

TABLE XI . SELF-ACTING FACE SEAL TEST DATA (TESTS IV - VII)

Test	Run	Speed (m/s)	Speed (ft/sec.)	Air Pressure (N/cm²)	Air Pressure (psia)	Cavity Pressure (N/cm²)	Cavity Pressure (psia)	Airflow (Two Seals) (kg/s)	Airflow (Two Seals) (scfm)	Airflow (Two Seals) (lb/sec)	Seal Temperature (K)	Seal Temperature (°F)
IV	34	91	300	34.3	49.7	10.5	15.2	<.0006	< 1	<.0013	347	164
	35	122	400	34.3	49.7	10.5	15.2	<.0006	< 1	<.0013	373	212
	36	152	500	34.3	49.7	11.5	16.7	.0006	1.0	.0013	393	247
	37	91	300	54.4	78.7	10.5	15.2	.0007	1.2	.0015	358	185
	38	122	400	55.0	79.7	11.5	16.7	.0009	1.5	.0019	380	224
	39	152	500	55.0	79.7	11.9	17.2	.0012	2.0	.0026	398	256
	40	91	300	79.1	114.7	11.5	16.7	.0011	1.9	.0024	373	212
	41	122	400	79.1	114.7	11.6	16.9	.0013	2.3	.0029	385	234
	42	152	500	79.1	114.7	12.5	18.2	.0017	2.9	.0037	402	262
	43	91	300	103.0	149.7	11.[illegible]	17.2	.0015	2.6	.0033	380	223
	44	122	400	103.0	149.7	12.[illegible]	17.7	.0018	3.1	.0040	396	25[illegible]
	45	152	500	103.0	149.7	12.9	18.7	.0023	4.0	.0051	412	282
V	46	91	300	34.3	49.7	10.8	15.7	<.0006	< 1	<.0013	333	140
	47	122	400	34.3	49.7	11.2	16.2	<.0006	< 1	<.0013	352	174
	48	152	500	34.3	49.7	11.2	16.2	<.0006	< 1	<.0013	371	210
	49	183	600	34.3	49.7	12.2	17.7	.0011	1.9	.0024	392	246
	50	91	300	55.0	79.7	11.2	16.2	.0008	1.3	.0017	348	166
	51	122	400	55.0	79.7	11.5	16.7	.0009	1.5	.0019	366	200
	52	152	500	55.0	79.7	11.9	17.2	.0012	2.1	.0027	381	226
	53	183	600	55.0	79.7	12.9	18.7	.0015	2.6	.0033	396	253
	54	91	300	103.0	149.7	11.9	17.2	.0017	3.0	.0038	359	186
	55	122	400	103.0	149.7	12.2	17.7	.0021	3.6	.0046	373	212
	56	152	500	103.0	149.7	13.6	19.7	.0029	5.0	.0064	387	237
	57	183	600	103.0	149.7	15.0	21.7	.0039	6.7	.0085	400	260
	58	91	300	123.9	179.7	12.5	18.2	.0023	3.9	.0050	364	196
	59	122	400	123.9	179.7	13.2	19.2	.0032	5.5	.0070	373	212
	60	152	500	123.9	179.7	14.3	20.7	.0036	6.2	.0079	386	236
	61	183	600	123.9	179.7	16.3	23.7	.0046	8.0	.0102	402	263
VI	62	122	400	34.3	49.7	11.5	16.7	<.0006	< 1	<.0013	365	198
	63	152	500	34.3	49.7	11.9	17.2	.0006	1.1	.0014	384	231
	64	183	600	34.3	49.7	12.9	18.7	.0010	1.7	.0022	405	270
	65	122	400	55.0	79.7	11.9	17.2	.0008	1.4	.0018	392	245
	66	152	500	55.0	79.7	12.2	17.7	.0011	1.9	.0024	405	270
	67	183	600	55.0	79.7	12.9	18.7	.0013	2.3	.0029	420	297
	68	122	400	103.0	149.7	12.9	18.7	.0021	3.7	.0047	371	208
	69	152	500	103.0	149.7	13.[illegible]	19.7	.0025	4.3	.0055	392	245
	70	183	600	103.0	149.7	13.9	20.2	.0029	5.0	.0064	415	286
	71	122	400	123.9	179.7	12.9	18.7	.0023	4.0	.0051	389	240
	72	152	500	123.9	179.7	13.6	19.7	.0028	4.9	.0062	403	265
	73	183	600	123.9	179.7	15.0	21.7	.0036	6.3	.0080	423	301
VII	74	91	300	34.3	49.7	11.5	16.7	<.0006	< 1	<.0013	-	-
	75	152	500	34.3	49.7	11.6	16.9	.0006	1.1	.0014	377	219
	76	183	600	34.3	49.7	11.9	17.2	.0008	1.3	.0017	397	255
	77	203	660	34.3	49.7	12.9	18.7	.0011	1.9	.0024	405	270
	78	152	500	103.0	149.7	14.6	21.2	.0032	5.6	.0071	376	216
	79	183	600	103.0	149.7	16.3	23.7	.0044	7.7	.0098	393	248
	80	203	660	103.0	149.7	17.7	25.7	.0054	9.5	.0121	405	270
	81	152	500	123.9	179.7	15.7	22.7	.0036	6.3	.0080	384	231
	82	183	600	123.9	179.7	17.7	25.7	.0059	10.2	.0130	400	260
	83	203	660	123.9	179.7	20.6	29.7	.0081	14.0	.0179	409	276
	84	152	500	148.2	214.7	17.4	25.2				393	248
	85	183	600	148.2	214.7	18.1	26.2	.0069	12.0	.0153	405	270
	86	203	660	148.2	214.7	23.7	34.7	.0107	18.5	.0236	420	297

Figure 28. Forward (Top) and Aft (Bottom) Self-Acting Seal Components After Test VI.

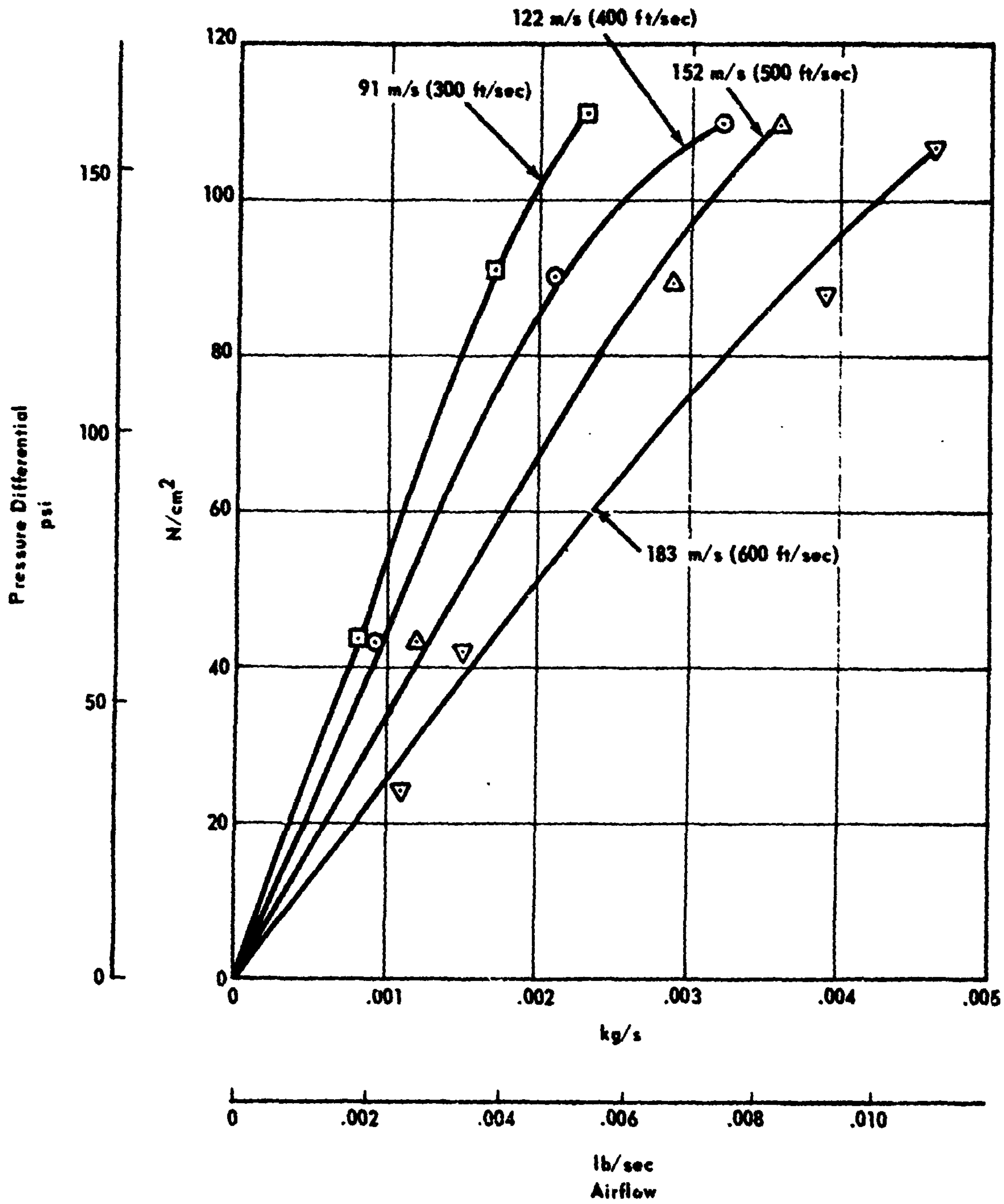

Figure 29. Airflow Through Two Self-Acting Face Seals Versus Pressure Differential at Various Speeds (Test V).

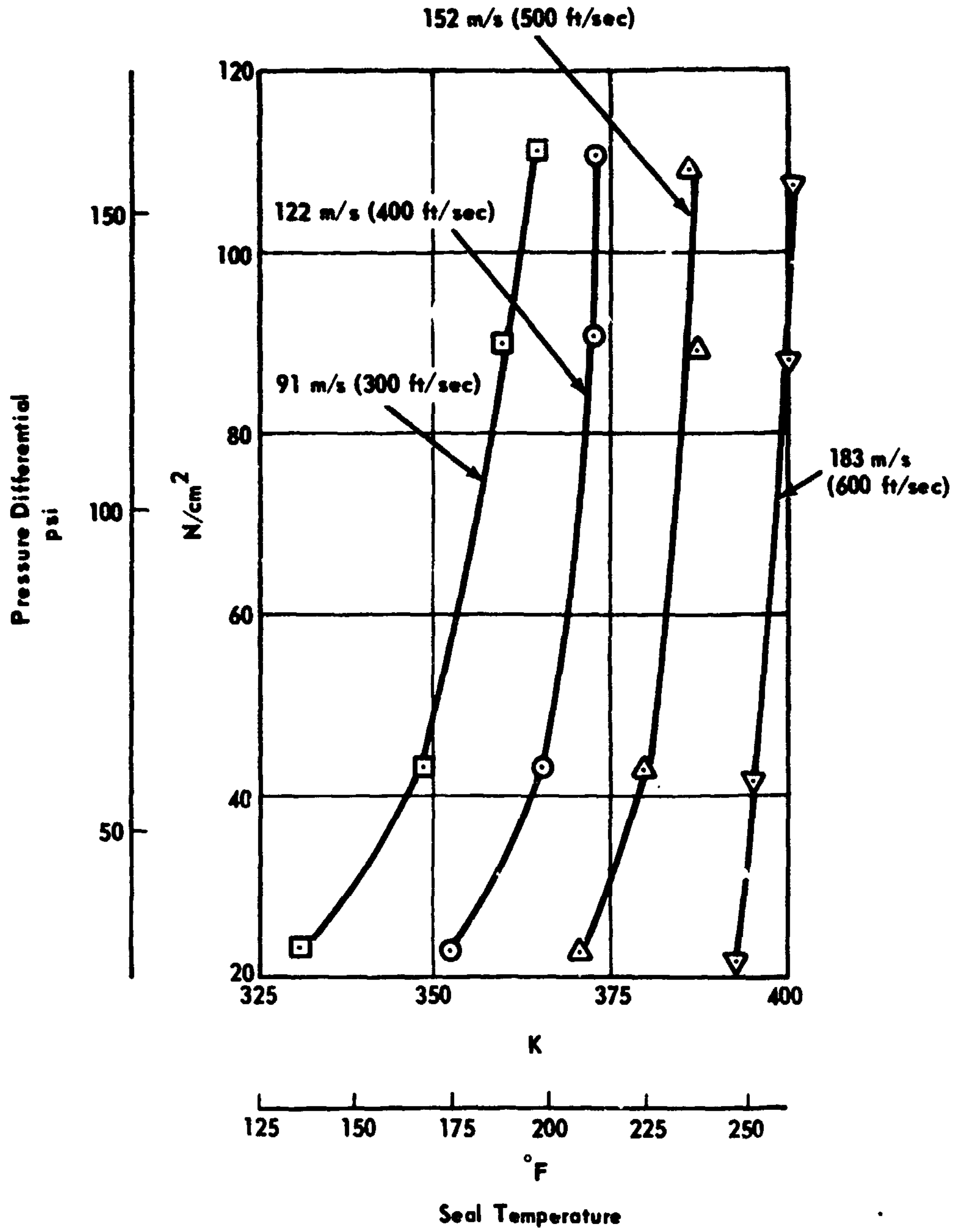

Figure 30. Self-Acting Face Seal Temperature Versus Pressure Differential at Various Speeds (Test V).

Following each test a visual and analytical inspection was performed on the primary ring (carbon) and the seat. Seats were traced for roughness and waviness. Flatness of the assembled seats clamped in place on the shaft was measured to be 0.0013 mm (0.000050 in.) on the forward seat and 0.0019 mm (0.000075 in.) on the aft seat. The forward seat roughness was 0.1016 mm (4 AA) and waviness was 0.254 mm (0.00001 in.) throughout the six tests. The aft seat roughness was 0.0762 mm (3 AA) through test V and increased to 0.2794 mm (11 AA) during test VI. Waviness was 0.254 mm (0.0001 in.) through test V and increased to 1.524 mm (0.0006 in.) during test VI. The 1.524 mm (0.0006 in.) is actually seat wear.

Measurement charts showing seat surface texture before testing and after test VI are presented in Figures 31 through 34.

The depth of the lift pads on the primary ring (carbon) was measured by taking a proficorder trace across the face. Traces of sealing faces of the forward and aft seals prior to testing are shown in Figure 35. Only one pad is depicted. Traces of four of twelve pads were taken before and after each test. The original lift pad depths varied from 0.0153 mm (0.00065 in.) to 0.0203 mm (0.00082 in.) on the forward seal. The lift pads on the aft seal were originally all 0.025 mm (0.0010 in.) Traces of the lift pads after test VI are shown in Figure 36.

Total oil flow to the bearing compartment was varied with speed as follows:

Shaft Speed		Oil Flow	
m/s	ft/sec	kg/hr	lb/hr
61	200	54	120
91	300	81	180
122	400	108	240
152	500	136	300
183	600	162	360
213	700	189	420

The bearing was fed by eight 0.81 mm (0.032 in.) jets and each seal face plate cooled by one 0.81 mm (0.032 in.) jet. Oil-in temperature was 366 K (200°F). MIL-L-23699 oil was used.

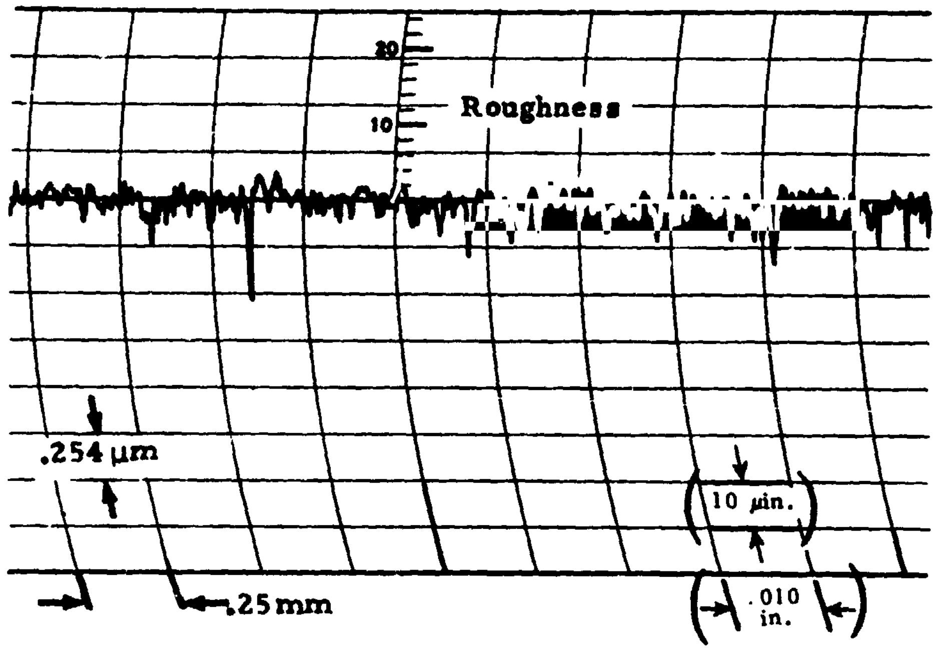

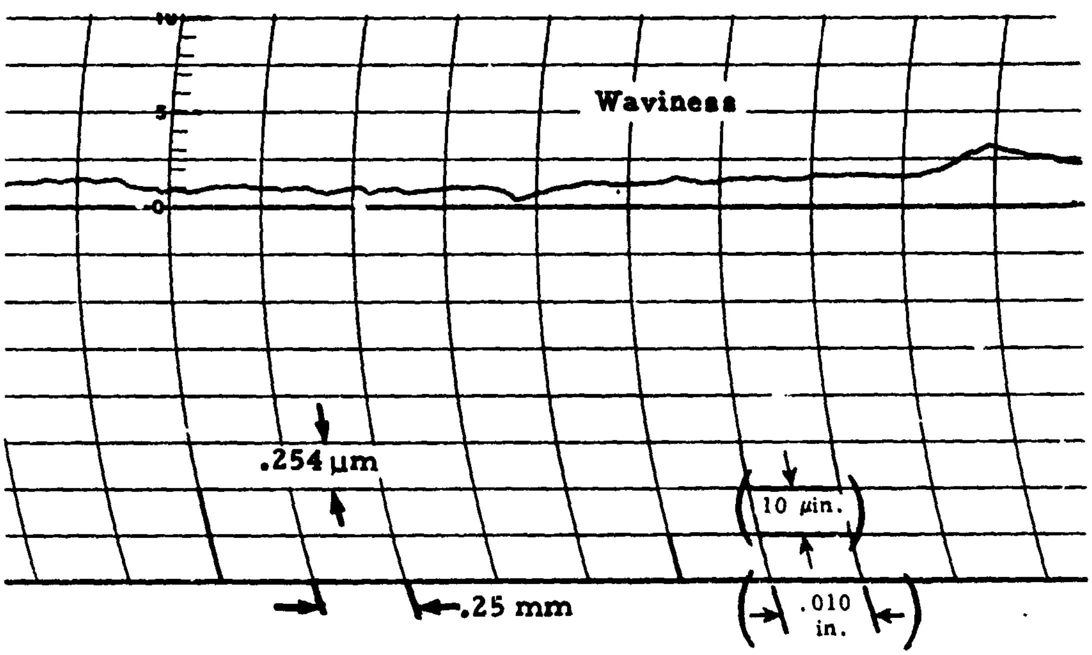

Figure 3.. Aft Self-Acting Face Seal Seat Trace of Roughness and Waviness Before Test.

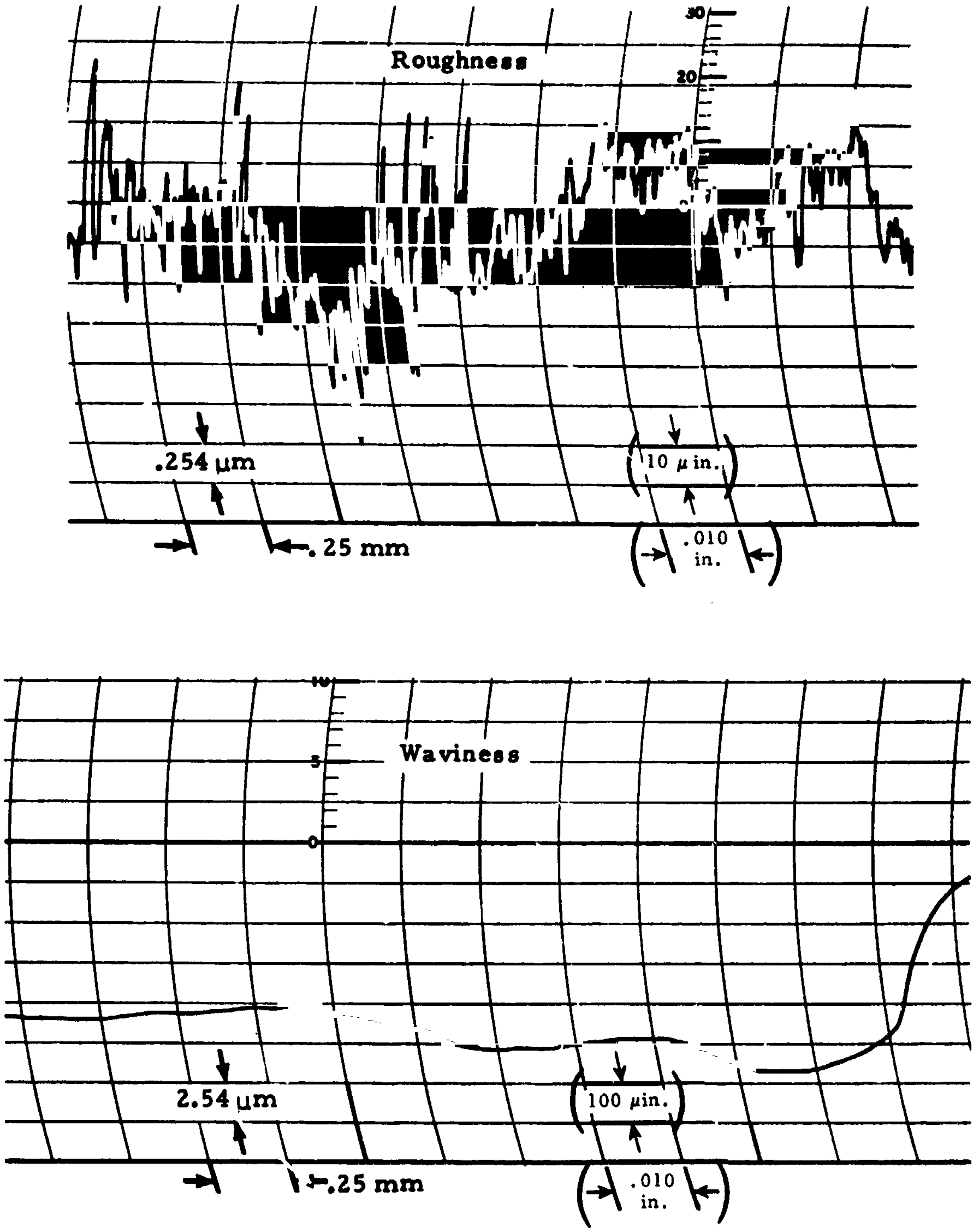

Figure 32. Aft Self-Acting Face Seal Seat Trace of Roughness and Waviness After Test VI.

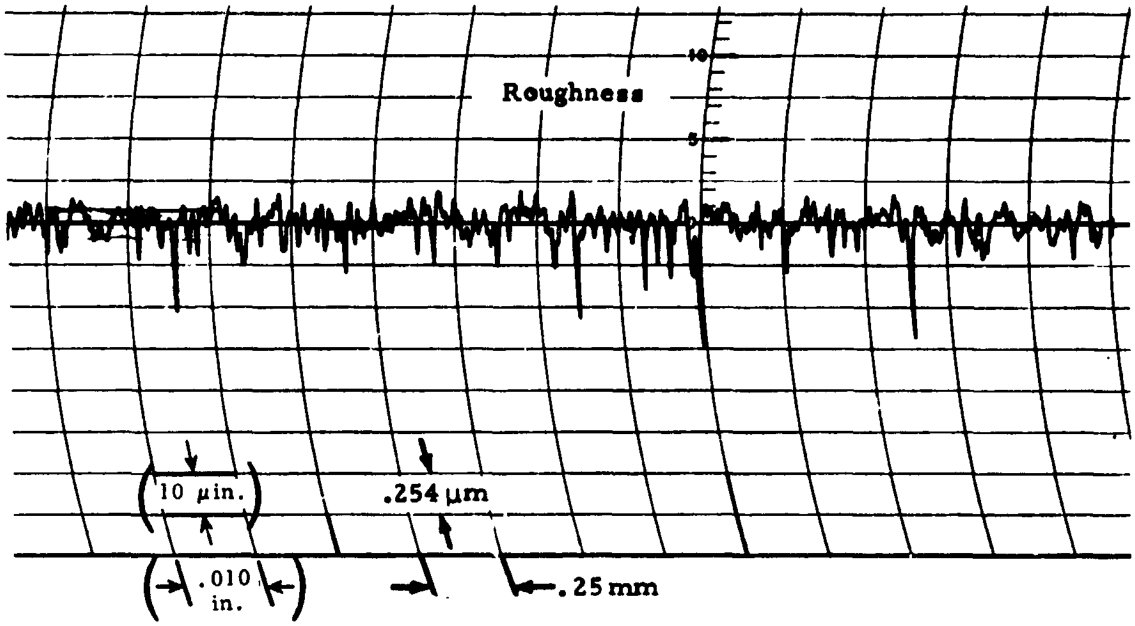

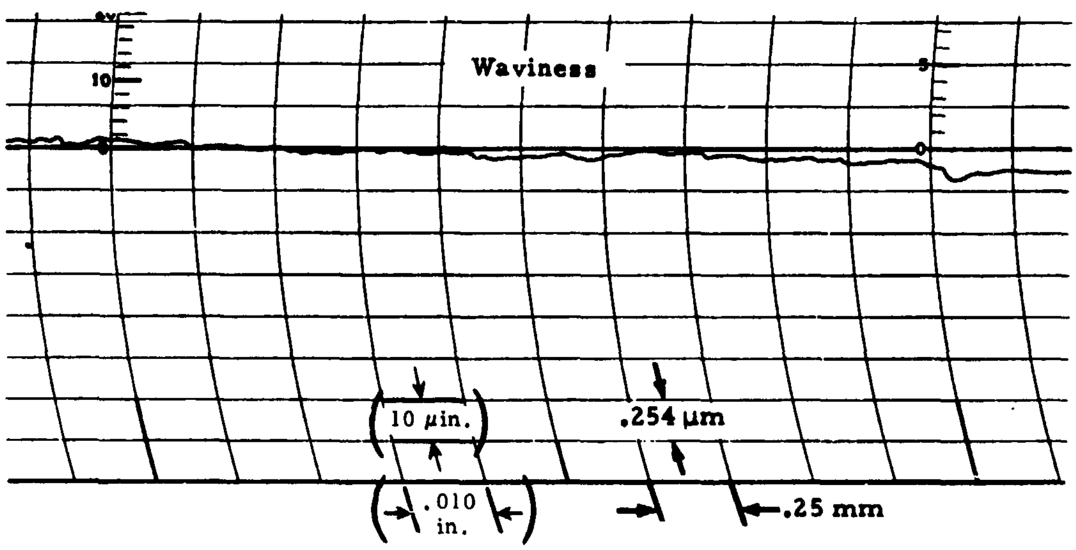

Figure 33. Forward Self-Acting Seal Seat Trace of Roughness and Waviness Before Test.

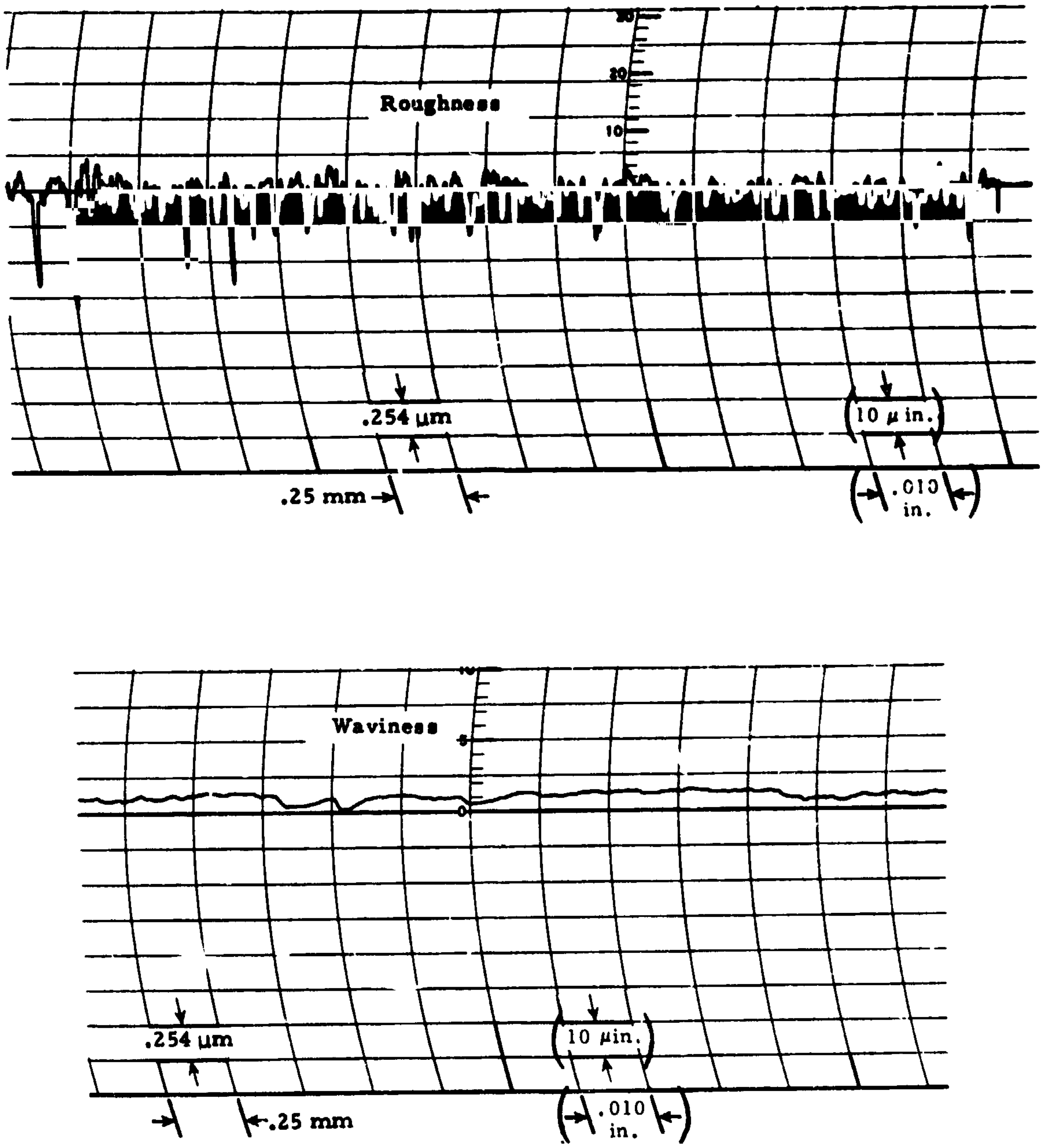

Figure 34. Forward Self-Acting Seal Seat Trace of Roughness and Waviness After Test VI.

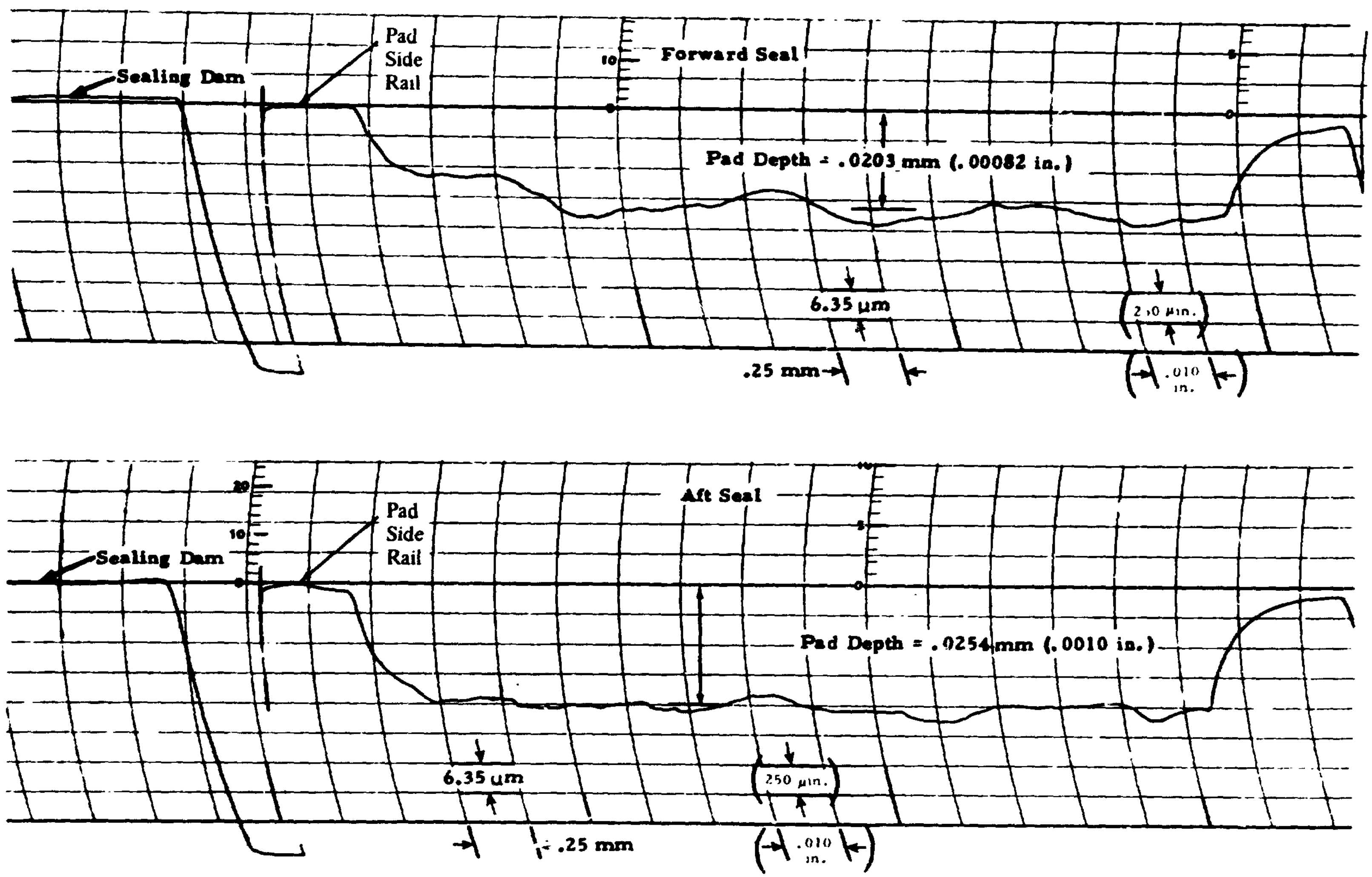

Figure 35. Trace of Forward and Aft Seal Carbon Ring Sealing Faces Before Operation, Self-Acting Seal.

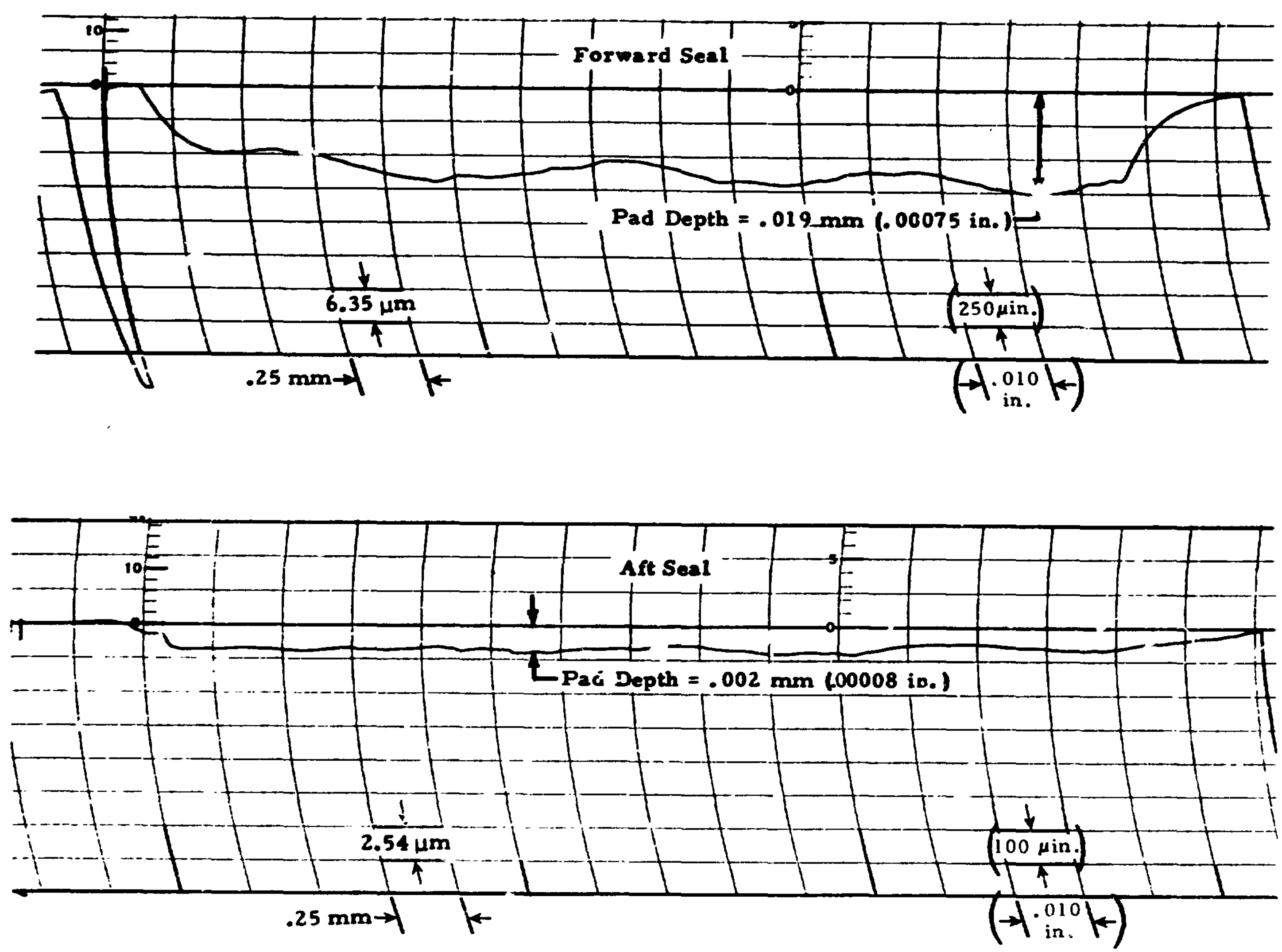

Figure 36. Trace of Forward and Aft Seal Carbon Ring Sealing Faces After Test VI, Self-Acting Seal

Immediately after test VII, without a teardown, an attempt was made to conduct endurance testing. A tentative 5-hour cycle had been set as follows:

Point	Speed m/s	Speed ft/sec	Air Pressure N/cm^2	Air Pressure psia	Air Temperature K	Air Temperature °F	Time at Point hr
1	91	300	34.3	49.7	478	400	1
2	122	400	55.0	79.7	478	400	1
3	152	500	103.0	149.7	590	600	1
4	183	600	123.9	179.7	700	800	1
5	203	660	148.2	214.7	812	1000	1

Points 1 and 2 were completed without incident, but 3/4 hour into point 3 the aft seal failed. The first indication of distress was smoke, and then seal temperature and bearing cavity pressure rose rapidly while rig speed decreased. The carbon lift pads had completely worn out and the seat was found to be burnt and distorted. The aft seal after the failure is shown in Figure 37. The forward seal had not worn during the endurance run. Test results during the endurance run are listed in Table XII.

Because two failures had occurred on the aft seal, it was decided to continue endurance testing with a conventional face seal in the aft position. The original self-acting face seal was still in the forward position.

Operation continued with 1/2 hour at points 1 and 2. An hour of operation at point 3 was completed and point 4 had been set when the forward self-acting face seal failed. Again, failure was characterized by a decrease in rig speed and a rapid increase in seal temperature. Inspection revealed that the lift pads had worn out and that the seat was burnt. Test results during the endurance run are listed in Table XIII. Note that airflows and cavity pressures are higher because of the use of the conventional seal in the aft position.

Inspection of the carbon nose revealed a taper of 0.0508 mm (0.0020 in.) from the outside diameter to the inside diameter, indicating the failure was associated with thermal distortion of the seat.

The face of the seat closest to the hot air expands faster than the face exposed to the oil side. This differential expansion tends to rotate the inside diameter of the seat toward the carbon sealing nose, which results in contact at the inside diameter of the sealing interface. This seat-carbon contact generates additional heat, which causes increasing distortion and further contact, heavier at the inside diameter.

Figure 37. Self-Acting Aft Seal Showing Condition After Failure.

TABLE XII. INITIAL ENDURANCE TEST RESULTS, SELF-ACTING SEAL

Speed		Air Pressure		Cavity Pressure		Airflow (Two Seals)			Aft Seal Temperature		Air Temperature	
(m/s)	(ft/sec)	(N/cm²)	(psia)	(N/cm²)	(psia)	(kg/s)	(scfm)	(lb/sec)	(K)	(°F)	(K)	(°F)
91	300	34.3	49.7	11.2	16.2	<.0006	<1	<.0013	407	273	426	307
91	300	34.3	49.7	11.5	16.7	.0006	1	.0013	415	288	448	347
91	300	34.3	49.7	11.5	16.7	.0006	1	.0013	421	298	465	376
91	300	34.3	49.7	11.5	16.7	.0006	1	.0013	434	321	488	418
122	400	55.0	79.7	11.6	16.9	.0013	2.2	.0028	440	333	479	404
122	400	55.0	79.7	11.5	16.7	.0012	2.0	.0025	421	298	448	346
122	400	55.0	79.7	11.5	16.7	.0010	1.8	.0023	427	310	472	390
122	400	55.0	79.7	11.6	16.9	.0010	1.8	.0023	442	336	488	418
152	500	103.0	149.7	13.6	19,7	.0032	5.5	.0070	493	428	525	486
152	500	103.0	149.7	14.3	20.7	.0038	6.5	.0083	509	454	544	520
152	500	103.0	149.7	14.3	20.7	.0046	8.0	.0010	511	460	554	536

TABLE XIII. SECOND ENDURANCE RUN RESULTS, SELF-ACTING SEAL

Speed		Air Pressure		Cavity Pressure		Airflow (Two Seals)			Forward Seal Temperature		Air Temperature	
(m/s)	(ft/sec)	(N/cm²)	(psia)	(N/cm²)	(psia)	(kg/s)	(scfm)	(lb/sec)	(K)	(°F)	(K)	(°F)
91	300	34.3	49.7	11.5	16.7	.0015	2.6	.0033	405	268	470	386
91	300	34.3	49.7	11.5	16.7	.0014	2.5	.0032	433	320	526	486
122	400	55.0	79.7	12.2	17.7	.0058	10.0	.0128	412	282	-	-
122	400	55.0	79.7	12.9	18.7	.0058	10.0	.0128	428	310	492	424
152	500	103.0	149.7	13.0	18.9	.0087	14.0	.0178	482	406	528	490
152	500	103.0	149.7	13.4	19.5	.0098	17.0	.0216	488	418	552	532
152	500	103.0	149.7	13.6	19.7	.0110	19.0	.0242	494	430	582	588
152	500	103.0	149.7	13.6	19.7	.0116	20.0	.0255	499	438	584	590

The final result is seal failure and the characteristic tapered wear.

To alleviate this problem, more oil flow was provided to cool the seat. Also, the spring force was reduced from 42 N (9.5 lb) to 31 N (7 lb).

A series of seven evaluation tests was then conducted as follows:

Test	Speed m/s	Speed ft/sec	Air Pressure N/cm^2	Air Pressure psia	Air Temperature K	Air Temperature ^oF	Total Package Oil Flow kg/hr	Total Package Oil Flow lb/hr	Time at Point hr
A	152	500	103.2	149.7	366	200	159	350	2.5
B	152	500	103.2	149.7	478	400	227	500	2.6
C	152	500	103.2	149.7	589	600	250	550	3.0
D	152	500	103.2	149.7	589	500	250	550	1.5
E	183	600	123.9	179.7	478	400	295	650	3.0
F	183	600	123.9	179.7	589	500	295	650	3.0
G	183	600	123.9	179.7	645	675	295	650	2.5

These tests were conducted with a self-acting face seal in the forward rig position and a conventional face seal in the aft postion.

During test B, airflow and cavity pressure readings were erratic, and package oil flow was increased to 227 kg/hr (500 lb/hr). During test C oil flow was increased again to 250 kg/hr (550 lb/hr).

For tests A and B the bearing and package incorporated eight 0.81 mm (0.032 in.) jets, six to the bearing and one to each of the seal runners. Therefore, 1/8 of the total package flow was for seal cooling. Prior to test C the rig was reworked with two bearing jets plugged and an additional jet opened to each seal runner. Therefore, from test C on, 1/4 of the total package flow was directed to the seal seat for cooling.

Test results for test G are listed in Table X. There was a normal shudown after the last point shown in Table XIV. At the next startup, bearing cavity pressure and air leakage were excessively high. Teardown revealed that the self-acting pads had worn out and the runner was burnt and discolored. The carbon face was worn on a 0.025 to 0.050 mm (0.001 to 0.002 in.) taper from the outside diameter to the inside diameter, again indicating that thermal distortion of the face plate caused initial contact at the inside diameter.

Some slight carbon wear occurred after each test. Average wear of four pads measured following each test is listed in Table XV.

TABLE XIV. EVALUATION TEST G RESULTS, SELF-ACTING SEAL

Speed	183 m/s (600 ft/sec)
Oil Flow	645 kg/hr (700 lb/hr)
Air Pressure	123.9 N/cm^2 (179.7 psia)
Time at Each Point	15 minutes

Cavity Pressure		Airflow			Seal Temperature		Air Temperature	
(N/cm^2)	(psia)	(kg/s)	(scfm)	(lb/sec)	(K)	(°F)	(K)	(°F)
37.8	54.7	.015	26.5	.034	500	440	623	660
37.0	53.7	.014	24.5	.031	511	460	631	675
37.8	54.7	.014	24.5	.031	524	484	623	660
37.8	54.7	.015	26.0	.033	526	486	609	636
38.4	55.7	.015	25.5	.032	522	480	-	-
38.4	55.7	.015	25.5	.032	512	462	-	-
38.4	55.7	.015	25.5	.032	513	464	-	-
37.8	54.7	.015	25.5	.032	518	474	-	-
38.4	55.7	.015	26.5	.034	527	488	-	-
38.4	55.7	.015	26.5	.034	526	486	-	-

TABLE XV. AVERAGE CARBON WEAR, SELF-ACTING SEAL

Test	Avg. Depth of Pockets		Avg. Wear	
	(mm)	(in.)	(mm)	(in.)
New	.0224	.000884	-	-
A	.0192	.000755	.0033	.000129
B	.0186	.000731	.0006	.000024
C	.0164	.000644	.0022	.000087
D & E	.0170	.000668	-	-
F	.0157	.000618	.0013	.000050

It was decided to continue endurance operation at reduced air temperatures to the following schedule:

Point	Speed m/s	Speed ft/sec	Air Pressure N/cm^2	Air Pressure psia	Air Temperature K	Air Temperature °F	Oil Flow kg/hr	Oil Flow lb/hr	Time hr
1	91	300	34.3	49.7	366	200	136	300	.5
2	122	400	55.0	79.7	366	200	182	400	.5
3	152	500	103.2	149.7	478	400	250	550	.5
4	183	600	123.9	179.7	589	500	295	650	4
5	152	500	103.2	149.7	478	400	250	550	.5
6	122	400	55.0	79.9	366	200	182	400	.5
7	91	300	34.3	49.7	366	200	136	300	.5

Self-acting face seals were installed in the forward and aft positions. Points 1 and 2 were completed, but as rig speed approached 152 m/s (500 ft/sec), a failure of the aft seal occurred. Inspection revealed the lift pads were completely worn out. Carbon face wear varied from 0.051 to 0.127 mm (0.002 to 0.005 in.). The forward seal carbon had worn approximately 0.0051 mm (0.0002 in.). Data taken are listed in Table XVI.

A conventional face seal was installed in the aft position and testing was contunued. As shown in Table XVI, test points 1 through 4 had been run when cavity pressure, seal temperature, and airflow readings started to fluctuate. The rig was disassembled and the self-acting seal was inspected. The seal was in good condition with no measureable wear.

Testing continued with oil flow increased 45.4 kg/hr (100 lb/hr) at each point. During test cycle point 4 the self-acting seal contacted the face plate. This occurrence was indicated by a reduction in rig speed and a rapid increase in seal temperature. The rig was shut down and restarted. Readings indicated that the seal had failed and was operating as a labyrinth. Disassembly confirmed this conclusion. The forward lift pads were completely worn out.

The test program to this point had indicated that thermal distortion of the face plate combined with dynamic effects resulted in failure of the self-acting seals.

TABLE XVI. CONTINUED ENDURANCE TEST RESULTS, SELF-ACTING SEAL

Test Cycle Point	Time min	Cavity Pressure (N/cm^2)	Cavity Pressure (psia)	Airflow (Two Seals) (kg/s)	Airflow (Two Seals) (scfm)	Airflow (Two Seals) (lb/sec)	Aft Seal Temperature (K)	Aft Seal Temperature (°F)
1	15	12.9	18.7	.0006	1.0	.0013	363	194
1	15	12.9	18.7	.0006	1.0	.0013	363	194
2	15	13.6	19.7	.0009	1.5	.0019	373	211
2	15	13.9	20.2	.0010	1.8	.0023	378	220
	Aft Seal Failure							
	Testing Continued With Conventional Seal in Aft Position							
							Fwd Seal Temperature	
1	15	13.9	20.2	.0013	2.3	.0029	368	204
1	15	13.9	20.2	.0013	2.2	.0028	370	205
2	15	16.4	23.7	.0026	4.6	.0059	381	226
2	15	16.4	23.7	.0028	4.8	.0061	382	228
3	15	23.2	33.7	.0064	11.0	.0140	409	276
3	15	23.2	33.7	.0066	11.5	.0147	424	304
4	15	30.8	44.7	.0121	21.0	.0268	472	390
4	15	35.7	51.7	.0159	27.5	.0350	474	394
4	15	35.7	51.7	.0144	25.0	.0320	498	437
4	15		Reading Fluctuations					
				Teardown				
1	15	14.6	21.2	.0013	2.4	.0031	371	208
1	15	15.0	21.7	.0016	2.7	.0034	371	208
2	15	17.0	24.7	.0024	4.2	.0053	382	228
2	15	17.0	24.7	.0026	4.5	.0057	382	228
3	15	24.6	35.7	.0066	11.5	.0146	410	279
3	15	26.7	38.7	.0078	13.5	.0172	430	314
4	15	33.6	48.7	.0116	20.0	.0254	465	378
4	15	35.7	51.7	.0133	23.0	.0293	499	438
4	15	35.0	50.7	.0133	23.0	.0293	498	436
				Shut Down				
3	15	37.0	53.7	.0156	27.0	.0344	455	360
3	15	41.2	59.7	.0182	31.5	.0402	578	580
4	15	44.7	64.7	.0231	40.0	.0510	567	560
4	15	48.8	70.7	.0231	40.0	.0510	565	558
4	15	48.8	70.7	.0231	40.0	.0510	567	560
4	15	49.4	71.7	.0231	40.0	.0510	567	560

To further explore the operating limits of the existing seals, 150 hours of endurance operation at ambient temperature was conducted as follows:

Speed		Air Pressure		Time
m/s	ft/sec	N/cm^2	psia	hr
102	334	103	149.7	28
122	400	103	149.7	22
137	450	103	149.7	65
145	475	103	149.7	20
145	475	124	179.7	15

Air temperature varied throughout the test but was generally from 372 to 408 K (200 to 275°F).

Test results are listed in Table XVII. Initially airflows were somewhat higher than in the evaluation testing performed previously, due probably to the lower spring force, 31 N (7 lb). After the 100-hour teardown, however, airflow increased significantly for no apparent reason. Teardown inspection revealed that an air leak had developed in the scavenge line. The test seals were in excellent condition after the 150-hour run. Seal components after testing are shown in Figure 38.

The aft seal carbon nose wore an average of 0.0044 mm (0.000175 in.) after the first 50 hours. No other wear occurred on the carbons or seats during the test.

Seal seat flatness in the assembled state was measured to be 1.8 μm (70 μin.). Axial runout was approximately 0.03 mm (0.0012 in.).

Oil flow to the bearing compartment was as follows:

Shaft Speed		Oil Flow	
m/s	ft/sec	kg/hr	lb/hr
102	334	182	400
122	400	182	400
137	450	205	450
145	475	205	450

	Speed		Air Pressure		Cavity Pressure		Airflow (Two Seals)			Fwd Seal Temp.		Aft Seal Temp.	
Hour	(m/s)	(ft/sec)	(N/cm²)	(psia)	(N/cm²)	(psia)	(kg/s)	(scfm)	(lb/sec)	(K)	(°F)	(K)	(°F)
1	102	334	103	149.7	15.1	21.9	.003	5.07	.006	362	191	360	189
2	102	334	103	149.7	15.0	21.7	.003	5.17	.007	367	200	366	198
Shut Down													
3	102	334	103	149.7	14.8	21.5	.003	5.30	.007	360	189	357	183
4	102	334	103	149.7	14.7	21.3	.003	4.95	.006	373	211	368	203
5	102	334	103	149.7	14.6	21.2	.003	4.85	.006	378	219	372	210
6	102	334	103	149.7	14.6	21.2	.003	4.80	.006	378	221	373	212
7	102	334	103	149.7	14.6	21.2	.003	4.68	.006	380	224	375	215
8	102	334	193	149.7	14.6	21.2	.003	4.70	.006	380	224	375	215
9	102	334	103	149.7	13.8	21.0	.003	4.68	.006	381	22[illegible]	377	218
Shut Down													
10	102	334	103	149.7	14.1	20.5	.003	4.95	.006	349	168	348	[illegible]
11	102	334	103	149.7	14.3	20.7	.003	4.90	.006	368	201	[illegible]	199
12	102	334	103	149.7	14.3	20.7	.003	4.90	.006	376	216	372	209
13	102	334	103	149.7	14.3	20.7	.003	4.88	.006	379	222	374	214
14	102	334	103	149.7	14.3	20.7	.003	5.00	.006	379	223	375	215
15	102	334	103	149.7	14.3	20.7	.003	4.98	.006	379	222	374	214
16	102	334	103	149.7	14.3	20.7	.003	4.98	.006	378	221	375	215
17	102	334	103	149.7	14.3	20.7	.003	4.90	.006	380	225	376	216
Shut Down													
18	102	334	103	149.7	14.3	20.7	.0[illegible]	5.13	.007	358	185	35[illegible]	182
19	102	334	103	149.7	14.3	20.7	[illegible]	5.20	.007	374	213	372	203
20	102	334	103	149.7	14.3	20.7	.003	5.35	.007	375	215	371	207
21	102	334	103	149.7	14.3	20.7	.003	5.25	.007	37[illegible]	21[illegible]	370	206
22	102	334	103	149.7	14.3	20.7	.003	5.05	.006	376	216	370	20[illegible]
23	102	334	103	149.7	14.3	20.7	.003	5.05	.006	377	218	371	208
24	102	334	103	149.7	14.3	20.7	.003	5.00	.006	378	220	372	209
Shut Down													
25	102	334	103	149.7	14.3	20.7	.003	5.22	.007	356	182	355	179
26	102	334	103	149.7	14.3	20.7	.003	5.17	.007	370	207	368	202
27	102	334	103	149.7	14.3	20.7	.003	5.22	.007	377	218	372	210
28	102	334	103	149.7	14.3	20.7	.003	5.30	.007	379	223	371	214
29	122	400	103	149.7	15.0	21.7	.004	6.25	.008	388	235	382	[illegible]
30	122	400	103	149.7	15.0	21.7	.004	6.30	.008	388	238	382	228
31	122	400	103	149.7	15.0	21.7	.004	6.30	.008	388	239	382	228
Shut Down													
32	122	400	103	149.7	14.3	20.7	.004	6.10	.008	354	176	350	170
33	122	400	103	149.7	14.8	21.4	.004	6.20	.008	366	198	364	196
34	122	400	103	149.7	14.8	21.5	.004	6.32	.008	379	223	374	213
35	122	400	103	149.7	15.0	21.7	.004	6.42	.008	384	232	378	220
36	122	400	103	149.7	15.0	21.7	.004	6.52	.008	385	233	378	221
37	122	400	103	149.7	15.0	21.7	.004	6.50	.008	382	228	378	220
38	122	400	103	149.7	15.0	21.7	.004	6.52	.008	386	234	379	222
39	122	400	103	149.7	15.0	21.7	.004	6.45	.008	387	236	379	223
Shut Down													
40	122	400	103	149.7	14.8	21.5	.004	6.25	.008	359	186	356	182
41	122	400	103	149.7	15.0	21.7	.004	6.30	.008	370	207	371	208
42	122	400	103	149.7	15.0	21.7	.004	6.38	.008	379	223	377	218
43	122	400	103	149.7	15.0	21.7	.004	6.45	.008	383	230	377	219
44	122	400	103	149.7	15.0	21.7	.004	6.43	.008	383	230	377	219
45	122	400	103	149.7	15.0	21.7	.004	6.38	.008	384	231	377	219
46	122	400	103	149.7	15.0	21.7	.004	6.35	.008	384	231	377	219
47	122	400	103	149.7	15.0	21.7	.004	6.48	.008	384	232	378	220
Shut Down													
48	122	400	103	149.7	14.8	21.5	.004	6.10	.008	364	195	362	191
49	122	400	103	149.7	15.0	21.7	.004	6.32	.008	379	222	375	215
50	122	400	103	149.7	15.0	21.7	.004	6.52	.008	384	232	380	224
Teardown for Inspection													

Table: TABLE XVII. 150-HOUR ENDURANCE TEST RESULTS SELF-ACTING SEAL

TABLE XVII - Continued

Hour	Speed (m/s)	Speed (ft/sec)	Air Pressure (N/cm²)	Air Pressure (psia)	Cavity Pressure (N/cm²)	Cavity Pressure (psia)	Airflow (Two Seals) (kg/s)	Airflow (Two Seals) (scfm)	Airflow (Two Seals) (lb/sec)	Fwd Seal Temp. (K)	Fwd Seal Temp. (°F)	Aft Seal Temp. (K)	Aft Seal Temp. (°F)
51	137	450	103	149.7	17.7	25.7	.004	7.6	.010	372	210	369	205
52	137	450	103	149.7	17.5	25.3	.004	7.5	.010	383	230	378	221
53	137	450	103	149.7	17.6	25.5	.005	7.9	.010	389	240	382	228
54	137	450	103	149.7	17.8	25.8	005	7.8	.010	391	244	384	232
55	137	450	103	149.7	17.7	25.7	.005	8.0	.010	390	243	383	230
56	137	450	103	149.7	17.4	25.2	.005	7.8	.010	390	243	385	233
Shut Down													
57	137	450	103	149.7	17.7	25.7	.005	9.0	.011	370	206	368	202
58	137	450	103	149.7	16.3	23.7	.004	6.8	.009	390	242	382	228
59	137	450	103	149.7	16.3	23.7	.004	6.6	.008	394	250	384	231
60	137	450	103	149.7	16.3	23.7	.004	6.6	.008	399	258	388	238
61	137	450	103	149.7	16.3	23.7	.004	6.7	.009	399	258	388	238
62	137	450	103	149.7	16.3	23.7	.004	6.7	.009	399	258	387	237
63	137	450	103	149.7	16.3	23.7	.004	6.7	.009	402	262	388	239
Shut Down													
64	137	450	103	149.7	16.2	23.5	.004	7.2	.009	374	213	372	210
65	137	450	103	149.7	16.0	23.2	.004	6.8	.009	387	236	381	227
66	137	450	103	149.7	15.9	23.0	.004	6.7	.009	397	255	389	240
67	137	450	103	149.7	15.7	22.7	.004	6.6	.008	403	264	393	247
68	137	450	103	149.7	15.7	22.7	.004	6.7	.009	404	265	392	246
69	137	450	103	149.7	15.7	22.7	.004	6.7	.009	403	264	390	243
70	137	450	103	149.7	15.7	22.7	.004	6.6	.008	403	264	392	246
71	137	450	103	149.7	15.7	22.7	.004	6.5	.008	403	264	392	246
Shut Down													
72	137	450	103	149.7	16.3	23.7	.004	7.1	.009	376	216	373	212
73	137	450	103	149.7	16.2	23.5	.004	7.0	.009	386	235	381	227
Shut Down													
74	137	450	103	149.7	15.7	22.7	.004	6.8	.009	397	254	387	237
75	137	450	103	149.7	15.7	22.7	.004	6.4	.008	403	264	391	244
76	137	450	103	149.7	15.7	22.7	.004	6.5	.008	402	262	389	241
77	137	450	103	149.7	16.3	23.7	.004	7.0	.009	395	251	386	235
78	137	450	103	149.7	15.9	23.0	.004	6.5	.008	400	259	389	241
Shut Down													
79	137	450	103	149.7	15.9	23.1	.004	7.2	.009	370	206	370	206
80	137	450	103	149.7	15.9	23.1	.004	7.0	.009	380	22[illegible]	378	220
81	137	450	103	149.7	16.0	23.2	.004	7.0	.009	392	246	384	232
82	137	450	103	149.7	15.9	23.1	.004	6.9	.009	394	249	384	232
83	137	450	103	149.7	15.9	23.1	.004	6.9	.009	396	252	385	233
84	137	450	103	149.7	15.7	22.8	.004	6.8	.009	396	253	387	236
85	137	450	103	149.7	15.7	22.7	.004	6.8	.009	397	254	388	238
86	137	450	103	149.7	15.7	22.7	.004	6.8	.009	397	254	388	238
Shut Down													
87	137	450	103	149.7	15.7	22.7	.004	7.0	.009	378	220	377	218
88	137	450	103	149.7	15.8	22.9	.004	6.8	.009	392	246	386	235
89	137	450	103	149.7	15.7	22.7	.004	6.4	.008	402	262	391	244
90	137	450	103	149.7	15.7	22.7	.004	6.4	.008	404	266	392	246
91	137	450	103	149.7	15.7	22.7	.004	6.4	.008	405	267	391	245
92	137	450	103	149.7	15.7	22.7	.004	6.5	.008	405	268	394	248
93	137	450	103	149.7	15.7	22.7	.004	6.6	.008	406	270	394	249
Shut Down													
94	137	450	103	149.7	15.9	23.0	.004	6.9	.009	374	214	374	213
95	137	450	103	149.7	15.8	22.9	.004	6.7	.009	390	242	386	234
96	137	450	103	149.7	15.8	22.9	.004	6.5	.008	400	260	390	243
97	137	450	103	149.7	15.7	22.8	.004	6.4	.008	404	266	392	246
98	137	450	103	149.7	15.7	22.8	.004	6.4	.008	405	267	393	247
99	137	450	103	149.7	15.7	22.7	.004	6.4	.008	405	268	394	248
100	137	450	103	149.7	15.7	22.7	.004	6.4	.008	405	268	393	247
Teardown for Inspection													

Hour	Speed (m/s)	Speed (ft/sec)	Air Pressure (N/cm²)	Air Pressure (psia)	Cavity Pressure (N/cm²)	Cavity Pressure (psia)	Airflow (Two Seals) (kg/s)	Airflow (Two Seals) (scfm)	Airflow (Two Seals) (lb/sec)	Fwd Seal Temp. (K)	Fwd Seal Temp. (°F)	Aft Seal Temp. (K)	Aft Seal Temp. (°F)
101	137	450	103	149.7	18.4	26.7	.005	9.5	.012	378	220	377	219
102	137	450	103	149.7	18.4	26.7	.005	9.2	.012	394	250	386	234
						Shut Down							
103	137	450	103	149.7	17.0	24.7	.005	9.5	.012	369	204	372	210
104	137	450	103	149.7	17.0	24.7	.005	8.8	.011	385	233	381	226
105	137	450	103	149.7	17.0	24.7	.005	9.0	.011	390	243	386	234
106	137	450	103	149.7	17.0	24.7	.005	8.7	.011	398	256	388	238
107	137	450	103	149.7	16.7	24.2	.005	8.4	.011	404	266	391	244
108	137	450	103	149.7	16.9	24.5	.005	8.2	.011	404	266	390	243
109	137	450	103	149.7	17.0	24.7	.005	9.0	.011	400	259	388	238
						Shut Dow							
110	137	450	103	149.7	17.0	24.7	.005	8.7	.011	367	200	368	202
111	137	450	103	149.7	17.0	24.7	.005	8.9	.011	382	227	378	220
112	137	450	103	149.7	17.0	24.7	.005	8.7	.011	395	251	386	234
113	137	450	103	149.7	17.0	24.7	.005	8.4	.011	400	259	388	238
114	137	450	103	149.7	17.0	24.7	.005	8.4	.011	401	260	388	238
115	137	450	103	149.7	17.0	24.7	.005	8.4	.011	401	260	388	239
116	145	475	103	149.7	17.0	24.7	.005	8.6	.011	405	268	393	247
117	145	475	103	149.7	17.0	24.7	.005	8.7	.011	406	270	393	247
						Shut Down							
118	145	475	103	149.7	17.4	25.2	.006	9.6	.012	378	221	378	220
119	145	475	103	149.7	17.4	25.3	.005	9.1	.012	[illegible]	247	387	236
120	145	475	103	149.7	17.1	24.8	.005	8.7	.011	400	260	389	241
121	145	475	103	149.7	17.2	24.9	.005	8.5	.011	405	268	393	247
122	145	475	103	149.7	17.0	24.7	.005	8.5	.011	403	264	392	246
123	145	475	103	149.7	17.0	24.7	.005	8.7	.011	402	262	390	242
124	145	475	103	149.7	17.0	24.7	.005	8.2	.010	407	271	394	250
						Shut Down							
125	145	475	103	149.7	17.4	25.2	.006	9.6	.012	377	219	377	218
126	145	475	103	149.7	17.4	25.2	.005	9.4	.012	392	246	384	232
127	145	475	103	149.7	17.1	24.8	.005	9.1	.012	402	262	389	240
128	145	475	103	149.7	17.0	24.7	.005	8.9	.011	405	267	390	242
129	145	475	103	149.7	17.0	24.7	.005	9.0	.011	406	270	391	244
130	145	475	103	149.7	17.0	24.7	.005	8.9	.011	407	272	392	246
131	145	475	103	149.7	17.2	24.9	.006	10.0	.013	397	255	387	236
						Shut Down							
132	145	475	103	149.7	16.7	24.3	.005	9.0	.011	388	239	383	229
133	145	475	103	149.7	17.0	24.7	.005	8.5	.011	399	258	390	242
134	145	475	103	149.7	16.7	24.2	.005	8.5	.011	402	263	390	242
135	145	475	103	149.7	16.7	24.2	.005	8.3	.011	405	268	394	248
136	145	475	124	179.7	19.1	27.7	.008	13.0	.017	404	266	388	238
137	145	475	124	179.7	19.1	27.7	.008	13.0	.017	402	262	386	234
138	145	475	124	179.7	19.1	27.7	.008	13.0	.017	398	256	383	230
						Shut Down							
139	145	475	124	179.7	18.4	26.7	.008	13.0	.017	394	[illegible]	380	225
140	145	475	124	179.7	19.1	27.7	.008	13.0	.017	396	253	379	222
141	145	475	124	179.7	20.1	28.2	.008	13.0	.017	392	246	377	218
142	145	475	124	179.7	20.1	28.2	.008	13.0	.017	390	244	377	219
143	145	475	124	179.7	19.2	27.8	.008	13.0	.017	391	245	378	220
144	145	475	124	179.7	19.1	27.7	.008	13.0	.017	391	245	378	220
145	145	475	124	179.7	20.1	28.2	.008	13.0	.017	394	250	379	223
146	145	475	124	179.7	19.1	27.7	.008	13.0	.017	394	250	379	223
						Shut Down							
147	145	475	124	179.7	19.1	27.7	.008	13.5	.017	392	246	382	228
148	145	475	124	179.7	19.1	27.7	.008	13.5	.017	391	245	301	227
149	145	475	124	179.7	18.4	26.7	.008	13.0	.017	392	246	381	227
150	145	475	124	179.7	18.4	26.7	.008	13.0	.017	395	251	384	231
End													

Table: TABLE XVII - Continued

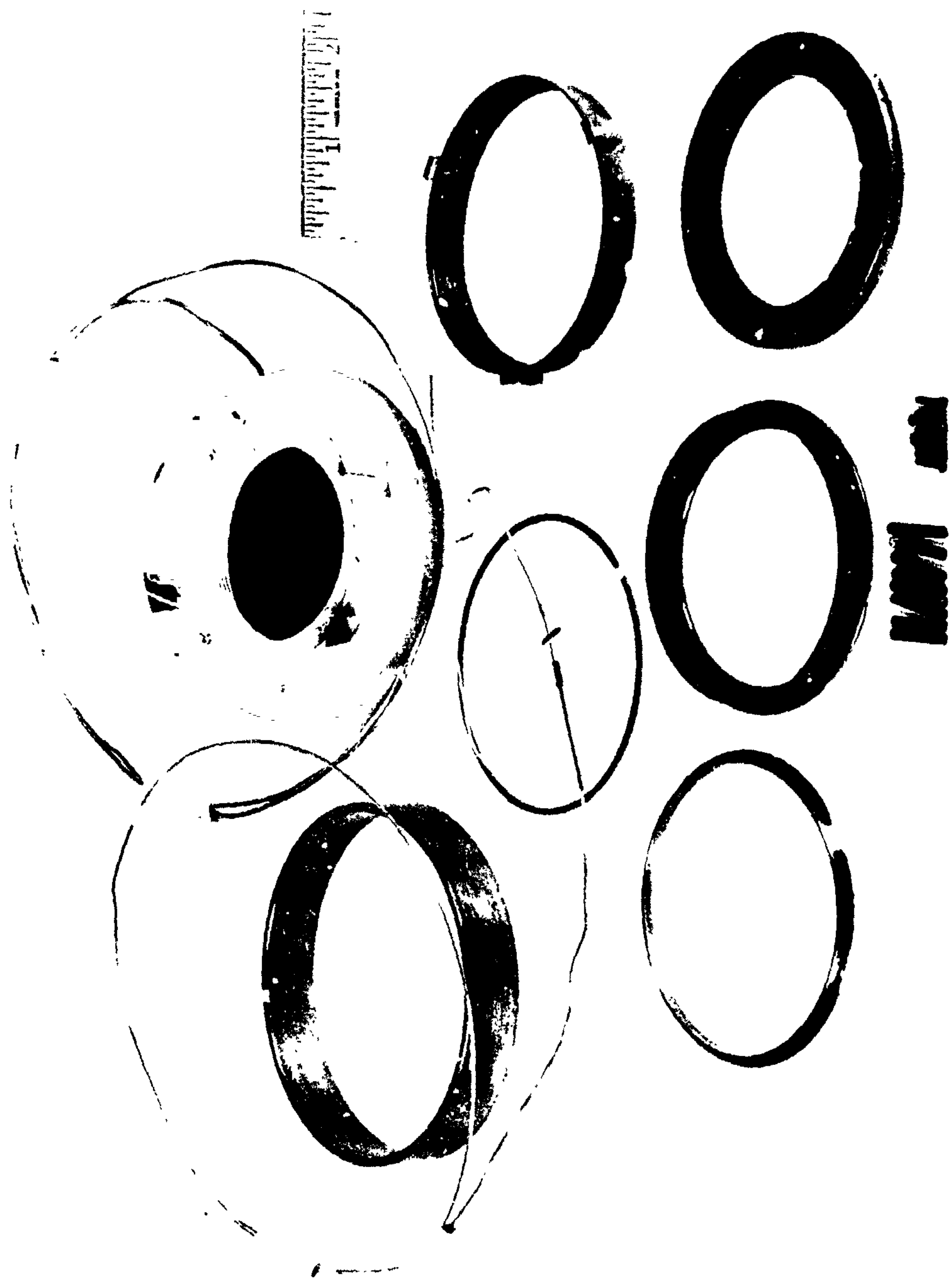

Figure 38. Self-Acting Face Seal Compcnents After 150-Hour Test.

The bearing was fed by four 0.81 mm (0.032 in.) diameter jets, and two 0.81 mm (0.032 in.) diameter jets were directed at each self-acting face seal dam. Oil-in temperature was 366 K (200°F), and MIL-L-23699 oil was used.

Self-Acting Circumferential Seal

Design

The self-acting circumferential seal configuration is shown in Figure 39. It is similar to a conventional circumferential seal with the addition of self-acting geometry on the carbon bore for lift augmentation. A detail of a carbon segment illustrating the self-acting geometry is shown in Figure 40.

The seal is internally pressurized with two rings, made up of three carbon segments each, comprising the sealing elements. The segment joints are overlapped and an antirotation lock in the center of the seal prevents the segments from turning with the shaft.

Test Results

Initially, two evaluation tests were conducted over a range of speeds and internal seal air pressures at ambient air temperatures. Test conditions and resulting airflows and bearing cavity pressures are listed in Table XVIII. Each run was of 15 minutes duration. Two thermocouples were placed adjacent to each oil-side and air-side carbon ring as shown in Figure 39, and resulting temperatures are listed in Table XIX. Some of the instrumentation was not operative in test II.

After test I, carbon wear was noted on the sealing dams and half way across the pad lands (Figures 41 and 42). The wear was in the order of 0.0102 mm (0.0004 in.) at the sealing dam. The carbon bores had been manufactured with a taper of 0.204 mm (0.0008 in.) from the sealing dam to the opposite end in order to account for possible distortion of the seal runner.

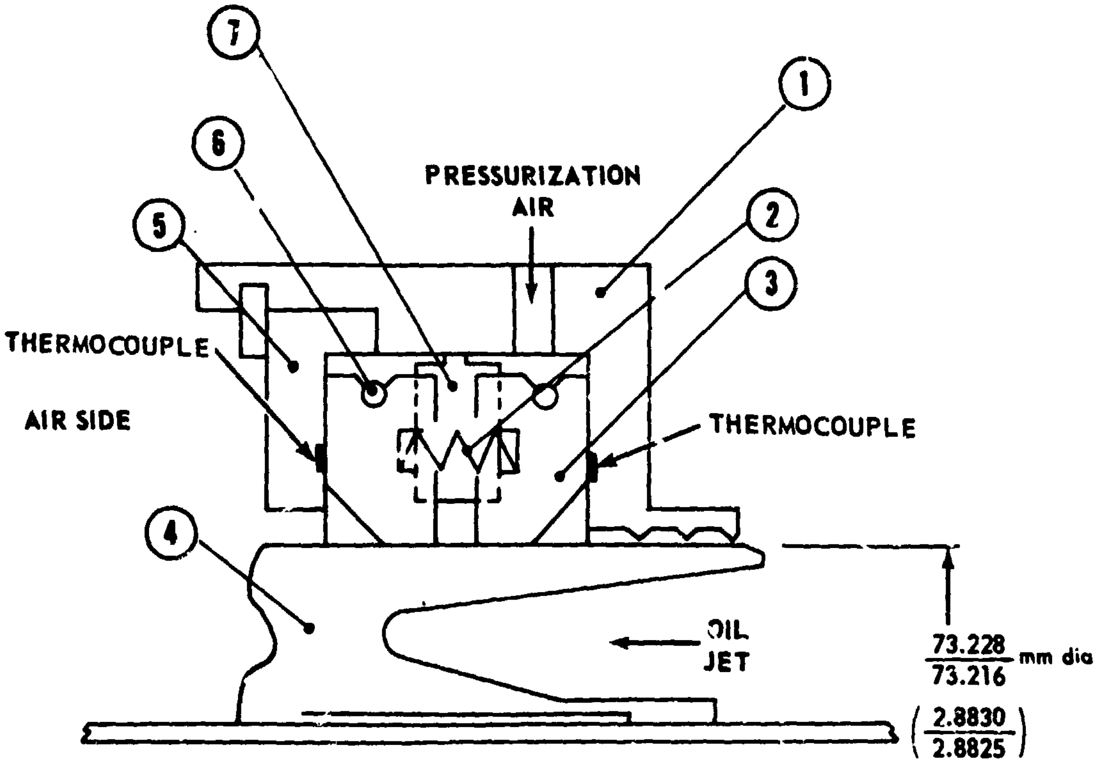

1. SEAL CASE	18-8 STAINLESS STEEL
2. COMPRESSION SPRING	INCONEL X
3. CARBON SEGMENT	HIGH-TEMPERATURE CARBON
4. RUNNER	AMS 6382 FLAME SPRAYED WITH LCIC CHROME CARBIDE
5. SEALING PLATE	18-8 STAINLESS STEEL
6. GARTER SPRING	INCONEL X .71 N (.159 lb)
7. ANTIROTATION LOCK	18-8 STAINLESS STEEL

Figure 39. Self-Acting Circumferential Seal.

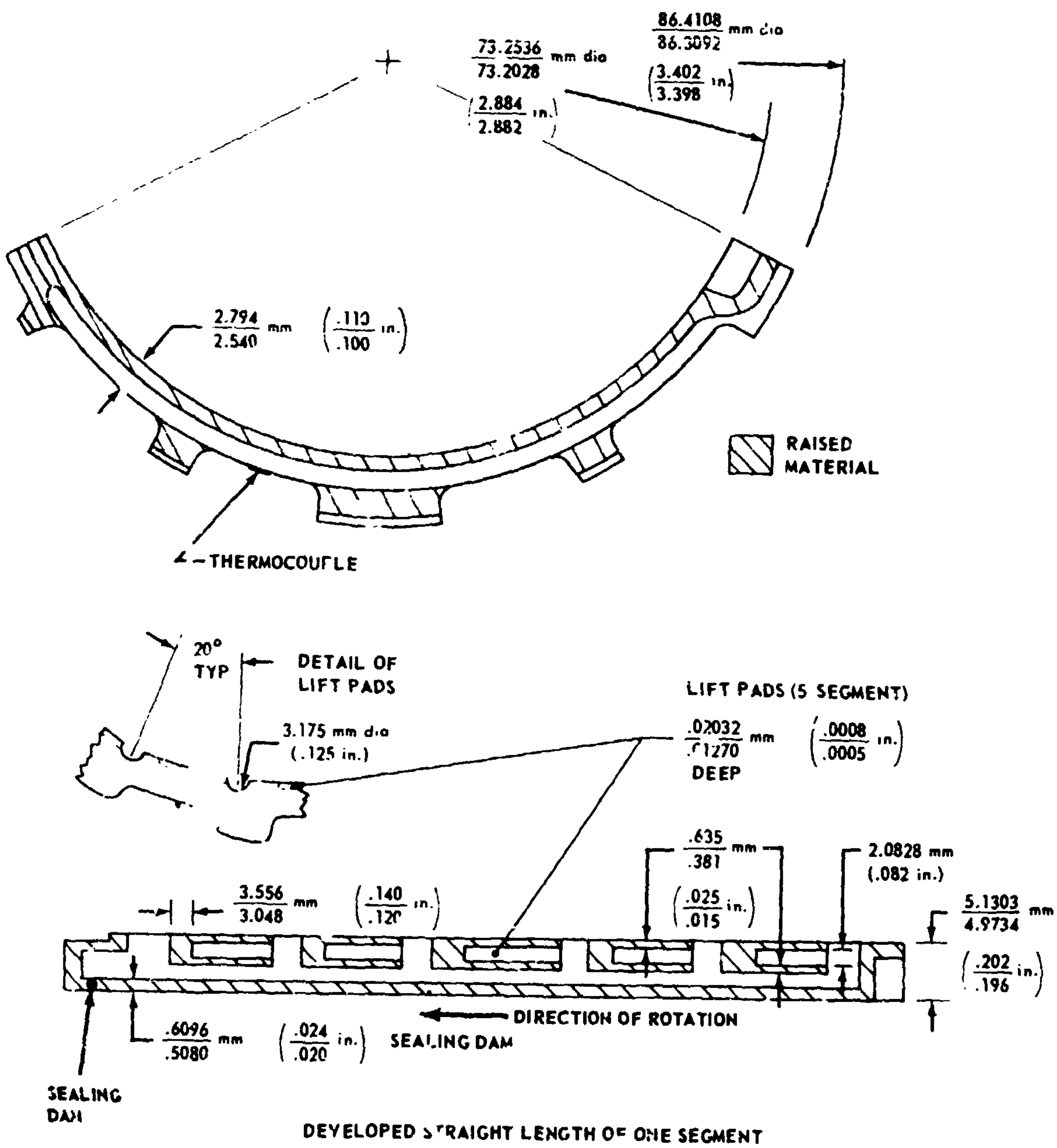

Figure 40. Details of Carbon Segment, Self-Acting Circumferential Seal.

TABLE XVIII. RESULTS OF TESTS I AND II, SELF-ACTING CIRCUMFERENTIAL SEAL

Test	Run	Speed (m/s)	Speed (ft/sec)	Air Pressure (N/cm²)	Air Pressure (psia)	Cavity Pressure (N/cm²)	Cavity Pressure (psia)	Airflow (Two Seals) (kg/s)	Airflow (Two Seals) (scfm)	Airflow (Two Seals) (lb/sec)	Oil Flow (kg/hr)	Oil Flow (lb/hr)
I	1	91	300	34.3	49.7	10.5	15.3	.0005	.8	.0011	75	166
	2	122	400	34.3	49.7	10.5	15.3	.0005	.8	.0011	95	210
	3	152	500	34.3	49.7	10.8	15.6	.0005	.8	.0011	115	254
	4	91	300	55	79.7	10.8	15.7	.0007	1.2	.0015	75	166
	5	122	400	55	79.7	10.8	15.7	.0007	1.2	.0015	95	210
	6	152	500	55	79.7	10.9	15.8	.0007	1.2	.0015	115	254
	7	91	300	34.3	49.7	10.6	15.4	.0005	.8	.0010	75	166
	8	122	400	34.3	49.7	10.6	15.4	.0005	.8	.0010	95	210
	9	152	500	34.3	49.7	10.8	15.6	.0005	.8	.0010	115	254
	10	183	600	34.3	49.7	11.0	15.9	.0005	.8	.0010	142	314
	11	91	300	55	79.7	10.8	15.7	.0005	.9	.0011	75	166
	12	122	400	55	79.7	10.8	15.7	.0005	.9	.0011	95	210
	13	152	500	55	79.7	10.9	15.8	.0005	.9	.0011	115	254
	14	183	600	55	79.7	11.2	16.3	-	-	-	142	314
	15	122	400	89.4	129.7	11.2	16.3	.0014	2.5	.0032	95	210
	16	152	500	89.4	129.7	11.5	16.7	.0018	3.2	.0041	115	254
II	17	91	300	34.3	49.7	10.8	15.7	.0005	.8	.0010	75	166
	18	122	400	34.3	49.7	10.8	15.7	.0005	.8	.0010	95	210
	19	152	500	34.3	49.7	10.8	15.7	.0005	.8	.0010	115	254
	20	183	600	34.3	49.7	11.0	16.0	.0005	.8	.0010	142	314
	21	213	700	34.3	49.7	11.2	16.3	.0005	.8	.0010	170	374
	22	122	400	55	79.7	10.8	15.7	.0006	1.0	.0013	95	210
	23	152	500	55	79.7	11.0	15.9	.0006	1.0	.0013	115	254
	24	183	600	55	79.7	11.1	16.1	.0006	1.0	.0013	142	314
	25	213	700	55	79.7	11.4	16.5	.0006	1.1	.0014	170	374
	26	122	400	79.1	114.7	11.5	16.7	.0016	2.7	.0034	95	210
	27	152	500	79.1	114.7	11.6	16.8	.0012	2.0	.0025	115	254
	28	183	600	79.1	114.7	11.9	17.3	.0014	2.5	.0032	142	314
	29	213	700	79.1	114.7	12.6	18.3	.0017	3.0	.0038	170	374
	30	152	500	103	149.7	12.9	18.7	.0021	3.6	.0046	115	254
	31	183	600	103	149.7	13.6	19.7	.0035	6.0	.0076	142	314
	32	213	700	103	149.7	13.7	19.9	.0023	4.0	.0051	170	374
	33	152	500	123.9	179.7	12.9	18.7	.0021	3.7	.0047	115	254
	34	183	600	123.9	179.7	13.2	19.2	.0017	3.0	.0038	142	314
	35	213	700	123.9	179.7	13.6	19.7	.0023	4.0	.0051	170	374

TABLE XIX. SEAL CARBON TEMPERATURES SELF-ACTING CIRCUMFERENTIAL SEAL

Test	Run	Aft Seal Temperature				Forward Seal Temperature			
		Oil Side		Air Side		Oil Side		Air Side	
		(K)	(°F)	(K)	(°F)	(K)	(°F)	(K)	(°F)
I	1	405/423	270/300	411/411	280/280	417/408	290/275	406/411	270/280
	2	433/450	320/350	444/450	340/350	436/428	325/310	423/423	300/300
	3	455/466	360/380	433/444	320/340	436/444	325/340	428/423	310/300
	4	461/455	370/360	455/428	360/310	444/450	340/370	439/439	330/330
	5	466/472	380/390	461/450	370/350	450/455	350/360	439/439	330/330
	6	466/478	380/400	458/455	365/360	461/461	370/370	439/439	330/330
	7	472/478	390/400	463/481	375/405	489/466	420/380	450/436	350/325
	8	439/455	330/360	444/450	340/350	423/423	305/300	423/423	300/300
	9	442/461	335/370	450/455	350/360	431/428	315/310	431/423	315/300
	10	442/466	335/380	452/461	355/370	433/433	320/320	433/428	320/310
	11	450/472	350/390	455/455	360/360	433/423	320/300	417/406	290/270
	12	455/458	360/365	461/466	370/380	442/428	335/310	423/417	300/290
	13	472/489	390/420	478/478	400/400	455/444	360/340	439/433	330/320
	14	472/492	390/425	478/492	400/425	469/452	385/355	444/444	340/340
	15	500/516	440/470	500/494	440/430	466/450	380/350	450/444	350/340
	16	494/516	430/470	489/494	420/430	463/450	375/350	461/455	370/360
II	17	378	220			383/394	230/250	361/378	190/220
	18	397	255			383/394	230/250	378/411	220/280
	19	414	285			408/411	265/280	400/405	260/270
	20	423	300			423/433	300/320	417/428	290/310
	21	433	320			447/461	345/370	439/453	330/355
	22	433	320			428/436	310/325	423/425	300/30[illegible]
	23	433	320			450/450	350/350	442/439	335/330
	24	436	325			453/461	355/370	436/453	325/355
	25	461	370			478/489	400/420	463/423	375/300
	26	444	340			423/439	300/330	455/428	360/310
	27	450	350			466/447	380/345	433/428	320/310
	28	461	370			450/453	350/355	439/444	330/340
	29	466	380			444/455	340/360	439/439	330/330
	30	500	440			444/455	340/360	423/405	300/270
	31	545	520			455/483	360/410	463/461	375/370
	32	534	500			461/534	370/500	466/522	380/480
	33	611	640			514/550	465/530	494/567	430/560
	34	617	650			628/606	670/630	597/600	615/620
	35	578	580			589/578	600/580	572/556	570/540

Figure 41. Condition of Carbon and Runners After Test I.

Figure 42. Carbon Segment After Test I, Self-Acting Circumferential Seal.

During test II, carbon wear was excessive: 0.305 to 0.737 mm (0.012 to 0.029 in.) radial wear. The lift pads had completely worn out and there was grooving on both runners. Seal carbon temperatures (Table XIX) were recorded as high as 628 K (670°F) and there were brief excursions as high as 700 K (800°F).

Typical traces of the lift pads prior to operation and after test I are shown in Figure 43. Note the taper on the sealing dam. In addition to tracing the lift pad profile, traces were taken of the runner, seal case, and seal plate. Inspection data are listed in Table XX. No axial wear of the carbon segments was noted throughout the test program.

Testing continued with an effort to determine the regimes of operation within which the seal could operate successfully. A 10-hour test was conducted at the following conditions:

Speed	91 m/s (300 ft/sec)
Air pressure	55 N/cm^2 (80 psia)
Air temperature	Ambient

Operating parameters held constant throughout the test as follows:

Airflow into bearing cavity through two seals - 0.0009 kg/s (0.0019 lb/sec or 1.5 scfm)

Bearing cavity pressure - 11.2 N/cm^2 (16.3 psia)

Carbon temperature

Forward seal

Oil-side carbon - Not instrumented
Air-side carbon - 428 K max (310°F)

Aft seal

Oil-side carbon - 450 K max (350°F)
Air-side carbon - 447 K max (345°F)

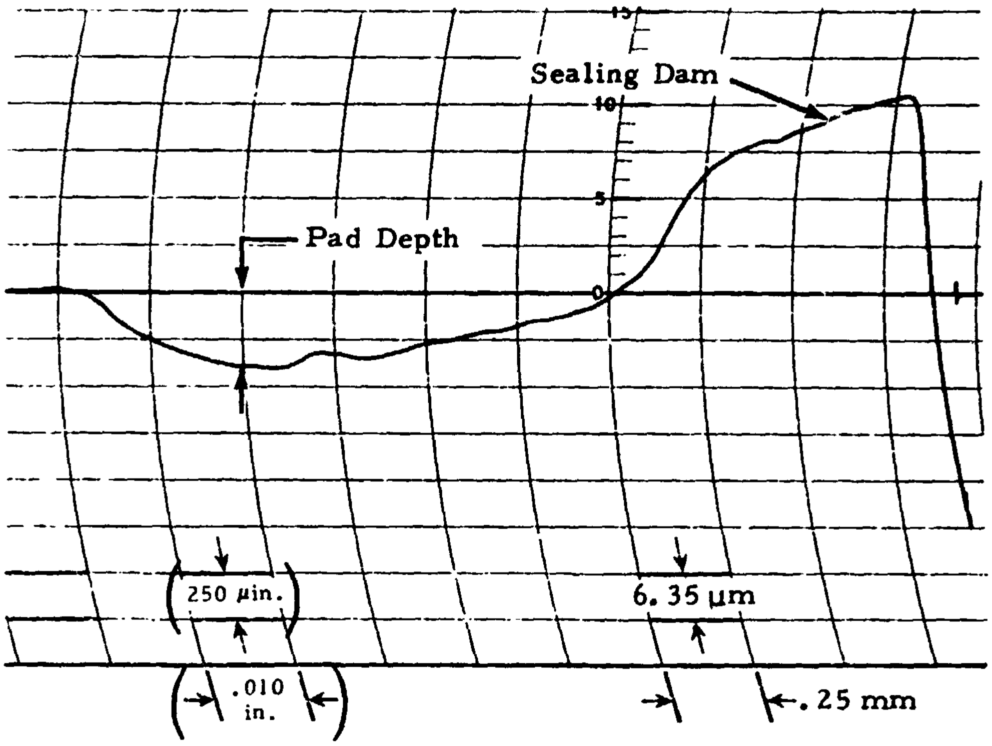

Before Operation

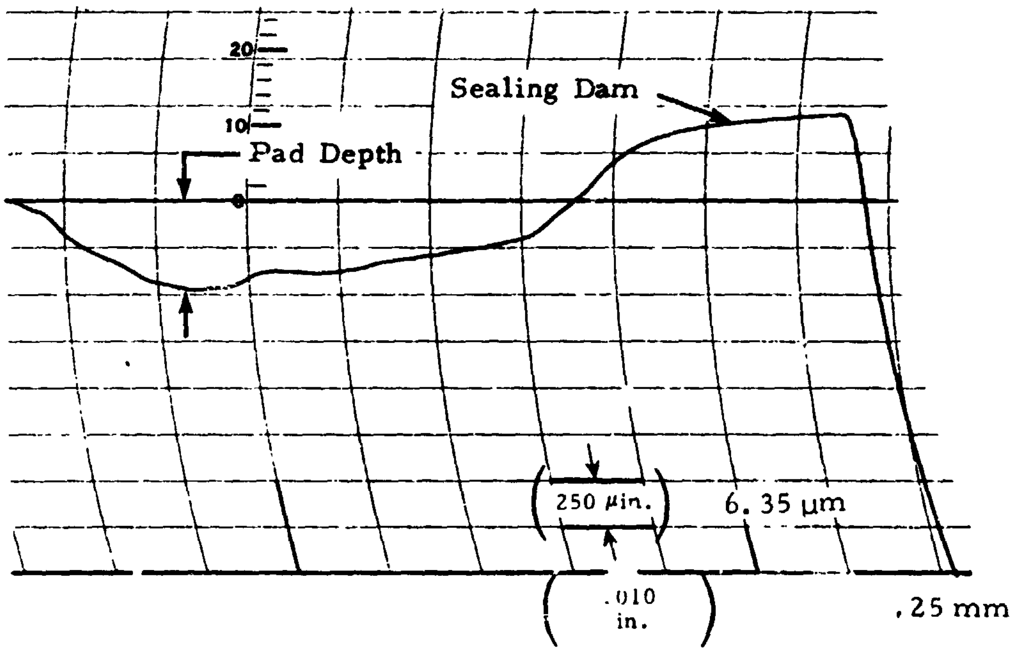

After Test I

Figure 43. Typical Lift Pad Trace, Self-Acting Circumferential Seal.

TABLE XX. SELF-ACTING CIRCUMFERENTIAL SEAL TEST DATA						
	New		After Test I		After Test II	
Fwd Seal						
Runner (Air-Side Contact)						
Roundness, µm (µin.)	.635	(25)	2.04	(80)	30.5	(1200)
Waviness, µm (µin.)	-	-	1.02	(40)	2.54	(100)
Roughness, µm (µin. AA)	.05	(2)	.38	(15)	-	-
Runner (Oil-Side Contact)						
Roundness, µm (µin.)	.635	(25)	2.04	(80)	22.8	(900)
Waviness, µm (µin.)	-	-	1.02	(40)	5.34	(210)
Roughness, µm (µin. AA)	.051	(2)	.38	(15)	-	-
Case						
Flatness, µm (µin.)	3.81	(150)	7.11	(280)	16.0	(630)
Waviness, µm (µin.)	.71	(28)	.51	(20)	1.14	(45)
Roughness, µm (µin. AA)	.38	(15)	.36	(14)	.25	(10)
Plate						
Flatness, µm (µin.)	1.27	(50)	21.4	(840)	30.5	(1200)
Waviness, µm (µin.)	.43	(17)	.41	(16)	.25	(10)
Roughness, µm (µin. AA)	.13	(5)	.18	(7)	.13	(5)
Aft Seal						
Runner (Air-Side Contact)						
Roundness, µm (µin.)	1.91	(75)	2.04	(80)	19.1	(750)
Waviness, µm (µin.)	1.52	(60)	1.27	(50)	9.4	(370)
Roughness, µm (µin. AA)	.08	(3)	.36	(14)	-	-
Runner (Oil-Side Contact)						
Roundness, µm (µin.)	1.91	(75)	2.04	(80)	38.1	(1500)
Waviness, µm (µin.)	1.52	(60)	1.27	(50)	58.5	(2300)
Roughness, µm (µin. AA)	.076	(3)	.36	(14)	-	-
Case						
Flatness, µm (µin.)	2.54	(100)	14.7	(580)	14.0	(550)
Waviness, µm (µin.)	.46	(18)	.76	(30)	.84	(33)
Roughness, µm (µin. AA)	.18	(7)	.18	(7)	.18	(7)
Plate						
Flatness, µm (µin.)	3.05	(120)	22.4	(880)	24.2	(950)
Waviness, µm (µin.)	.46	(18)	.64	(25)	.51	(20)
Roughness, µm (µin. AA)	.23	(9)	.25	(10)	.25	(10)

Inspection of the seals following test revealed light carbon wear at the sealing dams in the order of 0.0102 mm (0.0004 in.). The runners exhibited a full light carbon pattern on the oil side and a single light line corresponding to the sealing dam on the air side.

Testing continued with a 10-hour run at the following conditions:

Speed	122 m/s (400 ft/sec)
Air pressure	79 N/cm^2 (115 psia)
Air temperature	Ambient

Operating parameters held constant throughout the test as follows:

Airflow into bearing cavity through two seals - 0.012 kg/s (0.0026 lb/sec or 2.0 scfm)

Bearing cavity pressure - 11.2 N/cm^2 (16.3 psia)

Carbon temperature

Forward seal

Oil-side carbon - 514 K max (465°F)
Air-side carbon - 514 K max (465°F)

Aft seal

Oil-side carbon - 517 K max (470°F)
Air-side carbon - Not instrumented

Inspection of the seals following test revealed excessive wear of the forward seal. Seal dam wear varied from 0.036 to 0.228 mm (0.0014 to 0.009 in.). The lift pads were completely worn out.

The aft seal revealed carbon wear at the sealing dam of 0.0102 mm (0.0004 in.).

The runners after testing are shown in Figure 44. Surface roughness traces of the forward seal runner following the first and second 10-hour test are shown in Figure 45. During the self-acting circumferential seal test program, airflow into the bearing cavity and

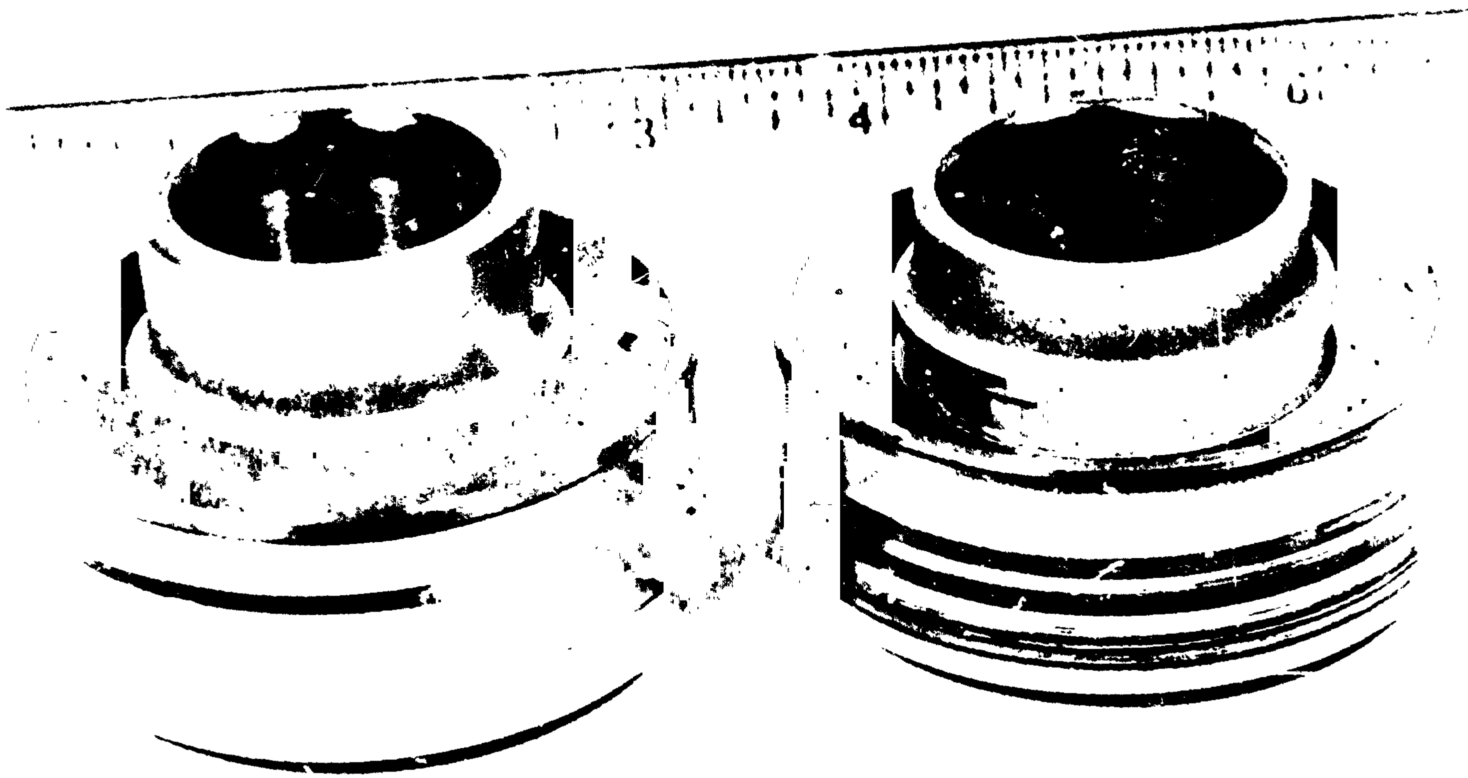

Figure 44. Seal Runners After Test, Self-Acting Circumferential Seal.

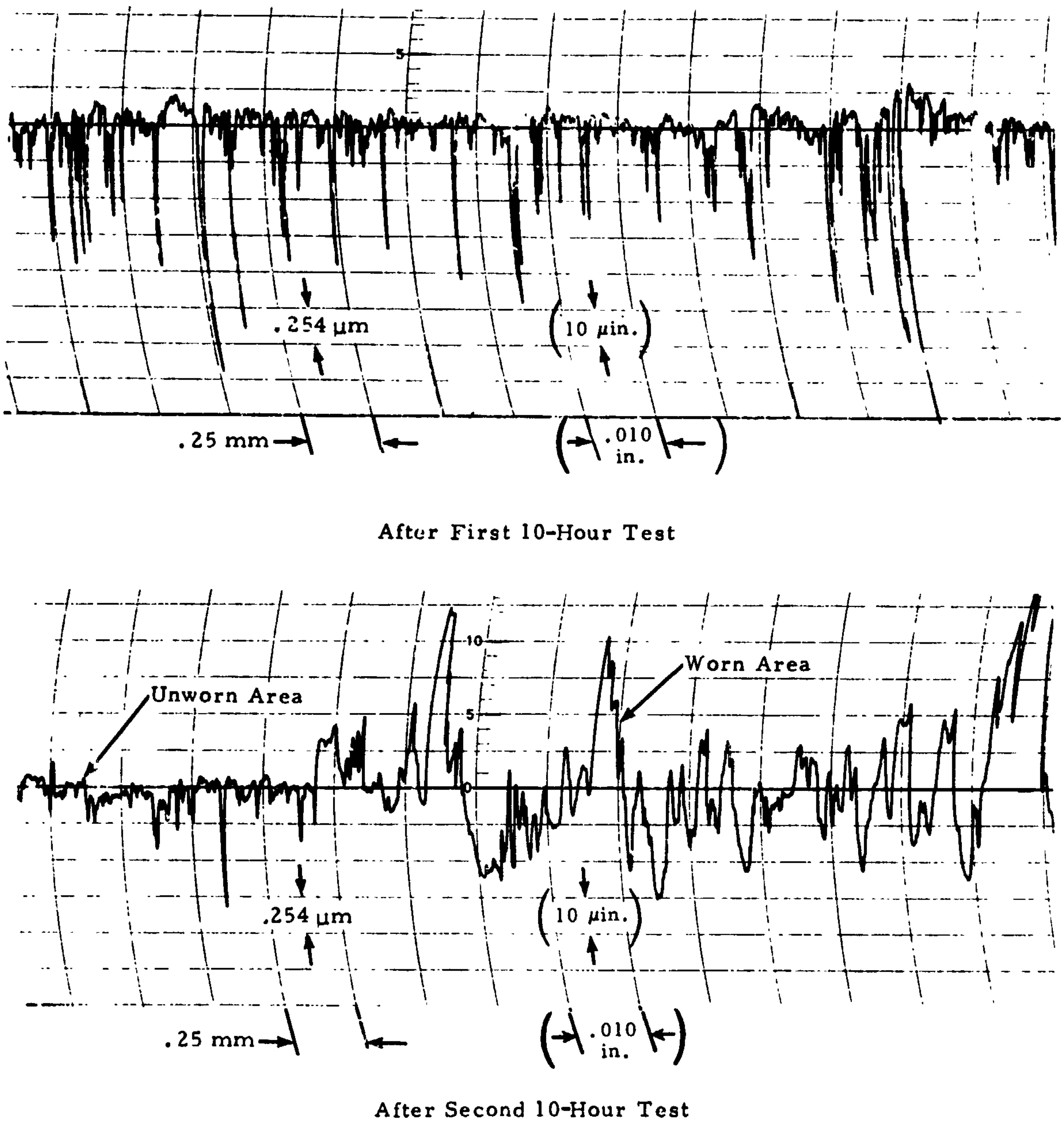

Figure 45. Roughness Traces of Forward Seal Runner, Self-Acting Circumferential Seal.

carbon temperature increased with increasing air pressure. These paremeters did not appear to change significantly with speed. Envelopes of the airflow and temperature data recorded in the test program are shown in Figures 46 and 47.

Total oil flow to the bearing compartment was varied with speed as follows:

Shaft Speed		Oil Flow	
m/s	ft/sec	kg/hr	lb/hr
91	300	75	166
122	400	95	210
152	500	115	254
183	600	143	314
213	700	170	374

The bearing was fed by four 0.81 mm (0.032 in.) jets and each seal runner was under cooled by one 0.81 mm (0.032 in.) jet. Oil-in temperature was 366 K (200°F). MIL-L-23699 oil was used.

Failure of the seal to operate successfully at speeds of 122 m/s (400 ft/sec) and pressure differentials of 79 N/cm^2 (115 psia) was attributed to insufficient lift force generated by the self-acting geometry. The 0.0204 mm (0.0008 in.) taper contributed to the inability of the pads to produce sufficient lift force. The self-acting geometry (Figure 48) was redesigned, which will increase the lift force. No taper will be incorporated.

Discussion of Test Results

A comparison of the performance of the various seal configurations is shown in Figure 49. The plot shows that self-acting face seals have the potential of significantly reducing airflow as compared to the conventional seals.

Of the conventional configurations, face seals allowed the least airflows at high pressure differentials. Circumferential segmented seals are as tight as face seals at moderate operating conditons; however, experience and the subject test program results have shown that at pressure differentials above approximately 41.4 N/cm^2 (60 psi) and speeds above approximately 107 m/s (350 ft/sec) circumferential segmented seals wear out and finally operate as labyrinths. In that case there is little to choose between circumferential, rotating ring, and labyrinth seals in terms of airflow.

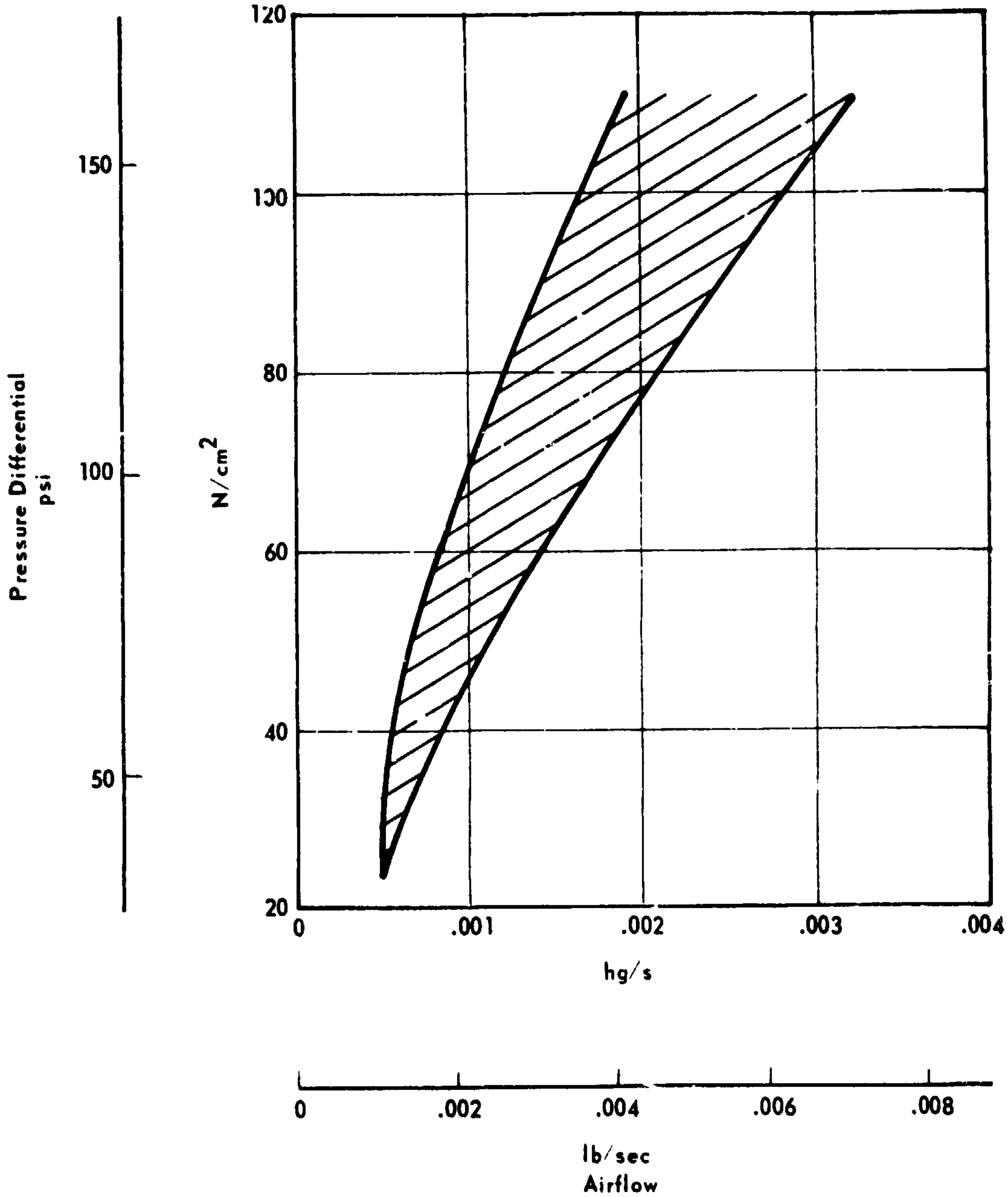

Figure 46. Envelope of Airflow Through Two Self-Acting Circumferential Seals Versus Pressure Differential.

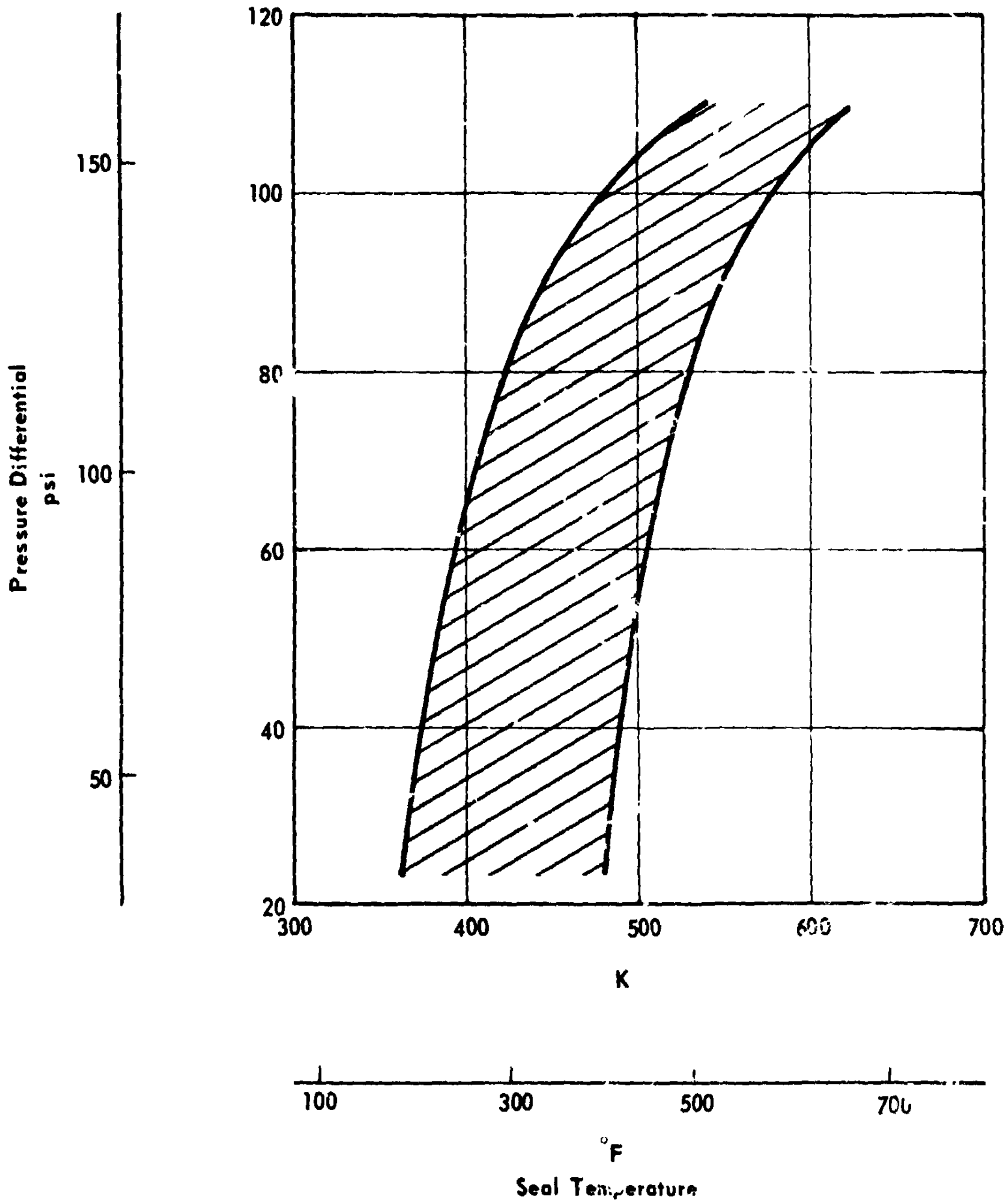

Figure 47. Envelope of Self-Acting Circumferential Seal Temperature Versus Pressure Differential.

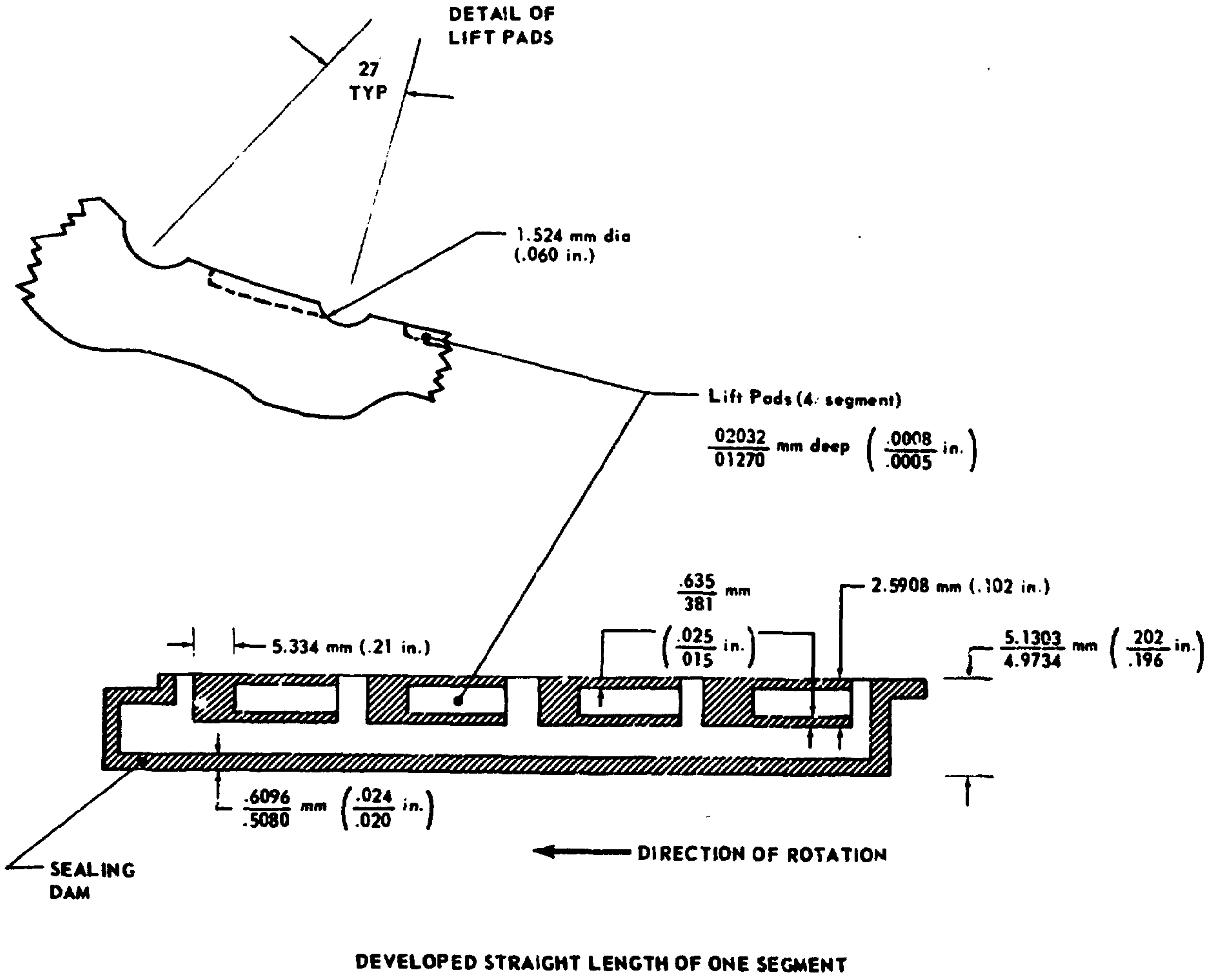

Figure 48. Details of Redesigned Carbon Segment, Self-Acting Circumferential Seal.

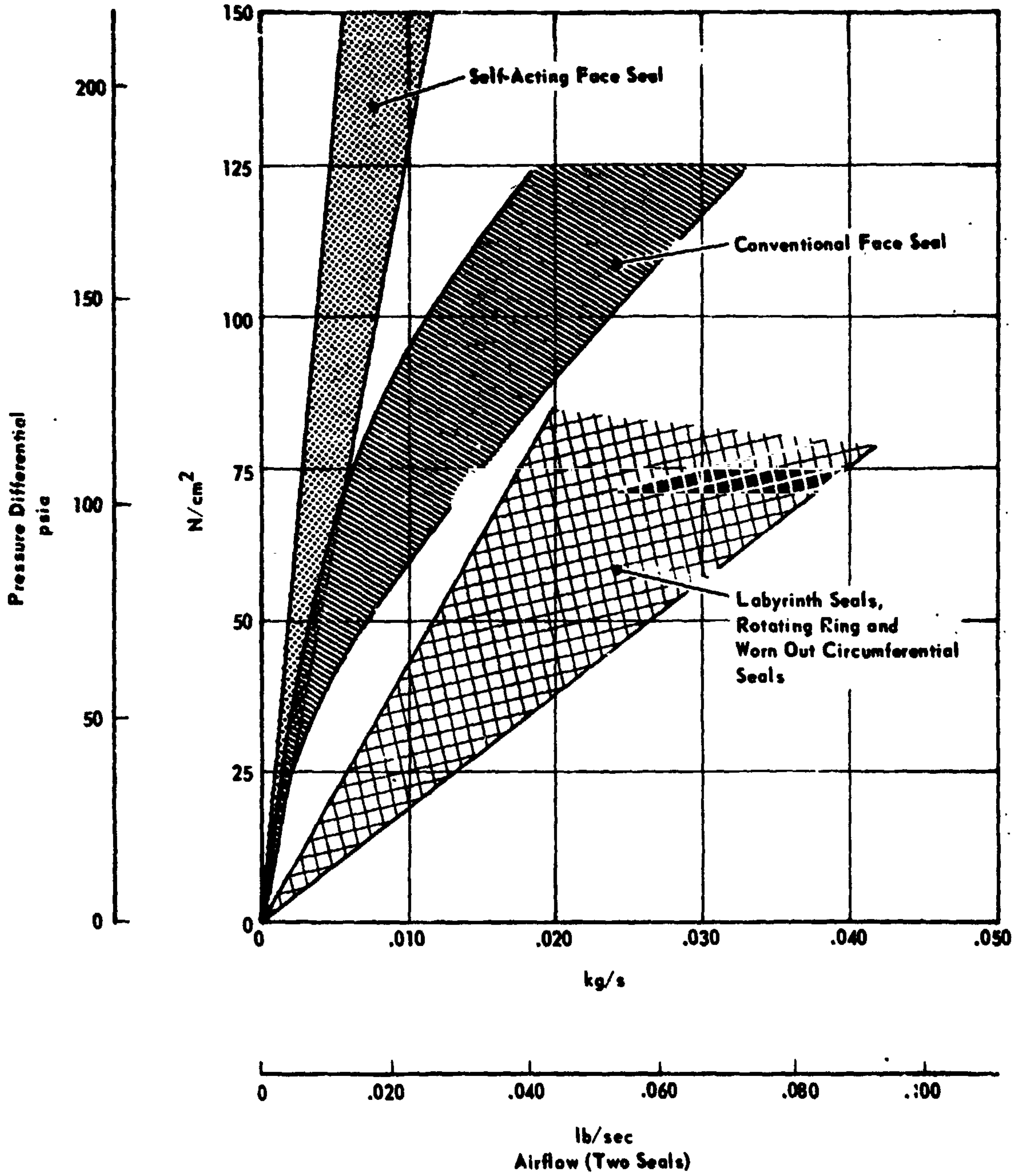

Figure 49. Comparison of Seal Configurations.

Several problems can occur as a result of high seal leakage airflow into the lubrication system:

1. The air-oil separation system may not be able to handle the volume of air, and accessory gearbox pressure will increase and back pressure the bearing cavities that are in low-pressure areas of the engine, causing oil leakage. Also, oil might be vented out of the air-oil separator.

2. Depending on the scavenge area of the bearing cavity and the pressure downstream, excessive airflow can pressurize the bearing cavity and limit the oil flow into it, thereby precipitating bearing failure.

3. Excessive hot air flowing into the bearing cavity can degrade the lubricant and be detrimental to the bearings.

To gain some perspective of the magnitude of airflow under discussion, engine experience has shown that excessive airflow into a bearing package incorporating seals of the size used in the test program would be in the order of 0.012 kg/s (0.028 lb/sec). Taking midpoint values of the range of pressure differentials in Figure 49, the face seal could not meet this criterion at pressure differentials above approximately 85 N/cm^2 (123 psia). The limiting pressure differential for worn out circumferential segmented seals, rotating ring seals, and simple labyrinths is approximately 40 N/cm^2 (58 psia).

Test program results indicated the effect of pressure differential on airflow was more significant than speed for circumferential segmented and conventional face seals. Airflow through the face seals decreased with increasing speed at a given air pressure. This is also the case with rotating ring seals and labyrinths since the leakage gap closes with speed. The self-acting face seal airflow increased with speed as would be expected since the lift force increases with speed and therefore the leakage gap increases.

CONCLUSIONS AND RECOMMENDATIONS

Self-Acting Face Seal

The self-acting face seal limited airflow successfully at operating conditions more severe than those of present small engine applications. Endurance running of 150 hours showed that the seal could operate without rubbing contact at high shaft rotative speed (43,000 rpm, 145 m/s (475 ft/sec)) with leakages less than conventional seals.

A redesign of the seal is required to overcome difficulties related to dynamic effects and distortion of the face plate, which led, in some runs, to contact of the sealing surfaces and excessive heat generation and wear.

It is recommended that a dynamic analysis of the redesigned seal be conducted to analytically determine the response of the seal to motions of the rotating face plate. Following the dynamic analysis, environmental testing should continue to determine the full potential of the self-acting face seal configuration.

Self-Acting Circumferential Seal

A 10-hour test was successfully conducted at a speed of 91 m/s (300 ft/sec) and air pressure of 55 N/cm^2 (80 psia). The self-acting circumferential seal did not develop sufficient lift force and wore excessively at speeds above 122 m/s (400 ft/sec) and at air pressure differentials above 79 N/cm^2 (115 psia).

The carbon bore, which was manufactured with a 0.0004 mm (0.0008 in.) taper from the sealing dam to the opposite end, proved detrimental to the self-acting lift pad performance. A redesigned seal with modified self-acting geometry and no bore taper should be evaluated.

Conventional Seals

Test results indicated that conventional seals may not be satisfactory in future advanced engines because of excessive airflow.

Of the conventional seals tested, the face seal configuration was most successful at limiting airflow; however, at air-to-oil pressure differentials above approximately 85 N/cm^2 (123 psia), airflow was considered excessive.

The circumferential segmented seal configuration operated well at moderate conditions, but at air-to-oil pressure differentials above approximately 41.4 N/cm^2 (60 psia) and speeds above approximately 107 m/s (350 ft/sec), it wore excessively and eventually operated as a labyrinth.

Airflow through worn out circumferential segmented seals, rotating ring seals, and simple labyrinths is comparable for a given air-to-oil pressure differential. At pressure differentials above 40 N/cm^2 (58 psia), airflow through these seal configurations was considered excessive.

In advanced engines, if conventional seals are to be used, complicated pressure-breakdown stages will be required, adding cost and weight. Incorporation of the self-acting concept offers an attractive alternate seal design for critical applications.

REFERENCES

1. Parks, A. J., McKibbin, A. H., Ng, C. C. W., and Slayton, R. M.: "Development of Mainshaft Seals for Advance Air Breathing Propulsion Systems," Pratt & Witney Aircraft Rep. PWA-3161, NASA CR-72338, 1967.

2. Povinelli, V. P., and McKibbin, A. H.: "Development of Mainshaft Seals for Advanced Air Breathing Propulsion Systems - Phase II, Pratt & Whitney Aircraft Rep. PWA-3933, NASA CR-72737, 1970.

3. Ludwig, L. P., and Johnson, R. L.: "Design Study of Shaft Face Seal with Self-Acting Lift Augmentation. III - Mechanical Components," NASA TN D-6164, 1971.

4. Ludwig, L. P., Zuk, J., and Johnson, R. L.: "Design Study of Shaft Face Seal with Self-Acting Lift Augmentation. IV - Force Balance," NASA TN D-6568, 1972.

5. Zuk, J., Ludwig, P., and Johnson, R. L.: "Quasi-One-Dimensional Compressible Flow Across Face Seals and Narrow Slots. I - Analysis," NASA TN D-6668, 1972.

6. Zuk, J., and Ludwig, L. P.: "Investigation of Isothermal, Compressible Flow Across a Rotating Sealing Dam. I - Analysis," NASA TN D-5344, 1969.

7. Zuk, J., and Smith, P. J.: "Computer Program for Viscous Isothermal Compressible Flow Across a Sealing Dam with Small Tilt Angle," NASA TN D-5373, 1969.

8. Zuk, J., Ludwig, L. P., and Johnson, R. L.: "Design Study of Shaft Face Seal with Self-Acting Lift Augmentation. I - Self-Acting Pad Geometry," NASA TN D-5744, 1970.

9. Colsher, R., and Shapiro, W.: "Steady State and Dynamic Performance of Gas-Lubricated Seals," NASA CR-121093 (in process).

10. Povinelli, V. P., and McKibbin, A. H.: "Development of Mainshaft Seals for Advanced Air Breathing Propulsion Systems - Phase III," Pratt & Whitney Aircraft Rep. PWA-4263, NASA CR-72987, 1971.

11. Elli, A.: "The Leakage of Steam Through Labyrinth Seals," Transactions of the ASME, Vol. 57, 1935.